

EXHIBIT 1

Exhibit 1
1

EXHIBIT 1



US006759038B2

(12) **United States Patent**
Tan et al.(10) **Patent No.:** **US 6,759,038 B2**
(45) **Date of Patent:** ***Jul. 6, 2004**(54) **METASTASIS MODELS USING GREEN FLUORESCENT PROTEIN (GFP) AS A MARKER**(75) **Inventors:** **Yuying Tan, San Diego, CA (US);**
Takashi Chishima, Yokohama (JP)(73) **Assignee:** **AntiCancer, Inc., San Diego, CA (US)**(*) **Notice:** Subject to any disclaimer, the term of this patent is extended or adjusted under 35 U.S.C. 154(b) by 0 days.

This patent is subject to a terminal disclaimer.

(21) **Appl. No.:** **09/870,268**(22) **Filed:** **May 29, 2001**(65) **Prior Publication Data**

US 2002/0026649 A1 Feb. 28, 2002

Related U.S. Application Data

(63) Continuation of application No. 09/226,856, filed on Jan. 7, 1999, now Pat. No. 6,251,384, which is a continuation-in-part of application No. 09/067,734, filed on Apr. 28, 1998, now Pat. No. 6,235,968, which is a continuation-in-part of application No. 09/049,544, filed on Mar. 27, 1998, now Pat. No. 5,235,967, which is a continuation-in-part of application No. 08/848,539, filed on Apr. 28, 1997, now Pat. No. 6,232,523.

(51) **Int. Cl.⁷** **A61K 48/00; C12N 5/00;**
C12N 15/63(52) **U.S. Cl.** **424/93.21; 800/8; 800/9;**
800/10; 435/320.1; 435/325; 435/455; 514/44(58) **Field of Search** **435/325, 320.1,**
435/455; 800/8, 9, 10; 514/44; 424/93.2,
93.21(56) **References Cited****U.S. PATENT DOCUMENTS**5,650,135 A 7/1997 Contag et al. 424/9.1
5,874,304 A 2/1999 Zolotukhin et al. 435/366**FOREIGN PATENT DOCUMENTS**WO WO 97/18841 5/1997
WO WO 97/45550 12/1997
WO WO 98/49336 11/1998**OTHER PUBLICATIONS**Merriam-Webster Online, <http://www.m-w.com/cgi-bin/dictionary>, definition of "intact". 2003.*Fu, X. et al., *Anticancer Res.* (1993) 13:283-286.Heim, R. et al., *Nature* (1995) 373:663-664.Hoffman, R.M., *Cancer Cells* (1991) 3:86-92.Hoffman, *Investigational New Drugs* (1999) 17(4):343-359.Hyer, M. L. et al., *Cancer Gene Therapy* (1997) 4(6):s29-s30.Kaufman, R.J. et al., *Nucleic Acids Res.* (1991) 19:4485-4490.Kaufman et al., *Annu. Rev. Immunol.* (1995) 13:339-367.Khokha, R. et al., *Cancer Metastasis Rev.* (1995) 14:279-301.Koop, S. et al., *Cancer Res.* (1995) 55:2520-2523.Leighton, J., *Cancer Res.* (1957) 17:929-941.Leighton, J., *Cancer Res.* (1960) 20:575-597.Levy, J.P. et al., *Nature Biotechnol.* (1996) 14:610-614.Li, Y. et al., *Biotechnologies*, (1997) 23:1026-1029.Lin, W.C. et al., *Cancer Res.* (1990) 50:2808-2817.Lin, W.C. et al., *Invasion and Metastasis* (1992) 12:197-209.Margolis, L.B. et al., *In Vitro Cell Dev. Biol.* (1995) 31:221-226.Margolis et al., *Annu. Rev. Immunol.* (1995) 13:339-367.Miller et al., *FASEB* (1995) 9:190-199.Morin, J. et al., *J. Cell. Physiol.* (1972) 77:313-318.Plautz, J. D. et al., *Gene* (1996) 173:83-87.Prasher, D.C. et al., *Gene* (1992) 111:229-233.Romer et al., *APMIS* (1995) 103:582-587.Vieweg et al., *Cancer Invest.* (1995) 13(2):193-201.Yang et al., *Cancer Research* (1999) 59(4):781-786.Yang et al., *Proc. SPIE-Int. Soc. Opt. Eng.* (1999) 117-124.Yokoe, H. et al., *Nature Biotechnol.* (1996) 14:1252-1256.Zolotukhin, S. et al., *J. Virol.* (1996) 70:4646-4654.Aboody-Guterman et al., *Society for Neuroscience Abstracts* (1996) 22:949-1998.Astoul, P. et al., *Anticancer Res.* (1994) 14:85-92.Astoul, P. et al., *J. Cell Biochem.* (1994) 56:9-15.Chalfie, M. et al., *Science* (1994) 263:802-805.Chishima et al., *Proc. Am. Assoc. Canc. Res* (1997) 38:489 (#3276-3/97).Chishima, T. et al., *Clinical and Experimental Metastasis* (1997) 15(5):547-552.Chishima, T. et al., *Anticancer Res.* (1997) 17:2377-2384.Chishima, T. et al., *Cancer Res.* (1997) 57(10):2042-2047.Chishima, T. et al., *Proc. Nat'l Academy of Sciences of USA* (1997) 94:11573-11576.Cody, C.W. et al., *Biochemistry* (1993) 32:1212-1218.Cormack, B. et al., *Gene* (1996) 173:33-38.Crameri, A. et al., *Nature Biotechnol.* (1996) 14:315-319.Delagrave, S. et al., *Biotechnology* (1995) 13:151-154.

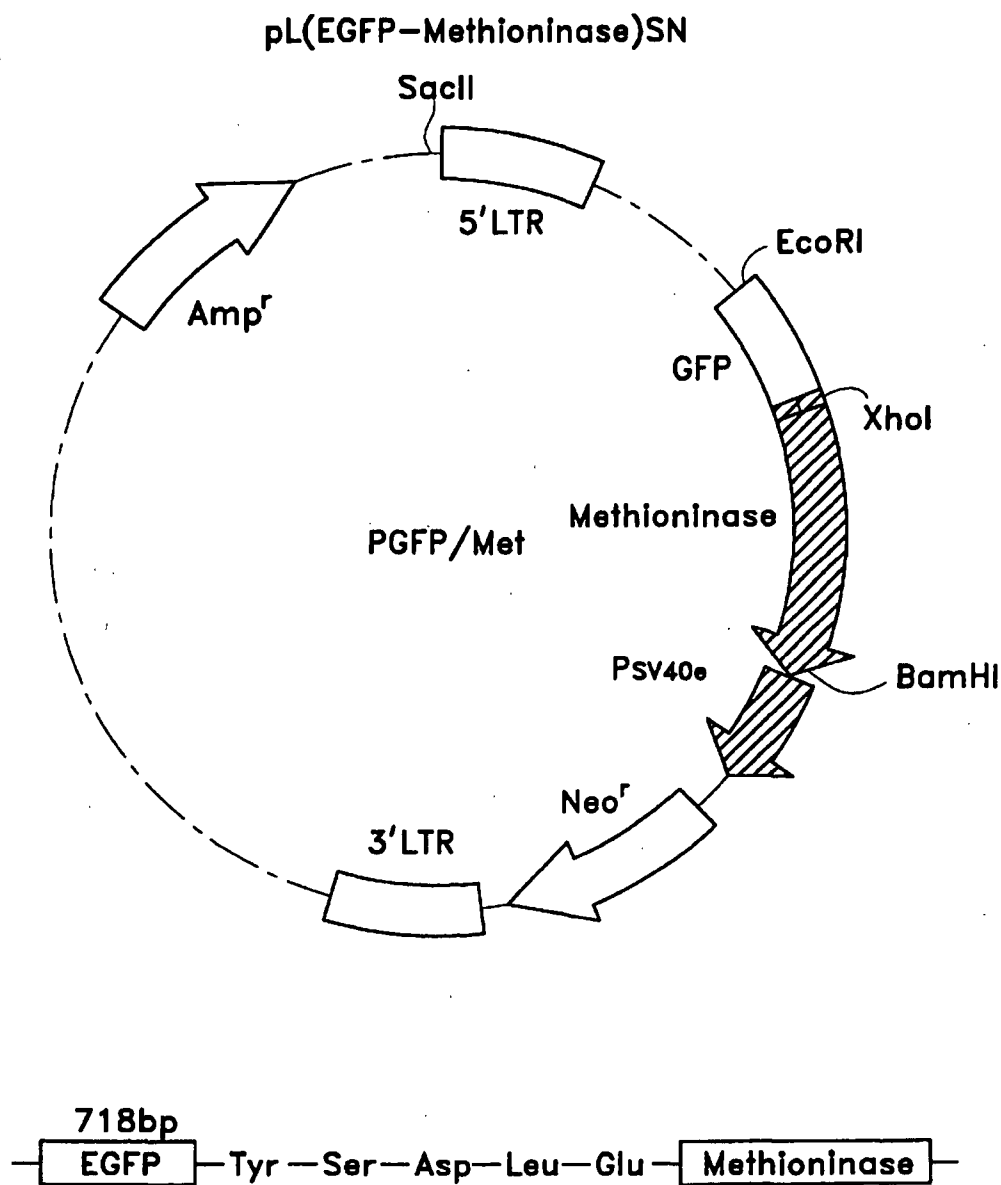
* cited by examiner

Primary Examiner—Anne M. Wehbe(74) *Attorney, Agent, or Firm*—Morrison & Foerster LLP(57) **ABSTRACT**

A method to follow the progression of metastasis of a primary tumor, which method comprises removing fresh organ tissues from a vertebrate subject which has been modified to contain tumor cells that express GFP and observing the excised tissues for the presence of fluorescence is disclosed. The fluorescence can also be monitored by observing the tissues in situ. Vertebrate subjects which contain GFP producing tumors are useful models to study the mechanism of metastasis, as well as to evaluate candidate protocols and drugs. In addition, subjects already harboring tumors can be treated so as to modify the endogenous tumors to contain GFP. This permits clinical applications. Finally, by injecting a contrast dye into a subject harboring a GFP-labeled tumor, angiogenesis in the tumor can be observed directly.

12 Claims, 2 Drawing Sheets

Exhibit 1**2**

**Fig. 1a****Exhibit 1****3**

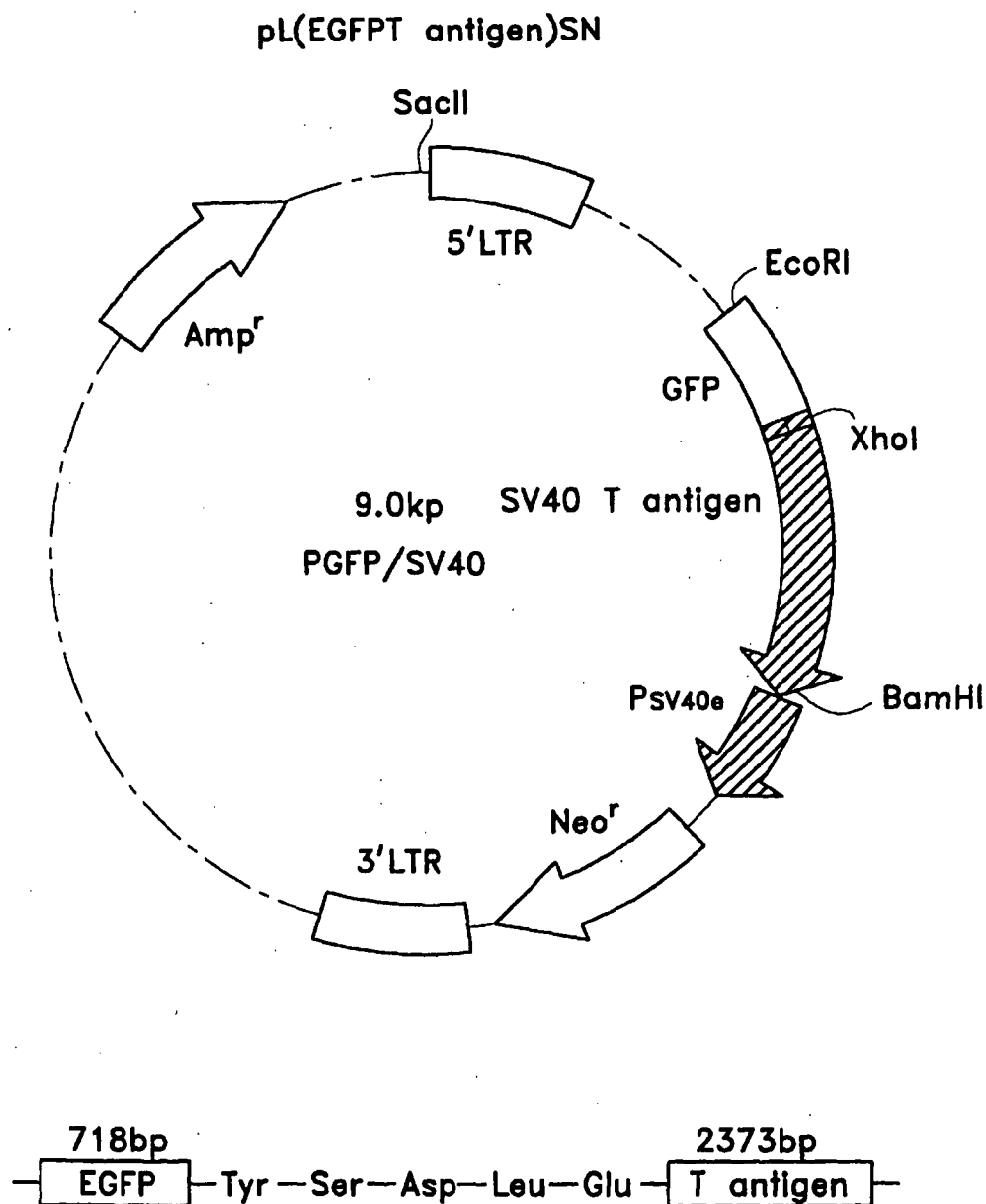


Fig. 1b

Exhibit 1

4

1

METASTASIS MODELS USING GREEN FLUORESCENT PROTEIN (GFP) AS A MARKER

This application is a Continuation of U.S. Ser. No. 09/226,856, filed Jan. 7, 1999, now U.S. Pat. No. 6,251,384, which is a Continuation-in-part of U.S. Ser. No. 09/067,734, filed Apr. 28, 1998, now U.S. Pat. No. 6,235,968, which is a Continuation-in-part of U.S. Ser. No. 09/049,544, filed March 27, 1998, now U.S. Pat. No. 5,235,967, which is a Continuation-in-part of U.S. Ser. No. 08/848,539, filed April 28, 1997, now U.S. Pat. No. 6,232,523, the contents of which are incorporated by reference.

TECHNICAL FIELD

The invention relates to the study of tumor progression. Specifically, it concerns model systems for studying the metastasis of tumors in vertebrate systems and to models and methods for evaluating candidate drugs.

BACKGROUND ART

It has long been recognized that the ability of tumor tissues to metastasize constitutes a major portion of the life-threatening aspects of malignancy. Metastasis is the growth of secondary tumors at sites different from the primary tumor. Thus, despite surgical removal of the primary tumor, it may not be possible to arrest the progress of this condition. An understanding of the mechanism whereby metastasis occurs will be crucial to the development of protocols whereby the growth of secondary tumors can be controlled. In order to understand the mechanism of metastasis, it will be necessary to provide a model which permits identification of small numbers of tumor cells against a background of many host cells so that secondary tumor emboli and micrometastases can be observed over the course of real time.

Others have demonstrated extravasation and initial seeding steps in tumor metastasis in vitro using externally fluorescently labeled tumor cells. Khokha, R. et al., *Cancer Metastasis Rev* (1995) 14:279-301; Koop, S. et al., *Cancer Res* (1995) 55:2520-2523. Further, Margolis, L. B. et al., *In Vitro Cell Dev Biol* (1995) 31:221-226 was able to visualize the migration of externally fluorescently labeled lung tumor cells in host mouse lung in histoculture. In all cases, however, long-term observation was not possible due to the limitation of exogenous fluorescent labels. Retroviral transfer of a green fluorescent protein (GFP) gene has been shown to result in stable transfectants of human cancer cells in vitro (Levy, J. P. et al., *Nature Biotechnol* (1996) 14:610-614), as well as of hematopoietic cells (Grignani, F. et al., *Cancer Res* (1998) 58:14-19 and by Cheng, L. et al., *Gene Therapy* (1997) 4:1013-1022).

Attempts have been made to provide such a model using the β -galactosidase gene as a marker (Lin, W. C. et al., *Cancer Res* (1990) 50:2808-2817; Lin, W. C. et al., *Invasion and Metastasis* (1992) 12:197-209). However, this marker has not proved satisfactory, as fresh or processed tissue cannot be used. The present invention provides a marker which permits visualization of tumor invasion and micrometastasis formation in viable fresh tissue. In addition, by providing suitable contrast media, the method of the invention can be adapted to visualize angiogenesis in established and growing tumors. The methods of the invention can be applied not only to models of tumor growth and metastasis, but, through the use of retroviral vectors, can be employed to obtain clinical data in human subjects bearing tumors.

2

The present invention utilizes green fluorescent protein (GFP) as a marker. Heterologous expression of this protein, principally to monitor expression of fused DNA, was disclosed in U.S. Pat. No. 5,491,084. This document describes the expression of GFP in *E. coli* and *C. elegans* and postulates that cells in general can be modified to express GFP. Such expression, according to this document, permits not only a method to monitor expression of fused DNA, but also a means of monitoring protein localization within the cell.

The aspect of the invention which provides a metastatic model has been reported and described in a series of publications. Chishima, T. et al. *Cancer Research* (1997) 57:2042-2047 describe the construction of a dicistronic vector containing the gene for humanized green fluorescent protein (GFP) and dihydrofolate reductase (DHFR). This vector was transfected into CHO-K1 cells to obtain clone-38. Clone-38 showed stable GFP expression which was maintained in the presence of methotrexate (MTX). Clone-38 cells were injected into mice to obtain tumor fragments which were then implanted by surgical orthotopic implantation (SOI) on the ovarian serosa in nude mice. Metastasis could be followed in this model.

Chishima, T. et al. *Proc Natl Acad Sci USA* (1997) 94:11573-11576 describe the preparation of clone-26 by transfection of Anip 973 human lung adenocarcinoma cells with the codon optimized hGFP-S65T clone obtained from Clontech. Clone-26 was injected intravenously into nude mice and the resulting tumors were followed in histoculture.

Chishima, T. et al. *Clin Exp Metastasis* (1997) 15:547-552 and Chishima, T. et al. *Anticancer Res* (1997) 17:2377-2384 describe similar work with clone-26 wherein the cells were inoculated subcutaneously into nude mice resulting in a visualizable tumor which was then implanted into the visceral pleura of nude mice by SOI. Metastases were observed in this model as well.

Chishima, T. et al. *In Vitro Cell Dev Biol* (1997) 33:745-747 describe histoculture of clone-26 and visualization of growth using the fluorescence emitted by GFP.

Yang, M., et al., *Cancer Res* (1998) 58:4217-4221 describe transduction of the human lung cancer cell line H460 with a retroviral expression vector containing enhanced GFP to obtain a stable high-GFP-expressing clone. Cells from this cell line were injected into nude mice and the resulting subcutaneously growing labeled tumors were transplanted by SOI into the left lung of nude mice. Fluorescence could then be observed from the metastases in the collateral lung, pleural membrane and throughout the skeletal system.

Yang, M., et al., *Cancer Res* (In Press) report similar studies using a model for prostate tumor and showing fluorescence throughout the skeletal system in nude mice.

The contents of the foregoing publications are incorporated herein by reference.

In addition to the foregoing, Cheng, L., et al., *Gene Therapy* (1997) 4:1013-1022, describe the modification of hematopoietic stem cells using the GFP gene under control of a retroviral promoter. Although the authors state that human stem cells are transfected with this system only with difficulty, by using an enhanced form of the GFP, satisfactory brightness could be achieved.

In addition, Grignani, F., et al., *Cancer Res* (1998) 58:14-19, report the use of a hybrid EBV/retroviral vector expressing GFP to effect high-efficiency gene transfer into human hematopoietic progenitor cells.

Vectors containing various modified forms of GFP to provide various colors are marketed by Clontech. The Clon-

Exhibit 1
5

3

tech vectors intended for mammalian cell expression place the GFP under control of the cytomegalovirus (CMV) promoter.

DISCLOSURE OF THE INVENTION

The invention provides models which permit the intimate study of formation of metastases from primary tumors in a realistic and real-time setting. By using green fluorescent protein (GFP) as a stable and readily visualized marker, the progression of such metastasis can be modeled and the mechanism elucidated.

Thus, in one aspect, the invention is directed to a method to follow the progression of metastasis of a primary tumor, which method comprises removing fresh organ tissues from a vertebrate subject which has been modified to contain tumor cells that express GFP and observing the excised tissues for the presence of fluorescence.

In one embodiment, however, it is unnecessary to remove organ tissues; rather, the fluorescence can be visualized in the whole animal by real-time fluorescence optical tumor imaging (FOTI).

In another aspect, the invention is directed to a vertebrate subject which has been modified to contain tumor cells expressing GFP.

In these aspects, the vertebrate subject may constitute a model system, such as an immunocompromised mouse wherein tumor cells or a tumor, modified to express green fluorescent protein has been introduced into the subject. The model system may be used to evaluate candidate drugs for their capacity to inhibit metastasis. Alternatively, the subject may be a human or other vertebrate which natively contains the tumor, but wherein the tumor has been subjected to viral infection or to transfection with a retroviral vector so as to produce said GFP. The efficacy of drugs administered to such patients can be evaluated by following the course of metastasis in the subject.

In still other aspects, the invention is directed to tumor cells modified to produce GFP under control of heterologous control elements, to cells that are immortalized to provide stable cell lines as well as comprising visible amounts of GFP, to tissues containing metastatic tumors that produce GFP, and to histocultures of tissues which contain such metastasized tumors.

The invention also includes a method to observe and follow angiogenesis in solid tumors which method comprises (usually) exposing and observing said tumors. The tumors will have been modified to express GFP, and the subject will have been administered a contrast dye to permit this observation.

BRIEF DESCRIPTION OF THE DRAWINGS

FIGS. 1a and 1b show the construction of expression vectors useful in the invention.

MODES OF CARRYING OUT THE INVENTION

The invention provides model systems for the study of the mechanism of metastasis of tumors generally, as well as to study angiogenesis in solid tumors. Advantage is taken of the visible marker green fluorescence protein (GFP) to label the tumor cells so that their migration and colonization in tissues distal to the tumor can be followed as the migration and colonization progresses. Further, by administering to the subject a contrast dye, such as rhodamine, the growth of blood vessels in solid tumors which have been labeled with GFP can also be observed.

4

Since sufficient intensity can be achieved to observe the migration of fluorescent cells in the intact animal, in addition to determining the migration of the cells by excising organs, the progression of metastasis can be observed in the intact subject. Either or both methods may be employed to observe metastasis in evaluating, in model systems, the efficacy of potential antimetastatic drugs. The success or failure of treatments provided to patients with potentially metastatic cancers can also be followed using the materials and methods of the invention.

The label used in the various aspects of the invention is green fluorescent protein (GFP). The native gene encoding this protein has been cloned from the bioluminescent jellyfish *Aequorea victoria* (Morin, J. et al., *J Cell Physiol* (1972) 77:313-318). The availability of the gene has made it possible to use GFP as a marker for gene expression. GFP itself is a 283 amino acid protein with a molecular weight of 27 kD. It requires no additional proteins from its native source nor does it require substrates or cofactors available only in its native source in order to fluoresce. (Prasher, D.C. et al., *Gene* (1992) 111:229-233; Yang, F. et al., *Nature Biotechnol* (1996) 14:1252-1256; Cody, C. W. et al., *Biochemistry* (1993) 32:1212-1218.) Mutants of the GFP gene have been found useful to enhance expression and to modify excitation and fluorescence. GFP-S65T (wherein serine at 65 is replaced with threonine) is particularly useful in the invention method and has a single excitation peak at 490 nm. (Heim, R. et al., *Nature* (1995) 373:663-664; U.S. Pat. No. 5,625,048. Other mutants have also been disclosed by Delagrade, S. et al., *Biotechnology* (1995) 13:151-154; Cormack, B. et al., *Gene* (1996) 173:33-38 and Cramer, A. et al. *Nature Biotechnol* (1996) 14:315-319. Additional mutants are also disclosed in U.S. Pat. No. 5,625,048. By suitable modification, the spectrum of light emitted by the GFP can be altered. Thus, although the term "GFP" is used in the present application, the proteins included within this definition are not necessarily green in appearance. Various forms of GFP exhibit colors other than green and these, too, are included within the definition of "GFP" and are useful in the methods and materials of the invention. In addition, it is noted that green fluorescent proteins falling within the definition of "GFP" herein have been isolated from other organisms, such as the sea pansy, *Renilla reniformis*. Any suitable and convenient form of the GFP gene can be used to modify the tumor cells useful in the models of the invention, and for retroviral transformation of endogenous tumors. The particular humanized hGFP-S65T clone is used in the examples set forth below for illustration.

Techniques for labeling cells in general using GFP are disclosed in U.S. Pat. No. 5,491,084 (supra).

In one application, the method of the invention provides a model system for studying the effects of various therapeutic candidate protocols and substances on metastatic growth of tumors.

In general, the model involves modifying a vertebrate, preferably a mammal, so as to contain tumor tissue, wherein the tumor cells have, themselves, been modified to contain an expression system for GFP. The tumor cells may arise from cell lines of the invention wherein tumor cells have been modified to contain expression systems for GFP and SV40 T-antigen. Tumors can be formed in such vertebrate systems by administering the transformed cells containing the GFP expression system and permitting these transformed cells to form tumors. Typically such administration is subcutaneous and the tumors are formed as solid masses. The tumors thus formed can be implanted in any suitable host tissue and allowed to progress, metastasize and develop.

Exhibit 1
6

5

Suitable procedures for growing the initial tumor, thus, involve transcutaneous injection of the tumor cells producing GFP, such as CHO cells, HeLa cells, carcinoma and sarcoma cell lines, well established cell lines such as the human lung adenocarcinoma line Anip 973, or lung cancer cell line H460 as well as GFP-containing human breast cancer lines MDA-MB468 and MDA-MB435; human prostate cancer lines PC3 and DU-145, human glioblastoma line 324, mouse melanoma B16 and others that may become available in the art, including the immortalized cells of the invention. The administered cells will have been modified to contain an expression system for GFP. After administration, solid tumors generally develop, typically at the site of subcutaneous injection. These tumors, which are themselves fluorescent, can then be removed and used for implantation in the model vertebrate.

Techniques for implantation of the solid tumors, now labeled with GFP, into vertebrates include direct implantation by surgical orthotopic implantation (SOI) at the desired site, typically the site from which the tumor cells were derived. Suitable sites include lung, liver, pancreas, stomach, breast, ovary, prostate, bone marrow, brain, and other tissues susceptible to malignancy. Once the solid tumors have been implanted, the vertebrate becomes a model system for studying metastasis. The tumor is thus allowed to progress and develop and the vertebrate is monitored for appearance of the GFP labeled cells at sites distal from the original implantation site. The monitoring can occur either on the whole vertebrate by opening the animal and observing the organs directly with a fluorescent microscope, or the tissues may be excised and examined microscopically. In some cases the tumors are sufficiently bright that opening the animal is unnecessary—they can be seen directly through the skin. In any case, as GFP is visible to the naked eye, no development systems to stain the tissue samples are required. Tissue samples are simply properly processed as fresh samples in slices of suitable size, typically 1 mm thick, and placed under a microscope for examination. Even colonies of less than 10 cells are thus visible. A variety of microscopic visualization techniques is known in the art and any appropriate method can be used.

It is particularly convenient to visualize the migration of tumor cells in the intact animal through fluorescent optical tumor imaging (FOTI). This permits real-time observation and monitoring of progression of metastasis on a continuous basis, in particular, in model systems, in evaluation of potential anti-metastatic drugs. Thus, the relative lack of metastasis observed directly in test animals administered a candidate drug in comparison to controls which have not been administered the drugs indicates the efficacy of the candidate and its potential as a treatment. In subjects being treated for cancer, the availability of FOTI permits those devising treatment protocols to be informed on a continuous basis of the advisability of modifying or not modifying the protocol.

In addition, the development of the tumor can be studied in vitro in histological culture. Suitable systems for such study include solid supported cultures such as those maintained on collagen gels and the like.

Suitable vertebrate subjects for use as models are preferably mammalian subjects, most preferably convenient laboratory animals such as rabbits, rats, mice, and the like. For closer analogy to human subjects, primates could also be used. Particularly useful are subjects that are particularly susceptible to tumor development, such as subjects with impaired immune systems, typically nude mice or SCID mice. Any appropriate vertebrate subject can be used, the

6

choice being dictated mainly by convenience and similarity to the system of ultimate interest.

Any suitable expression system operable in the tumor cells to be implanted may be used. A number of vectors are commercially available that will effect expression in tumor cells of various types. The nature of the vector may vary with the nature of the tumor and the vertebrate in which it finds its origin. However, when GFP is used to visualize metastasis in a model system, it is preferred to utilize vectors which do not use retroviral or other viral promoters which may complicate the nature of the model.

In order to provide cell lines that are helpful in establishing tumors for these model systems, it is also advantageous to employ expression vectors which provide the cells with the SV40 T-antigen. The presence of this antigen ensures immortality of the culture. Thus, particularly useful in the invention are vectors which comprise expression systems that result in the production both of GFP and SV40 T-antigen.

In order to transfect and modify the transformed cells which are effective in generating tumors, any suitable transfection method may be used, such as liposomes, calcium phosphate precipitation, electroporation and use of a gene gun. Lipofection is preferred.

In contrast, when the method of the invention is used to visualize metastasis in tumors that natively occur in a subject such as a human cancer patient, vectors that employ retroviral or other viral promoters are preferred. The use of such vectors permits the insertion of an expression system for GFP into the already existent tumor. In addition, the expression system may contain nucleotide sequence encoding other useful proteins such as therapeutic proteins which permit simultaneous diagnosis of metastasis and treatment. Among such suitable proteins are included methioninase (see, for example, PCT/US93/11311 and PCT/US96/09935). Such proteins may be produced either as fusions with the GFP, or independently either using a dicistronic expression system or independent expression systems, one for the therapeutic protein and the other for the GFP.

Retroviral based expression systems for GFP have already been described by Grignani, F. et al. *Cancer Res* (1998) 58:14-19 and by Cheng, L. et al. *Gene Therapy* (1997) 4:1013-1022. In these reports, the retroviral expression system itself was used to transfect hematopoietic progenitor cells or packaging cells were employed to provide virus-containing supernatants which can be used directly for infection of the mammalian cells. Thus, in the method of the invention, the tumor contained in the vertebrate subject is typically infected with virus which has been modified and packaged to contain the expression system for GFP. In situ infection with virus results in the ability of the tumor to produce GFP and, in effect, label itself.

Various retroviral systems useful in producing proteins in mammalian cells are known in the art. Examples include commercially available vector and packaging systems such as those sold by Clontech, San Diego, Calif., including their Retro-X vectors pLNCX and pLXSN which permit expression of GFP under a variety of promoters by insertion into the multiple cloning site. These vectors contain ψ^* (the extended viral packaging signal) and antibiotic resistance genes for selection. A number of these systems have been developed for use in gene therapy, including vectors which provide a multiple cloning site sandwiched between 5' and 3' LTR derived from retroviral sources, and thus would be useful in labeling the tumors of human patients.

Thus, retroviral based vectors such as those set forth in FIGS. 1a-1b can be transfected into packaging cells and

Exhibit 1

7

transferred directly to targeted cancer cells or supernatants from the packaging cells can be used to infect tumor cells with the retrovirus. Preferred combinations of retrovirus and packaging cells include the GFP-retrovirus vector pLEIN in PT-67 packaging cells. Co-culture of the packaging cells with colon cancer cells results in transfer of the GFP-retrovirus to the cancer cells.

Using histoculture techniques, and supernatants from PT-67 packaging cells generating GFP-pLEIN virus, the successful modification of a human cancer tissue to display the fluorescence associated with GFP has been demonstrated. For use in vivo, the virus is administered, preferably locally to the tumor, which can be observed within hours after injection either of packaging cells or of the viral containing supernatants. The malignant cells can be identified by their green color, sometimes sufficiently bright so that the tumors can be seen through the skin.

In addition to direct observation of tumor metastasis and growth either in a model system or in a vertebrate, typically mammalian and more typically a human subject which is already afflicted by a tumor, the methods of the invention can be adapted to observe angiogenesis in solid tumors. The tumor is itself labeled with GFP as described above. The subject is then administered a contrast dye, typically by injection, preferably intravenous injection, which allows blood vessels in the tumor to be observed. Suitable dyes include rhodamine and other contrast dyes. Any dye which forms a contrasting color with the green color of the GFP can be used. Preferably, the dye is coupled to an inert polymer such as polyethylene glycol to increase the length of time the dye will remain in the blood vessel. A sufficient amount of dye is provided to permit ready visualization; the amount of dye required will depend on the choice of dye, the location of the tumor, the nature of the background GFP, and the method used for observation. Within a few minutes, vessels growing into the solid tumors in such areas as the mesentery, colon wall, and omentum can be observed. Observations can be continued over substantial periods; for example, angiogenesis after several hours is still observed by using this method.

The following examples are intended to illustrate but not to limit the invention.

EXAMPLE 1

Preparation of Tumor Cells that Produce GFP

The humanized hGFP-S65T clone described by Zolotukhin, S. et al., *J Virol* (1996) 70:4646-4654 was used as the green fluorescent protein coding sequence. This codon-optimized gene was purchased from Clontech Laboratories, Inc. (Palo Alto, Calif.) and ligated into the dicistronic expression vector (pED-mtx¹) obtained from Genetics Institute, Cambridge, Mass. and described in Kaufman, R. J. et al., *Nucleic Acids Res* (1991) 19:4485-4490. hGFP-S65T was digested with HindIII and blunt-ended; the entire hGFP coding region was excised with XbaI and then unidirectionally subcloned into pED-mtx¹ which had been digested with PstI, blunt-ended and then further digested with XbaI.

CHO-K1 cells were cultured in DMEM containing 10% fetal calf serum, 2 mM L-glutamine and 100 μ M nonessential amino acids. Near confluent cells were incubated with a precipitated mixture of LipofectAMINETM reagent (GIBCO) and saturating amounts of plasmids for six hours and then replenished with fresh medium. The cells were harvested by trypsin/EDTA 48 hours later and subcultured at

1:15 into selective medium containing 1.5 μ M methotrexate (MTX). Cells with stably integrated plasmids were selected in MTX-containing medium and isolated with cloning cylinders (Bel-Art Products, Pequannock, N.J.) by EDTA. After amplification and transfer, Clone-38 was selected because of its high-intensity GFP fluorescence and stability.

In a similar manner, Anip 973 cells, a human lung cancer cell line obtained from Harbin Medical University, China, were cultured as described above for CHO-K1 cells except using RPMI1640 (GIBCO) in place of DMEM. Transfection, selection and amplification and transfer were conducted as described above. Clone-26 was chosen because of its high-intensity GFP fluorescence and stability.

EXAMPLE 2

Mouse Model Using Modified CHO Cells

Clone-38, which was stable at 1.5 μ M MTX and which proliferated at the same rate as the parental CHO-K1 cells as ascertained by comparing doubling times, was used in this model.

Three six-week old Balb/C nu/nu female mice were injected subcutaneously with a single dose of 10^7 Clone-38 cells that had been harvested by trypsinization and washed three times with cold serum-containing medium and then kept on ice. The cells were injected in a total volume of 0.4 ml within 40 minutes of harvesting and the nude mice sacrificed three weeks after injection. All of the mice had a subcutaneous tumor ranging in diameter from 13.0 mm to 18.5 mm (mean=15.2 mm \pm 2.9 mm). The tumor tissue was strongly fluorescent. It was shown by extracting GFP from cultured Clone-38 cells in comparison to Clone-38 cells prepared from the tumor that the levels of production of GFP were the same in both.

To construct the model, tumor fragments (1 mm³) derived from the nude mouse subcutaneous Clone-38 tumor grown as described above, were implanted by surgical or surgical orthotopic implantation (SOI) on the ovarian serosa in six nude mice as described by Fu, X. et al., *Anticancer Res* (1993) 13:283-286, incorporated herein by reference. Briefly, the mice were anesthetized by isoflurane inhalation and an incision was made through the left lower abdominal pararectal line and peritoneum to expose the left ovary and part of the serosal membrane, which was scraped with a forceps. Four 1 mm³ tumor pieces were fixed on the scraped site with an 8-0 nylon suture and the ovary then returned to the peritoneal cavity. The abdominal wall and skin were closed with 6-0 silk sutures.

Four weeks later, the mice were sacrificed and lung and various other organs were removed. The fresh samples were sliced at approximately 1 mm thickness and observed directly under fluorescent and confocal microscopy. Samples were also processed for histological examination for fluorescence and conventional staining. Frozen sections were prepared wherein the slides were rinsed with phosphate buffer saline and fixed for 10 minutes at 4° C.; 10% formaldehyde plus 0.2% glutaraldehyde and PBS were added and the slides were then washed with PBS. The fixed tissue was stained with hematoxylin and eosin using standard techniques.

Light and fluorescence microscopy were carried out using a Nikon microscope equipped with a Xenon lamp power supply and a GFP filter set (Chromotechnology Corp., Brattleboro, Vt.). Confocal microscopy was with an MRC-600 Confocal Imaging System (Bio-Rad) mounted on a Nikon microscope with an argon laser.

The mice, at sacrifice, had tumors in the ovaries ranging in diameter from 18.7 mm–25.3 mm (mean 21.9±3.1 mm). The fresh organ tissues examined under fluorescence microscopy with no treatment of the tissues showed seeding of the tumor throughout the peritoneal cavity, including the colon (6/6 mice), cecum (5/6), small intestine (4/6), spleen (1/6), and peritoneal wall (6/6). Numerous micrometastases were detected in the lungs of all mice and multiple micrometastases were also detected on the liver (1/6), kidney (1/6), contralateral ovary (3/6), adrenal gland (2/6), para-aortic lymph node (5/6) and pleural membrane (5/6). Single-cell micrometastases could not be detected by the standard histological techniques described above and even the multiple cell colonies were difficult to detect using them. As the colonies developed, the density of tumor cells decreased markedly in the center.

In an additional experiment, 5×10^6 Clone-38 cells were injected into a nude mouse through the tail vein and the mouse sacrificed after two minutes. Fresh visceral organs were analyzed by fluorescence microscopy and showed the presence of fluorescent cells in peritoneal wall vessels which formed emboli in the capillaries of the lung, liver, kidney, spleen, ovary, adrenal gland, thyroid gland and brain.

Thus, using these techniques, progression of micrometastasis can be observed as seeded cells develop into colonies within the relevant target organs. Further, screening for micrometastases can be done easily and quickly in all systemic organs.

EXAMPLE 3

Murine Model Using Human Lung Cancer Cells

The procedures are generally those set forth in Example 2 except that Clone-26 cells as prepared in Example 1 were used instead of Clone-38 CHO cells.

A. As in Example 2, tumors were grown in six-week-old Balb/C nu/nu male mice injected subcutaneously with a single 0.4 ml dose of 10^7 Clone-26 cells within 40 minutes of harvesting by trypsinization and washing three times with cold serum-containing medium. The cells were kept on ice prior to injection. The animals were sacrificed when the tumors had reached approximately 1.2 cm diameters. The 1.2 cm tumors formed after about 5 weeks.

B. The tumor pieces, 1 mm^3 , were implanted by SOI into the left visceral pleura of 8 mice as described by Astoul, P. et al., *Anticancer Research* (1994) 14:85–92; Astoul, P. *J Cell Biochem* (1994) 56:9–15, both incorporated herein by reference. Briefly, the mice were anesthetized by isofluran inhalation and a small 1 cm transverse incision made on the left lateral chest, via the fourth intercostal space, resulting in total lung collapse. Five tumor pieces were sewn together with a 7-0 nylon surgical suture and fixed by making one knot. The lung was taken up by forceps and the tumor sewn into the lower part of the lung with one suture, after which the lung was returned to the chest cavity and the muscles and skin closed with a single layer of 6-0 silk sutures. The lung was reinflated by withdrawing air from the chest cavity with a 23-gauge needle.

C. Four of the mice were sacrificed at 4 weeks and another 4 at 8 weeks. Pleural tumors for the 4-week group ranged from 244.40 mm^3 – 522.88 mm^3 ; those from the 8 week group from 1279.08 mm^3 – 2714.40 mm^3 . This represented mean volumes of 371 mm^3 and 1799 mm^3 . Specimens of tissue were sliced at 1 mm thickness and observed directly under fluorescent microscopy using a Nikon microscope equipped with a Xenon lamp power supply and a Leica

stereo fluorescence microscope equipped with a mercury lamp power supply and GFP filter sets. All of the animals showed chest wall invasion and local and regional spread of the tumor, but in the 8-week mice, all tumors involved the mediastinum and contralateral pleural cavity as well as metastases on the visceral and parietal pleura. Pulmonary hilum lymph nodes were involved in 3 of 4 mice of the 4-week group and all of the mice in the 8-week group. Cervical node involvement was detected in one of the mice of the 8-week group, but no other metastases were observed. The animals were also observed directly before the tissues were excised. The margin of the invading tumor in normal lung tissue could be detected by GFP fluorescence and a small vessel could be seen developing at the margin of the tumor.

D. In an additional experiment, 8 nude mice were injected in the tail vein with a single dose of 1×10^7 Clone-26 cells that had been harvested by trypsinization and washed 3 times with cold serum-containing medium. The injection contained a total volume of 0.8 ml within 40 min. of harvesting. Again, 4 mice were sacrificed at 4 weeks and another 4 at 8 weeks and tissue specimens were obtained and studied by microscopy as described above. Numerous micrometastatic colonies were detected in whole lung tissue in both groups ranging from $5.2 \mu\text{m}$ to $32.5 \mu\text{m}$ in the 4-week group and $5.5 \mu\text{m}$ – $178.3 \mu\text{m}$ in the 8-week group. The colonies from the 8-week group did not appear further developed as compared with those from the 4-week group. Numerous small colonies ranging in number to less than 10 cells were detected at the lung surface in both groups and brain metastases were detected in 1 mouse of the 4-week group and 2 from the 8-week group. One mouse in the 8-week group had systemic metastases in the brain, the submandibular gland, the whole lung, the pancreas, the bilateral adrenal glands, the peritoneum and the pulmonary hilum lymph nodes.

E. In an additional experiment, similar to that set forth in the previous paragraph, the mice injected in a tail vein with 10^7 Clone-26 cells were sacrificed at 4, 8 and 12 weeks and the tissues examined as described. Most of the colonies and mice sacrificed at 8 weeks were not obviously further developed compared with those sacrificed at 4 weeks, but numerous small quantities ranging in number down to less than 10 cells and ranging in size from $5.5 \mu\text{m}$ – $110 \mu\text{m}$ were detected at the lung surface. At 12 weeks, there were many small metastatic colonies which appeared dormant, although other colonies grew extensively by this time, reaching a size up to $1100 \mu\text{m}$, suggesting a heterogeneity of dormant and active tumor colonies in the lung.

EXAMPLE 4

Growth of Clone-26 Tumor Cells in Histoculture

Six-week old SCID/SCID mice were injected intravenously with a single dose of 7.5×10^7 Clone-26 cells which had been harvested by trypsinization and washed 3 times with cold serum-containing medium and kept on ice as described above. The cells were injected in a total volume of 0.5 ml within 40 minutes of harvesting. After 3 weeks, numerous micrometastatic colonies were detected in whole lung tissue up to approximately $550 \mu\text{m}$. After 5 weeks, the mice were sacrificed and the Clone-26 seeded mouse lungs were removed and histocultured on spun gels using the histoculture methods developed by Leighton, J. *Cancer Res* (1957) 17:929–941; Leighton, J. et al., *Cancer Res* (1960) 20:575–597; Hoffman, R. M. *Cancer Cells* (1991) 3:86–92. Tumor colonies spread rapidly in the lung tissue over time

11

and after 1 week the tumor cells started to invade and colonize supporting collagen sponge-gel. After 2 weeks, tumor cells formed satellite colonies in the sponge-gel distant from the primary colonies in the lung tissue, thus growing faster in histoculture than in SCID mice. Tumor colonies could grow in histoculture for more than 1 month.

EXAMPLE 5

Construction of a Retroviral Expression Vector for GFP and Preparation of Labeled Tumor Cell Lines

FIGS. 1a and 1b show the construction of expression vectors for GFP under control of the SV40 promoter. The constructs employ commercially available pEGFP series vectors available from Clontech. Both bacterial and mammalian expression vectors are available which permit production of additional proteins, as well as GFP, either as fusions or in dicistronic systems. FIG. 1a shows the construction of an expression vector, pGFP/Met, for a fusion of GFP with methioninase; FIG. 1b shows the construction of a vector pGFP/SV40 for production of a fusion protein of GFP with the SV40 T-antigen.

Commercial vectors containing the GFP coding sequence of the desired spectral characteristics using the pLEIN system described in Example 6 were transfected into cell lines originating from tumors, such as human breast cancer, human prostate cancer, human glioblastoma and mouse melanoma. In this manner, human breast cancer cell lines MF-7, MDA-MB468 and MDA-MB435, human prostate cancer cell lines PC3 and DU145, human glioblastoma cell line 324, human lung cancer cells Anip-73 and H460, human colon cancer cells lines Colo-205, HCT-15 and WiDr, human gastric cancer cell line NVGC-4, human kidney cancer cell line SN12C, human tongue cancer cell line SCC-25, human melanomas LOX and SK-mel-5, labeled Chinese hamster ovary cells from cell line CHO-K1 and mouse melanoma cell line B16 labeled with green fluorescent protein were established.

The SV40 T-antigen protein is useful to immortalize cultured cells so as to establish permanent cell lines. Accordingly, the vector pGFP/SV40 is transfected into a series of tumor cell cultures to provide fluorescent immortalized cell lines.

EXAMPLE 6

In Vivo Labeling of Established Tumors

Unlabeled tumors derived from the human lung cancer cell line Anip973 were established in mice using the procedure set forth in Example 3, paragraphs A and B, but substituting unlabeled Anip973 cells for clone 26. The mice were then injected with 1×10^7 packaging cells containing the retroviral vector GFP-retrovirus pLEIN contained in PT67 cells. This virus packaging system is available from Clontech, San Diego, Calif. pLEIN contains an insert of the coding sequence for EGFP, a red-shifted variant of wild-type GFP that has been optimized for brighter fluorescence and higher expression in mammalian cells. It has an excitation maximum of 488 nm and an emission maximum at 507 nm. This mutant contains a double amino acid substitution at position 64 from Phe to Leu and at position 65 from Ser to Thr. It is described by Comack, B. et al. *Gene* (1996) 173:31-38. There are more than 190 silent base changes to maximize human codon usage preferences as described by Haas, J. et al. *Curr Biol* (1996) 6:315-324. Thus, pLEIN contains the above-described GFP coding sequence inserted

12

into the multiple cloning site of pLXIN to obtain a dicistronic expression system which permits coordinated translation of the GFP and neomycin resistance. Three days after injection of the cells into the peritoneal cavity of the mice, the tumor cells could be seen in the seminal vesicles under bright-field microscopy and under fluorescent microscopy.

EXAMPLE 7

Observation of Angiogenesis

A suspension containing 1×10^7 clone-38 cells, described in Example 1, were injected into the peritoneal cavity of a mouse. Five days later, the mouse was injected in the tail with rhodamine and the mouse was then put under anesthesia and the abdominal cavity opened sufficiently to visualize the tumor. Recovery from this surgery is straightforward. In some cases, abdominal opening is unnecessary as the intraperitoneal tumors can be visualized through intact skin. Tumors were visible in the abdominal cavity and angiogenesis was apparent as identified by the rhodamine fluorescence. Similar results were found in tumors growing in the omentum in the wall of the small intestine, and in the mesentery.

In an analogous experiment, a suspension containing 1×10^7 cells of clone-26, described in Example 1, were injected into the peritoneal cavity of a mouse. After one day, tumors appeared in the mesentery and in the colon wall. These were observed by anesthetizing the mouse and a minimal opening of the abdomen. Observations on day 3 of a similarly treated mouse showed tumors in the wall of the small intestine and in the omentum as well as in the colon wall and mesentery. On day 5, a similarly treated mouse was injected in the tail with $100 \mu\text{l}$ of 2×10^3 M rhodamine and a few vessels could be seen in the tumor growing in the mesentery. After day 60, numerous vessels were seen in the tumor growing in the colon wall.

EXAMPLE 8

Construction of Metastatic Models

Using the labeled human cancer cell lines described in Example 5, murine models are established for various types of cancer. The cell lines are implanted into 6-week-old nu/nu female mice with a single dose of 10^7 GFP expressing human tumor cells which had been harvested by trypsinization and washed three times with cold, serum-containing medium and then kept on ice. The cells are injected in subcutaneous space in the flank of the animal at a total volume of 0.4 ml within 40 min of harvesting. The nude mice are sacrificed to harvest the tumor fragments 3 weeks after tumor cell injection. These tumor fragments are then used for surgical implantation into the corresponding tissue (surgical orthotopic implantation (SOI)) in nude mice as recipients.

The recipient mice are first anesthetized and then implanted using established SOI techniques with fragments of the subcutaneously grown colon cancer, lung cancer, breast cancer, prostate cancer or melanoma. In all cases, except for melanoma, the size of the fragment is 1 mm^3 ; for melanoma, 0.025 mm^3 fragments are prepared from the human melanoma LOX-GFP subcutaneous tumor and 5-6 fragments are implanted. The progress of metastasis is then observed using FOTI with a Leica Stereomicroscope MZ12 with a mercury lamp source. GFP is excited with a D425/60 bandpass filter and a 470DCXR dichroic mirror; fluorescence is emitted through a GG475 longpass filter (Chroma

13

Technology, Brattle-boro, Vt.) and collected by a thermoelectrically cooled ST-133 Micromass High-Speed Controlled Camera—TEA/CCD-1317K1 (Princeton Instruments, Trenton, N.J.) with a 17x1035 pixels chip. The images are processed and analyzed with ImagePro+3.1 Software (Media Cybernetics, Silver Spring, Md.). High resolution images are captured by computer, or continuously through video output onto video tape.

In the colon cancer model, a small midline incision is made in the abdomen and the colorectal part of the intestine is exteriorized. The serosa is removed and 8–15 pieces of tumor fragments are implanted. An 8–0 surgical suture is used to penetrate the small tumor pieces and suture them to the wall of the intestine. The intestine is returned to the abdominal cavity and abdominal wall is closed. The animals are then observed for metastases.

For lung cancer models, a small 1 cm transverse incision is made on the left lateral chest via the fourth intercostal space; total lung collapse results. Five tumor pieces sewn together with 8–0 nylon surgical suture are fixed by making one knot; the lung is taken out by forceps and the tumor sewn into the lower part of the lung with one suture. After returning the lung to the chest cavity, the chest muscles and skin are closed. The lung is reinflated by withdrawing air from the chest cavity with a 23-gauge needle. The animals can then be observed for metastasis either by FOTI or by excising various tissues.

For breast cancer, an incision of 1.5 cm is made along the medial side of the nipple and after blunt dissection, the fat pad is exposed. A small incision is made and a small pocket formed to accommodate 2 fragments of the tumor tissue; an 8–0 suture is made to close the pocket. The skin layer is then closed. The animals are then observed by FOTI or by tissue excision.

For prostate cancer, an opening is made above the pubic symphysis to expose the prostate gland. The fascia surrounding the dorsal portion of the prostate and the dorsal lateral lobes of the gland are separated by a small incision. Five randomized fragments are sutured into the incision using a 8–0 nylon suture. The two parts of the separated lobes are sutured together and the surrounding fascia used to wrap this portion of the gland to consolidate the incision. The abdomen is then closed and the animals maintained for observation.

For melanoma, 5–6 fragments are transplanted subdermally into the flank with a 13x¼ cancer implant needle (Popper & Sons, New Hyde Park, N.Y.).

Images can be obtained as described above showing metastases to various locations in the animal.

The animals treated as described above, can then be used to evaluate potential protocols for treatment of cancer and metastasis inhibition. The metastatic progress of the fluorescent tumors in animals administered the protocols is compared to similar animals lacking treatment. The efficacy of the protocols can then be directly observed.

What is claimed is:

1. A method to evaluate a candidate protocol or drug for the inhibition of metastasis of a primary tumor which method comprises:

administering said protocol or drug to a subject which is a mouse, rat or rabbit which contains a primary tumor that stably expresses green fluorescent protein (GFP) in cells of said tumor when said tumor metastasizes and monitoring the progression of metastasis by observing the presence, absence or intensity of the fluorescence at various locations in the treated subject;

14

wherein said subject contains said tumor that expresses GFP and wherein said subject is a genetically immunocompromised mouse, rat or rabbit, or a mouse, rat or rabbit which is syngeneic to said tumor;

monitoring the progression of metastasis in a control, which contains a similar tumor that expresses green fluorescent protein;

wherein said control subject contains said tumor that expresses GFP wherein said control subject is an immunocompromised mouse, rat or rabbit, or a mouse, rat or rabbit which is syngeneic to said tumor; and

comparing the progression of metastasis in said treated subject with the progression of metastasis in said control subject wherein the control subject and treated subject are intact;

whereby a diminution of the progression of metastasis in said treated subject as compared to said control subject identifies the protocol or drug as effective in inhibiting metastasis.

2. The method of claim 1 wherein the progression of metastasis is monitored by fluorescent optical tumor imaging in the intact subject.

3. The method of claim 1 wherein said subject contains said tumor by virtue of surgical orthotopic implantation of said tumor.

4. The method of claim 1 wherein said subject contains said tumor by virtue of injecting cells of a stably transformed tumor cell line which has been transfected with an expression vector containing a first nucleotide sequence encoding green fluorescent protein (GFP) and a second nucleotide sequence encoding a selection marker, both said first and second nucleotide sequences being under control of a viral promoter and wherein said cell line stably effects high level expression of said GFP in the absence of selection agent and maintains a high level expression of GFP when said cell line proliferates through multiple passages of said cell line.

5. A method to monitor metastasis of a primary tumor in a subject which is a mouse, rat or rabbit which contains said primary tumor, and wherein said tumor stably expresses green fluorescent protein (GFP) in cells of said tumor when said tumor metastasizes,

wherein said subject contains said tumor that expresses GFP and wherein said subject is a genetically immunocompromised mouse, rat or rabbit, or a mouse, rat or rabbit which is syngeneic to said tumor;

which method comprises monitoring the progression of metastasis by observing the presence, absence or intensity of the fluorescence as a function of time at various locations in said subject wherein the subject is intact.

6. The method of claim 5 wherein the progression of metastasis is monitored by fluorescent optical tumor imaging in the intact subject.

7. The method of claim 5 wherein said subject contains said tumor by virtue of surgical orthotopic implantation of said tumor.

8. The method of claim 5 wherein said subject contains said tumor by virtue of injecting cells of a stably transformed tumor cell line which has been transfected with an expression vector in containing a first nucleotide sequence encoding green fluorescent protein (GFP) and a second nucleotide sequence encoding a selection marker, both said first and second nucleotide sequences being under control of a viral promoter and wherein said cell line stably effects high level expression of said GFP in the absence of selection agent and maintains a high level expression of GFP when said cell line proliferates through multiple passages of said cell line.

Exhibit 1
11

15

9. A method to monitor metastasis of a primary tumor in a mammalian subject which contains said primary tumor, and wherein said tumor stably expresses green fluorescent protein (GFP) in cells of said tumor when said tumor metastasizes,

wherein said primary tumor is endogenous to said mammalian subject and expresses said GFP as a result of locally administering a retroviral vector to said subject in the vicinity of said tumor, said retroviral vector containing an expression system for said GFP;

which method comprises monitoring the progression of metastasis by observing the presence, absence or inten-

16

sity of the fluorescence as a function of time at various locations in said subject.

10. The method of claim 9 wherein the subject is human.

11. The method of claim 9 wherein the progression of metastasis is monitored by excising fresh organ tissues from various locations in said subject.

12. The method of claim 11 wherein said excised tissues are observed by microscopic examination of fresh tissue slices.

* * * * *

Exhibit 1
12

EXHIBIT 2

Exhibit 2
13

EXHIBIT 2



US006649159B2

(12) **United States Patent**
Yang et al.

(10) **Patent No.:** **US 6,649,159 B2**
(45) **Date of Patent:** **Nov. 18, 2003**

(54) **WHOLE-BODY OPTICAL IMAGING OF GENE EXPRESSION AND USES THEREOF**

(75) Inventors: **Meng Yang**, San Diego, CA (US);
Eugene Baranov, San Diego, CA (US)

(73) Assignee: **AntiCancer, Inc.**, San Diego, CA (US)

(*) Notice: Subject to any disclaimer, the term of this patent is extended or adjusted under 35 U.S.C. 154(b) by 0 days.

(21) Appl. No.: **09/812,710**

(22) Filed: **Mar. 19, 2001**

(65) **Prior Publication Data**

US 2002/0013954 A1 Jan. 31, 2002

Related U.S. Application Data

(60) Provisional application No. 60/190,196, filed on Mar. 17, 2000.

(51) Int. Cl.⁷ **A61K 48/00**; **A61K 49/00**;
A01N 63/00; **C12N 15/63**; **C12N 15/85**

(52) U.S. Cl. **424/93.21**; **424/93.1**; **424/93.2**;
424/9.1; **435/320.1**; **435/325**

(58) Field of Search **800/8**; **435/320.1**,
435/325; **536/24.5**; **424/93.1**

(56) **References Cited**

U.S. PATENT DOCUMENTS

5,650,135 A 7/1997 Contag et al. 424/9.1
5,876,711 A 3/1999 Fattaey 424/932
6,020,192 A 2/2000 Muzyczka et al. 435/320.1

OTHER PUBLICATIONS

Yang et al., Whole-body optical imaging of green fluorescent protein-expressing tumors and metastases, 2000, PNAS, vol. 97, pp. 1206-1211.*

Edinger et al., Noninvasive assessment of tumor cell proliferation in animal models, 1999, NEOPLASIA, vol. 1, pp. 303-310.*

Zhang et al., An enhanced green fluorescent protein allows sensitive detection of gene transfer in mammalian cells, 1996, Biochemical and Biophysical Communications, vol. 227, pp. 707-711.*

Yang, M. et al. "Whole-Body Optical Imaging of Green Fluorescent Protein-Expressing Tumors and Metastases" PNAS 97(3): 1206-1211 (2000).

Yang, M. et al. "Visualizing Gene Expression by Whole-Body Fluorescence Imaging" PNAS 97(22):12278-12282 (2000).

Benard et al., J. Nucl. Med. (1999) 40(8):1257-1263.

Brenner et al., Eur. J. Nucl. Med. (1999) 26(12):1567-1571.

Engelson et al., Am. J. Clin. Nutr. (1999) 69(9):1162-1169.

Eustace et al., Magn. Reson. Imaging Clin. (N. Am.) (1999) 7(2):209-236.

Jerusalem et al., Blood (1999) 94(2):429-433.

Saunders et al., Ann. Thorac. Surg. (1999) 67(3):790-797.

Valk et al., Arch. Surg. (1999) 134(5):503-511.

Yang et al., Proc. Natl. Acad. Sci. USA (2000) 97(3):1206-1211.

* cited by examiner

Primary Examiner—Anne-Marie Falk

Assistant Examiner—Celine Qian

(74) *Attorney, Agent, or Firm*—Morrison & Foerster LLP

(57) **ABSTRACT**

The invention relates to the whole-body external optical imaging of gene expression. Specifically, methods for whole-body external optical imaging of gene expression and methods for evaluating a candidate protocol or drug for treating diseases or disorders using a fluorophore operatively linked to the promoter of a gene and external optical imaging are provided herein. Methods to screen for substances or genes that regulate target promoters are also provided.

13 Claims, 2 Drawing Sheets

Exhibit 2
14

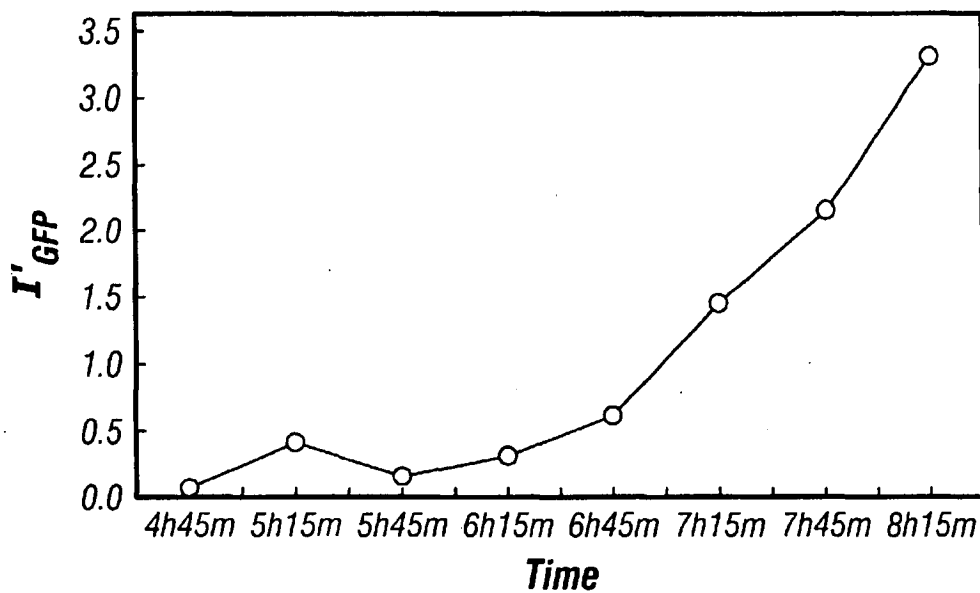


FIG. 1A

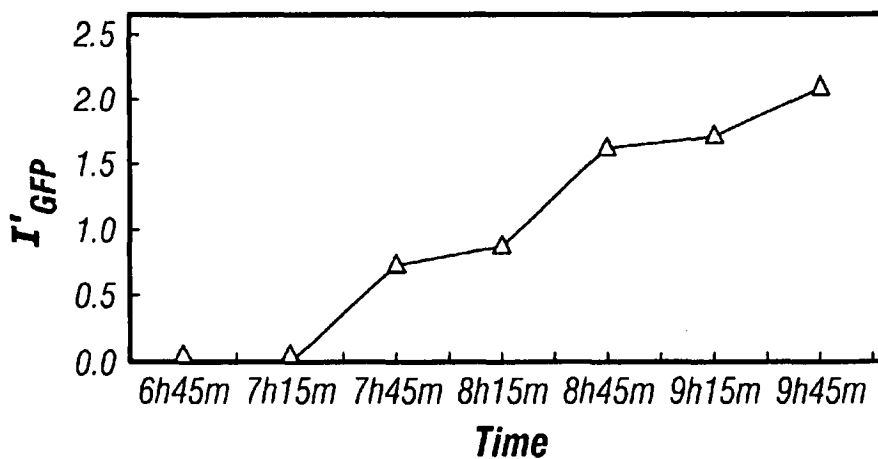
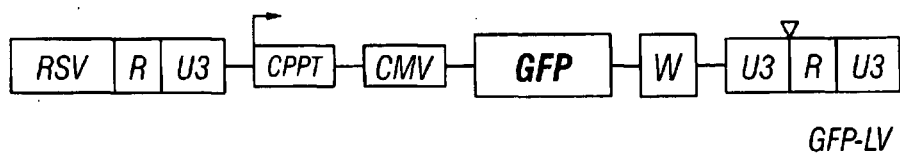
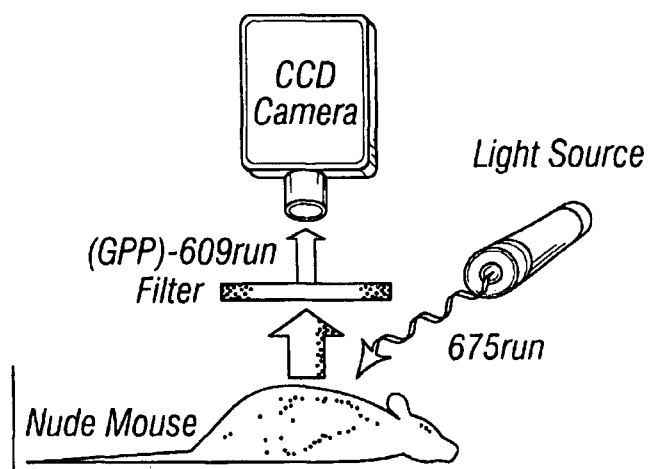


FIG. 1B

Exhibit 2
15

**FIG. 2A****FIG. 2B****Exhibit 2****16**

1

WHOLE-BODY OPTICAL IMAGING OF GENE EXPRESSION AND USES THEREOF

This application claims priority under 35 U.S.C. 119 from provisional application U.S. Ser. No. 60/190,196 filed Mar. 17, 2000, the contents of which are incorporated herein by reference.

TECHNICAL FIELD

The invention relates to the whole-body external optical imaging of gene expression. Specifically, methods for whole-body external optical imaging of gene expression and methods for evaluating a candidate protocol or drug for treating diseases or disorders using a fluorophore operatively linked to the promoter of a gene and external optical imaging are provided herein. Methods to screen for substances or genes that regulate target promoters are also provided.

BACKGROUND ART

Whole-body imaging technology has been used to monitor "tracer molecules" in the intact body. For example, Brenner et al. studied the diagnostic value of iodine-123-2-hydroxy-3-iodo-6-methoxy-N-[(1-ethyl-2-pyrrolidinyl)methyl] benzamide (IBZM) whole-body imaging in comparison to thallium-201 scintigraphy in patients with metastatic malignant melanoma (Brenner et al., *Eur. J. Nucl. Med.*, 26(12):1567-71 (1999)). Benard et al. conducted clinical evaluation of processing techniques for attenuation correction with ¹³⁷Cs in whole-body PET imaging (Benard et al., *J. Nucl. Med.*, 40(8):1257-63 (1999)). Jerusalem et al. showed that whole-body positron emission tomography using ¹⁸F-fluorodeoxyglucose for posttreatment evaluation in Hodgkin's disease and non-Hodgkin's lymphoma has higher diagnostic and prognostic value than classical computed tomography scan imaging (Jerusalem et al., *Blood*, 94(2):429-33 (1999)). Eustace et al. discussed practical issues, clinical applications, and future directions of whole-body MR imaging (Eustace et al., *Magn. Reson. Imaging Clin. (N. Am)*, 7(2):209-36 (1999)). Engelson et al. studied fat distribution in HIV-infected patients reporting truncal enlargement quantified by whole-body magnetic resonance imaging (Engelson et al., *Am. J. Clin. Nutr.*, 69(6):1162-9 (1999)). Valk et al. used whole-body positron emission tomography (PET) imaging with [¹⁸F]fluorodeoxyglucose in management of recurrent colorectal cancer (Valk et al., *Arch. Surg.*, 134(5):503-11 (1999)). Saunders et al. evaluated fluorine-18-fluorodeoxyglucose whole body positron emission tomography imaging in the staging of lung cancer (Saunders et al., *Ann. Thorac. Surg.*, 67(3):790-7 (1999)).

U.S. Pat. No. 5,650,135 discloses a noninvasive method for detecting the localization of an entity under study from within a mammalian subject, which method comprises: (a) administering to the subject a conjugate of the entity and a light-generating moiety or a transformed cell expressing the light-generating moiety; (b) after a period of time in which the conjugate or transformed cell can achieve localization in the subject, immobilizing the subject within the detection field of a photodetector device; (c) maintaining the subject in an immobilized condition, (d) during said maintaining, measuring photon emission from the light-generating moiety, localized in the subject, with the photodetector device until an image of photon emission can be constructed; and (e) detecting said image through an opaque tissue of said mammal. U.S. Pat. No. 5,650,135 also discloses a noninvasive method for detecting the level of an entity under study in a mammalian subject over time, which

2

method comprises: (a) administering to the subject a conjugate of the entity and a light-generating moiety or a transformed cell expressing the light-generating moiety; (b) placing the subject within the detection field of a photodetector device; (c) maintaining the subject in the detection field of the device; (d) during said maintaining, measuring photon emission from the light-generating moiety, in the subject, with the photodetector device; and (e) repeating steps (b) through (d) at selected intervals, wherein said repeating is effective to detect changes in the level of the entity in the subject over time.

Recently, Yang et al. conducted whole-body optical imaging of green fluorescent protein-expressing tumors and metastases (Yang et al., *Proc. Natl. Acad. Sci. (USA)*, 97(3):1206-11 (2000)). Yang et al. have imaged, in real time, fluorescent tumors growing and metastasizing in live mice. The whole-body optical imaging system is external and noninvasive. It affords unprecedented continuous visual monitoring of malignant growth and spread within intact animals. Yang et al. have established new human and rodent tumors that stably express very high levels of the Aequorea victoria green fluorescent protein (GFP) and transplanted these to appropriate animals. B16F0-GFP mouse melanoma cells were injected into the tail vein or portal vein of 6-week-old C57BL/6 and nude mice. Whole-body optical images showed metastatic lesions in the brain, liver, and bone of B 16F0-GFP that were used for real time, quantitative measurement of tumor growth in each of these organs. The AC3488-GFP human colon cancer was surgically implanted orthotopically into nude mice. Whole-body optical images showed, in real time, growth of the primary colon tumor and its metastatic lesions in the liver and skeleton. Imaging was with either a trans-illuminated epifluorescence microscope or a fluorescence light box and thermoelectrically cooled color charge-coupled device camera. The depth to which metastasis and micrometastasis could be imaged depended on their size. A 60-micrometer diameter tumor was detectable at a depth of 0.5 mm whereas a 1, 800-micrometer tumor could be visualized at 2.2-mm depth. The simple, noninvasive, and highly selective imaging of growing tumors, made possible by strong GFP fluorescence, enables the detailed imaging of tumor growth and metastasis formation. This should facilitate studies of modulators of cancer growth including inhibition by potential chemotherapeutic agents.

Methods for monitoring gene expression are known in the art (see generally, Ausubel et al. (Ed.), *Current Protocols in Molecular Biology*, John Wiley & Sons, Inc.). However, whole-body external optical imaging of gene expression, which offers simple, noninvasive, highly selective, and real-time recording and analysis of gene expression in an intact multi-cellular organisms, e.g., animals, is not available currently. The present invention addresses this and other related needs in the art.

DISCLOSURE OF THE INVENTION

The invention provides for whole-body external optical imaging of gene expression and methods for evaluating a candidate protocol or drug for treating diseases or disorders. The method uses a fluorophore operatively linked to the promoter of a gene and external optical imaging. Methods to screen for substances or genes that regulate target promoters are also provided.

In a specific embodiment, a method to monitor the expression of a gene is provided, which method comprises: a) delivering to a multi-cellular organism a nucleic acid encod-

Exhibit 2
17

3

ing a fluorophore operatively linked to the promoter of a gene whose expression is to be analyzed or delivering a cell containing said nucleic acid; and b) observing the presence, absence or intensity of the fluorescence generated by said fluorophore at various locations in said organism by whole-body external fluorescent optical imaging, whereby the expression of said gene is monitored.

In a preferred embodiment, a nucleic acid encoding a fluorophore operatively linked to the promoter of the gene is delivered directly to the organism. Also preferably, the nucleic acid encoding a fluorophore operatively linked to the promoter of the gene is in a viral vector such as a viral vector derived from adenovirus or a lentivirus.

In another preferred embodiment, a cell containing a nucleic acid encoding a fluorophore operatively linked to the promoter of the gene is delivered to the organism. More preferably, the cell is delivered to the organism via a surgical procedure such as direct implantation by surgical orthotopic implantation (SOI) at a desired site.

In still another preferred embodiment, the fluorophore operatively linked to the promoter of a gene is a humanized fluorophore. Also preferably, the fluorophore is a green fluorescent protein (GFP), a blue fluorescent protein (BFP) or a red fluorescent protein (RFP). More preferably, the GFP is the humanized hGFP-S65T.

In yet another preferred embodiment, the multi-cellular organism to be analyzed is a plant or an animal, including a transgenic animal. More preferably, the animal is a mammal. A human can also be analyzed by the present method.

In yet another preferred embodiment, the gene to be analyzed is expressed in a tissue or organ specific manner. More preferably, the gene is expressed in connective, epithelium, muscle or nerve tissue. Also more preferably, the gene is expressed in an internal animal organ such as brain, lung, liver, spleen, bone marrow, thymus, heart, lymph, blood, bone, cartilage, pancreas, kidney, gall bladder, stomach, intestine, testis, ovary, uterus, rectum, nervous system, gland, internal blood vessels, etc. Yet more preferably, the gene to be analyzed is a tumor or cancer associated gene such as an oncogene or a tumor suppressor gene.

In yet another preferred embodiment, the expression of more than one gene is monitored simultaneously.

In another specific embodiment, a method to evaluate a candidate protocol or drug for treating a disease or disorder is provided, which method comprises: a) administering said protocol or drug to a non-human mammalian subject which expresses a fluorophore under the direction of a promoter of a gene associated with a disease or disorder, and determining the expression of said promoter via observing the presence, absence or intensity of the fluorescence generated by said fluorophore at various locations in said mammalian subject by whole-body external fluorescent optical imaging; b) determining the expression of said promoter, via observing the presence, absence or intensity of the fluorescence generated by said fluorophore at various locations in said mammalian subject by whole-body external fluorescent optical imaging, in a control non-human mammalian subject which expresses said fluorophore under the direction of said promoter of said gene; and c) comparing the expression of said promoter determined in steps a) and b), wherein the expression determined in step a) is different from that in step b) identifies said protocol or drug as effective in treating the disease or disorder.

If overexpression of the gene is associated with the disease or disorder, the expression determined in step a) is

4

lower than that in step b) when said protocol or drug is effective in treating the disease or disorder.

If underexpression of the gene is associated with the disease or disorder, the expression determined in step a) is higher than that in step b) when said protocol or drug is effective in treating the infection.

Preferably, the disease or disorder is a cancer, an immune system disease or disorder, a metabolism disease or disorder, a muscle and bone disease or disorder, a nervous system disease or disorder, a signal disease or disorder, or a transporter disease or disorder.

Preferably, the non-human mammalian subject which expresses a fluorophore under the direction of a promoter of the gene is produced by delivering a nucleic acid encoding the fluorophore operatively linked to the promoter of the gene, or a cell containing the nucleic acid, to the non-human mammalian subject. Alternatively, the non-human mammalian subject used in the screen is a transgenic animal.

The non-human mammalian subject used in the screening is preferably a well established laboratory animal such as a mice, a rabbit or a non-human primate.

The fluorophore used in the screening is preferably a green fluorescent protein (GFP), a blue fluorescent protein (BFP) or a red fluorescent protein (RFP).

More than one candidate protocol or candidate drug is preferably screened for simultaneously.

If the non-human mammalian subject expresses a fluorophore under the direction of a promoter of an infectious organism, the expression determined in step a) is lower than that in step b) when said protocol or drug is effective in treating infection caused by the infectious organism.

The non-human mammalian subject used in the screening is preferably an infectious disease animal model.

The infectious organism screened against is preferably a fungus such as a yeast, a bacterium such as an eubacteria or an archaeobacteria, or a virus such as a Class I virus, a Class II virus, a Class III virus, a Class IV virus, a Class V virus or a Class VI virus.

If the infection is caused by a bacterium, the candidate drug to be screened is preferably an antibiotic.

In still another specific embodiment, a method to screen for a modulator of the expression of a gene in a non-human multi-cellular organism is provided, which method comprises: a) administering a test substance to a non-human multi-cellular organism which expresses a fluorophore under the direction of a promoter of a gene, and determining the expression of said promoter via observing the presence, absence or intensity of the fluorescence generated by said fluorophore at various locations in said multi-cellular organism by whole-body external fluorescent optical imaging; b) determining the expression of said promoter, via observing the presence, absence or intensity of the fluorescence generated by said fluorophore at various locations by whole-body external fluorescent optical imaging, in a control multi-cellular organism which expresses said fluorophore under the direction of said promoter of said gene; and c) comparing the expression of said promoter determined in steps a) and b), wherein the expression determined in step a) is different from that in step b) identifies said test substance as a modulator of said gene expression. Preferably, the promoter is an endogenous promoter of the multi-cellular organism.

In yet another specific embodiment, a method to screen for a non-human multi-cellular organism that expresses a gene at an altered level is provided, which method com-

5

prises: a) administering a mutation-inducing agent or treatment to a non-human multi-cellular organism which expresses a fluorophore under the direction of a promoter of a gene, and determining the expression of said promoter via observing the presence, absence or intensity of the fluorescence generated by said fluorophore at various locations in said multi-cellular organism by whole-body external fluorescent optical imaging; b) determining the expression of said promoter, via observing the presence, absence or intensity of the fluorescence generated by said fluorophore at various locations by whole-body external fluorescent optical imaging in an untreated control multi-cellular organism which expresses said fluorophore under the direction of said promoter of said gene; and c) comparing the expression of said promoter determined in steps a) and b), wherein the expression determined in step a) is different from that in step b) identifies a multi-cellular organism that expresses said gene at the altered level. Preferably, the mutation-inducing agent or treatment causes a mutation in germ-line cells of the multi-cellular organism so that the desired mutation is stably-transferable to offspring of the multi-cellular organism.

BRIEF DESCRIPTION OF THE DRAWINGS

FIGS. 1A and 1B show the time course of expression of adenoviral-administered GFP in brain and liver respectively. Fluorescence first becomes visible in the brain within six (6) hours after local delivery and liver fluorescence became detectable at about seven (7) hours after injection into the tail vein.

FIGS. 2A and 2B are pertinent to administration of lentiviral vectors. FIG. 2A is a diagram of lentiviral vector GFP-LV. FIG. 2B is a diagram of a control observation method; whole body measurement involved use of a light box.

MODES FOR CARRYING OUT THE INVENTION

A. Definitions

Unless defined otherwise, all technical and scientific terms used herein have the same meaning as is commonly understood by one of ordinary skill in the art to which this invention belongs. All patents, applications, published applications and other publications and sequences from GenBank and other data bases referred to herein are incorporated by reference in their entirety.

As used herein, "delivering a nucleic acid to a multi-cellular organism" refers to a process in which the nucleic acid is either administered directly into the body of the multi-cellular organism, or the nucleic acid is administered into a cell first, and then the cell containing the nucleic acid is administered into the body of the multi-cellular organism. After delivery into the organism, the nucleic acid may exist independently from the genome of the host organism or may be integrated into the genome of the host organism. If the nucleic acid is integrated into a germline cell of the host organism, such nucleic acid may be transmitted into the host organism's offspring.

As used herein, "whole-body external fluorescent optical imaging" refers to an imaging process in which the presence, absence or intensity of the fluorescence generated by the fluorophore at various locations in the host organism is monitored, recorded and/or analyzed externally without any procedure, e.g., surgical procedure, to expose and/or to excise the desired observing site from the host organism. To achieve the whole-body external fluorescent optical

6

imaging, it is necessary that the intensity of the fluorescence generated by the fluorophore is sufficiently high so that, even when the fluorescence site is an internal one within the host organism body, the fluorescence signal can be analyzed externally without exposing or excising the site from the host body, or while the animal is not controlled.

As no invasive procedures are required and the intensity of the signal is sufficiently great for direct observation, the animal may remain completely mobile and need not be restrained. The ability to provide a completely non-invasive observation protocol is highly significant. If the animal is traumatized either by, e.g., incision or by physical restraint, e.g., straps or pins, the alteration in metabolism may affect the expression of the genes in organs or tissues.

Since whole-body external fluorescent optical imaging are quick and easily amenable to automation, it can be used for monitoring large number of gene expression simultaneously. In addition, it can be employed in high-throughput screening methods for identifying protocols, substances including candidate drugs, and cis-acting regulators that regulate the expression of a target gene. Using the whole-body external fluorescent optical imaging provided in this application, multiple candidate protocols, substances, drugs, and cis-acting regulators can be screened for, either against a single target gene or against multiple target genes, in either a single animal or in multiple animals, simultaneously.

As used herein, "fluorophore" refers to a protein that is auto-fluorescent such that no other substrates or co-factors are needed for it to fluoresce. Non-limiting examples of such fluorophores include green fluorescent proteins (GFPs), blue fluorescent proteins (BFPs) and red fluorescent protein (RFPs), and functional fragments, derivatives and analogues thereof.

As used herein, "a promoter region or promoter element" refers to a segment of DNA or RNA that controls transcription of the DNA or RNA to which it is operatively linked. The promoter region includes specific sequences that are sufficient for RNA polymerase recognition, binding and transcription initiation. This portion of the promoter region is referred to as the promoter. In addition, the promoter region includes sequences that modulate this recognition, binding and transcription initiation activity of RNA polymerase. These sequences may be cis acting or may be responsive to trans acting factors. Promoters, depending upon the nature of the regulation, may be constitutive or regulated.

As used herein, "operatively linked or operationally associated" refers to the functional relationship of DNA with regulatory and effector sequences of nucleotides, such as promoters, enhancers, transcriptional and translational stop sites, and other signal sequences. For example, operative linkage of DNA to a promoter refers to the physical and functional relationship between the DNA and the promoter such that the transcription of such DNA is initiated from the promoter by an RNA polymerase that specifically recognizes, binds to and transcribes the DNA. In order to optimize expression and/or in vitro transcription, it may be necessary to remove, add or alter 5' untranslated portions of the clones to eliminate extra, potential inappropriate alternative translation initiation (i.e., start) codons or other sequences that may interfere with or reduce expression, either at the level of transcription or translation. Alternatively, consensus ribosome binding sites (see, e.g., Kozak, *J. Biol. Chem.*, 266:19867-19870 (1991)) can be inserted immediately 5' of the start codon and may enhance expression. The desirability of (or need for) such modification may be empirically determined.

Exhibit 2
19

As used herein, "humanized fluorophore" refers to a fluorophore whose codon is modified according to the codon usage pattern in human genome to enhance its expression while substantially maintaining its fluorescent characteristics.

As used herein, "multi-cellular organism" refers to an organism with certain cell numbers, mass, and internal structure so that internal sites of such multi-cellular organism are not externally detectable by non-fluorescent optical imaging without exposing the internal sites. Sufficiently high intensity of internal fluorescence is needed for external fluorescent optical imaging of the internal site.

As used herein, "plant" refers to any of various photosynthetic, eucaryotic multi-cellular organisms of the kingdom Plantae, characteristically producing embryos, containing chloroplasts, having cellulose cell walls and lacking locomotion.

As used herein, "animal" refers to a multi-cellular organism of the kingdom of Animalia, characterized by a capacity for locomotion, nonphotosynthetic metabolism, pronounced response to stimuli, restricted growth and fixed bodily structure. Non-limiting examples of animals include birds such as chickens, vertebrates such fish and mammals such as mice, rats, rabbits, cats, dogs, pigs, cows, ox, sheep, goats, horses, monkeys and other non-human primates.

As used herein, "expressed in a tissue or organ specific manner" refers to a gene expression pattern in which a gene is expressed, either transiently or constitutively, only in certain tissues or organs, but not in other tissues or organs.

As used herein, "tissue" refers to a collection of similar cells and the intracellular substances surrounding them. There are four basic tissues in the body: 1) epithelium; 2) connective tissues, including blood, bone, and cartilage; 3) muscle tissue; and 4) nerve tissue.

As used herein, "organ" refers to any part of the body exercising a specific function, as of respiration, secretion or digestion.

As used herein, "disease or disorder" refers to a pathological condition in an organism resulting from, e.g., infection or genetic defect, and characterized by identifiable symptoms.

As used herein, neoplasm (neoplasia) refers to abnormal new growth, and thus means the same as tumor, which may be benign or malignant. Unlike hyperplasia, neoplastic proliferation persists even in the absence of the original stimulus.

As used herein, cancer refers to a general term for diseases caused by any type of malignant tumor.

As used herein, "oncogene" refers to a mutated and/or overexpressed version of a normal gene of animal cells (the proto-oncogene) that in a dominant fashion can release the cell from normal restraints on growth, and thus alone, or in concert with other changes, convert a cell into a tumor cell. Exemplary oncogenes include, but are not limited to, abl, erbA, erbB, ets, fes (fps), fgr, fms, fos, hst, int1, int2, jun, hit, B-lym, mas, met, mil (raf), mos, myb, myc, N-myc, neu (ErbB2), ral (mil), Ha-ras, Ki-ras, N-ras, rel, ros, sis, src, ski, trk and yes.

As used herein, "tumor suppressor gene" (or anti-oncogene, cancer susceptibility gene) refers to a gene that encodes a product which normally negatively regulates the cell cycle, and which must be mutated or otherwise inactivated before a cell can proceed to rapid division. Exemplary tumor suppressor genes include, but are not limited to, p16, p21, p53, RB (retinoblastoma), WT-1 (Wiln's tumor), DCC

(deleted in colonic carcinoma), NF-1 (neurofibrosarcoma) and APC (adenomatous polyposis coli).

As used herein, "an immune system disease or disorder" refers to a pathological condition caused by a defect in the immune system. The immune system is a complex and highly developed system, yet its mission is simple: to seek and kill invaders. If a person is born with a severely defective immune system, death from infection by a virus, bacterium, fungus or parasite will occur. In severe combined immunodeficiency, lack of an enzyme means that toxic waste builds up inside immune system cells, killing them and thus devastating the immune system. A lack of immune system cells is also the basis for DiGeorge syndrome: improper development of the thymus gland means that T cell production is diminished. Most other immune disorders result from either an excessive immune response or an 'autoimmune attack'. For example, asthma, familial Mediterranean fever and Crohn disease (inflammatory bowel disease) all result from an over-reaction of the immune system, while autoimmune polyglandular syndrome and some facets of diabetes are due to the immune system attacking 'self' cells and molecules. A key part of the immune system's role is to differentiate between invaders and the body's own cells—when it fails to make this distinction, a reaction against 'self' cells and molecules causes autoimmune disease.

As used herein, "a metabolism disease or disorder" refers to a pathological condition caused by errors in metabolic processes. Metabolism is the means by which the body derives energy and synthesizes the other molecules it needs from the fats, carbohydrates and proteins we eat as food, by enzymatic reactions helped by minerals and vitamins. There is a significant level of tolerance of errors in the system: often, a mutation in one enzyme does not mean that the individual will suffer from a disease. A number of different enzymes may compete to modify the same molecule, and there may be more than one way to achieve the same end result for a variety of metabolic intermediates. Disease will only occur if a critical enzyme is disabled, or if a control mechanism for a metabolic pathway is affected.

As used herein, "a muscle and bone disease or disorder" refers to a pathological condition caused by defects in genes important for the formation and function of muscles, and connective tissues. Connective tissue is used herein as a broad term that includes bones, cartilage and tendons. For example, defects in fibrillin—a connective tissue protein that is important in making the tissue strong yet flexible—cause Marfan syndrome, while diastrophic dysplasia is caused by a defect in a sulfate transporter found in cartilage. Two diseases that originate through a defect in the muscle cells themselves are Duchenne muscular dystrophy (DMD) and myotonic dystrophy (DM). DM is another 'dynamic mutation' disease, similar to Huntington disease, that involves the expansion of a nucleotide repeat, this time in a muscle protein kinase gene. DMD involves a defect in the cytoskeletal protein, dystrophin, which is important for maintaining cell structure.

As used herein, "a nervous system disease or disorder" refers to a pathological condition caused by defects in the nervous system including the central nervous system, i.e., brain, and the peripheral nervous system. The brain and nervous system form an intricate network of electrical signals that are responsible for coordinating muscles, the senses, speech, memories, thought and emotion. Several diseases that directly affect the nervous system have a genetic component: some are due to a mutation in a single gene, others are proving to have a more complex mode of

inheritance. As our understanding of the pathogenesis of neurodegenerative disorders deepens, common themes begin to emerge: Alzheimer brain plaques and the inclusion bodies found in Parkinson disease contain at least one common component, while Huntington disease, fragile X syndrome and spinocerebellar atrophy are all 'dynamic mutation' diseases in which there is an expansion of a DNA repeat sequence. Apoptosis is emerging as one of the molecular mechanisms invoked in several neurodegenerative diseases, as are other, specific, intracellular signaling events. The biosynthesis of myelin and the regulation of cholesterol traffic also figure in Charcot-Marie-Tooth and Neimann-Pick disease, respectively.

As used herein, "a signal disease or disorder" refers to a pathological condition caused by defects in the signal transduction process. Signal transduction within and between cells mean that they can communicate important information and act upon it. Hormones released from their site of synthesis carry a message to their target site, as in the case of leptin, which is released from adipose tissue (fat cells) and transported via the blood to the brain. Here, the leptin signals that enough has been eaten. Leptin binds to a receptor on the surface of hypothalamus cells, triggering subsequent intracellular signaling networks. Intracellular signaling defects account for several diseases, including cancers, ataxia telangiectasia and Cockayne syndrome. Faulty DNA repair mechanisms are also invoked in pathogenesis, since control of cell division, DNA synthesis and DNA repair all are inextricably linked. The end-result of many cell signals is to alter the expression of genes (transcription) by acting on DNA-binding proteins. Some diseases are the result of a lack of or a mutation in these proteins, which stop them from binding DNA in the normal way. Since signaling networks impinge on so many aspects of normal function, it is not surprising that so many diseases have at least some basis in a signaling defect.

As used herein, "a transporter disease or disorder" refers to a pathological condition caused by defects in a transporter, channel or pump. Transporters, channels or pumps that reside in cell membranes are key to maintaining the right balance of ions in cells, and are vital for transmitting signals from nerves to tissues. The consequences of defects in ion channels and transporters are diverse, depending on where they are located and what their cargo is. For example, in the heart, defects in potassium channels do not allow proper transmission of electrical impulses, resulting in the arrhythmia seen in long QT syndrome. In the lungs, failure of a sodium and chloride transporter found in epithelial cells leads to the congestion of cystic fibrosis, while one of the most common inherited forms of deafness, Pendred syndrome, looks to be associated with a defect in a sulphate transporter.

As used herein, "infection" refers to invasion of the body of a multi-cellular organism with organisms that have the potential to cause disease.

As used herein, "infectious organism" refers to an organism that is capable to cause infection of a multi-cellular organism. Most infectious organisms are microorganisms such as viruses, bacteria and fungi.

As used herein, "bacteria" refers to small prokaryotic organisms (linear dimensions of around 1 μ m) with non-compartmentalized circular DNA and ribosomes of about 70S. Bacteria protein synthesis differs from that of eukaryotes. Many anti-bacterial antibiotics interfere with bacteria proteins synthesis but do not affect the infected host.

As used herein, "eubacteria" refers to a major subdivision of the bacteria except the archaeobacteria. Most Gram-

positive bacteria, cyanobacteria, mycoplasmas, enterobacteria, pseudomonas and chloroplasts are eubacteria. The cytoplasmic membrane of eubacteria contains ester-linked lipids; there is peptidoglycan in the cell wall (if present); and no introns have been discovered in eubacteria.

As used herein, "archaeobacteria" refers to a major subdivision of the bacteria except the eubacteria. There are 3 main orders of archaeobacteria: extreme halophiles, methanogens and sulphur-dependent extreme thermophiles. Archaeobacteria differs from eubacteria in ribosomal structure, the possession (in some case) of introns, and other features including membrane composition.

As used herein, "virus" refers to obligate intracellular parasites of living but non-cellular nature, consisting of DNA or RNA and a protein coat. Viruses range in diameter from about 20 to about 300 nm. Class I viruses (Baltimore classification) have a double-stranded DNA as their genome; Class II viruses have a single-stranded DNA as their genome; Class III viruses have a double-stranded RNA as their genome; Class IV viruses have a positive single-stranded RNA as their genome, the genome itself acting as mRNA; Class V viruses have a negative single-stranded RNA as their genome used as a template for mRNA synthesis; and Class VI viruses have a positive single-stranded RNA genome but with a DNA intermediate not only in replication but also in mRNA synthesis. The majority of viruses are recognized by the diseases they cause in plants, animals and prokaryotes. Viruses of prokaryotes are known as bacteriophages.

As used herein, "fungi" refers to a division of eucaryotic organisms that grow in irregular masses, without roots, stems, or leaves, and are devoid of chlorophyll or other pigments capable of photosynthesis. Each organism (thallus) is unicellular to filamentous, and possess branched somatic structures (hyphae) surrounded by cell walls containing glucan or chitin or both, and containing true nuclei.

As used herein, "antibiotic" refers to a substance either derived from a mold or bacterium or organically synthesized, that inhibits the growth of certain microorganisms without substantially harming the host of the microorganisms to be killed or inhibited.

As used herein, "test substance" refers to a chemically defined compound (e.g., organic molecules, inorganic molecules, organic/inorganic molecules, proteins, peptides, nucleic acids, oligonucleotides, lipids, polysaccharides, saccharides, or hybrids among these molecules such as glycoproteins, etc.) or mixtures of compounds (e.g., a library of test compounds, natural extracts or culture supernatants, etc.) whose effect on the promoter to be analyzed is determined by the disclosed and/or claimed methods herein.

For clarity of disclosure, and not by way of limitation, the detailed description of the invention is divided into the subsections that follow.

B. Methods of Whole-Body External Optical Imaging of Gene Expression

In a specific embodiment, a method to monitor the expression of a gene is provided herein, which method comprises: a) delivering to a multi-cellular organism a nucleic acid encoding a fluorophore operatively linked to the promoter of a gene whose expression is to be analyzed or a cell containing said nucleic acid; and b) observing the presence, absence or intensity of the fluorescence generated by said fluorophore at various locations in said organism by whole-body external fluorescent optical imaging, whereby the expression of said gene is monitored.

The present methods can be used to monitor gene expression for any suitable purposes including prognostic, diag-

nostic and screening purposes. For example, if abnormal gene expression is associated with a disease or disorder in a multi-cellular organism such as a plant or an animal, the present method can be used in prognosis or diagnosis by monitoring the abnormal gene expression. The present monitoring methods are advantageous over the currently available gene expression monitoring methods in several aspects. First, the present monitoring methods can avoid any invasive procedures and this is particularly advantageous for human clinical uses. Second, the present monitoring methods offer in vivo, real-time and continuous monitor and analysis of gene expression in plants or animals, which cannot be accomplished using the currently available monitoring methods. Third, the present monitoring methods are quick and easily amenable to automation, which are important for monitoring large number of gene expression simultaneously. Since many diseases or disorders involve abnormal gene expression of more than gene, the present monitoring methods are particularly suitable for the prognosis and diagnosis of these diseases or disorders. Besides prognosis or diagnosis, if expression of certain genes is a good indicator of tissue or organ health or functionality, the present monitoring methods can also be used in monitoring the health or functionality of these tissues or organs without any invasive procedures.

1. Methods for Delivering the Nucleic Acids into the Multi-Cellular Organism

The nucleic acids encoding a fluorophore operatively linked to the promoter of a gene whose expression is to be analyzed can be a DNA or a RNA. Such nucleic acids can be delivered into the body of the multi-cellular organism by any methods known in the art.

For example, if the host multi-cellular organism is an animal, the DNA or RNA sequence can be delivered to the interstitial space of tissues of the animal body, including those of muscle, skin, brain, lung, liver, spleen, bone marrow, thymus, heart, lymph, blood, bone, cartilage, pancreas, kidney, gall bladder, stomach, intestine, testis, ovary, uterus, rectum, nervous system, eye, gland, and connective tissue. Interstitial space of the tissues comprises the intercellular, fluid, mucopolysaccharide matrix among the reticular fibers or organ tissues, elastic fibers in the walls of vessels or chambers, collagen fibers of fibrous tissues, or that same matrix within connective tissue ensheathing muscle cells or in the lacunae of bone. It is similarly the space occupied by the plasma of the circulation of the lymph fluid of the lymphatic channels.

The DNA or RNA sequence can be conveniently delivered by injection into the tissues comprising these cells. They are preferably delivered to and expressed in persistent, non-dividing cells which are differentiated, although delivery and expression can be achieved in non-differentiated or less completely differentiated cells, such as, for example, stem cells of blood or skin fibroblasts.

In a specific embodiment, the DNA or RNA sequence is delivered directly to a tissue of the host animal. Preferably, the DNA or RNA sequence is delivered directly to muscle, skin or mucous membrane. Delivery to the interstitial space of muscle tissue is preferred because muscle cells are particularly competent in their ability to take up and express polynucleotides.

The DNA or RNA sequence can be delivered directly to a tissue of the host animal by injection, by gene gun technology or by lipid mediated delivery technology. The injection can be conducted via a needle or other injection devices. The gene gun technology is disclosed in U.S. Pat.

No. 5,302,509 and the lipid mediated delivery technology is disclosed in U.S. Pat. No. 5,703,055.

In still another specific embodiment, the DNA or RNA sequence is delivered to a cell of host animal and said cell containing the DNA or RNA sequence is delivered to a suitable tissue of the host animal. Preferably, the DNA or RNA sequence is delivered to tail or portal vein of the host animal.

The DNA or RNA sequence can be delivered to the cells of the host animal by a number of methods (see generally Koprowski & Weiner, DNA vaccination/genetic vaccination, 1998. Springer-verlag Berlin Heidelberg) including $\text{Ca}_3(\text{PO}_4)_2$ -DNA transfection (Sambrook et al., *Molecular Cloning*, 2nd Edition, Plainview, N.Y. Cold Spring Harbor Press, 1989), DEAE dextran-DNA transfection (Sambrook et al., *Molecular Cloning*, 2nd Edition, Plainview, N.Y. Cold Spring Harbor Press, 1989), electroporation (e.g., protocols from Bio-Rad), transfection using "LIPOFECTIN"™ reagent (e.g., protocols from BRL-Life Science), gene gun technology (U.S. Pat. No. 5,302,509), or viral gene delivery system (Kaplit et al., *Viral Vectors*, Academic Press, Inc., 1995).

Gold-particle based gene gun delivery is disclosed in U.S. Pat. No. 5,302,509. In a specific embodiment, Bio-Rad helios gene gun system is used in the DNA delivery. (BIO-RAD Inc. New England). The helios gene gun is a convenient, hand-held device that provides rapid and direct gene transfer in vivo. The device employs an adjustable, helium pulse to sweep DNA coated gold microcarriers from the inner wall of a small plastic cartridge directly into the target cells. The tubing preposition and tubing cutter provide a simple way to prepare 50 cartridge "bullets" at a time.

In a preferred embodiment, a nucleic acid encoding a fluorophore operatively linked to the promoter of the gene is delivered directly to the organism. More preferably, the nucleic acid encoding a fluorophore operatively linked to the promoter of the gene is delivered to the organism, or to a cell to be delivered to the organism, in a viral vector such as a viral vector derived from adenovirus or a lentivirus.

Any viral vectors known in the art can be used. For example, vectors derived from a parvovirus (U.S. Pat. Nos. 5,252,479 and 5,624,820), a paramyxovirus such as simian virus 5 (SV5) (U.S. Pat. No. 5,962,274), a retrovirus such as HIV (U.S. Pat. Nos. 5,753,499 and 5,888,767), and a baculovirus such as a nuclear polyhedrosis virus (U.S. Pat. No. 5,674,747) can be used. Preferably, a vector derived from adenovirus can be used (U.S. Pat. Nos. 5,670,488, 5,817,492, 5,820,868, 5,856,152, 5,981,225).

U.S. Pat. No. 5,670,488 discloses an adenoviral vector comprising an adenovirus genome from which one or more of the E4 open reading frames has been deleted, but retaining sufficient E4 sequences to promote virus replication in vitro, and additionally comprising a DNA sequence of interest operably linked to expression control sequences and inserted into said adenoviral genome.

U.S. Pat. No. 5,817,492 discloses a recombinant adenoviral vector comprising: two DNA sequences which serve as a substrate for a recombinase enzyme, an origin of replication which is operable in an animal cell, a promoter, a foreign gene and a poly(A) sequence, wherein said origin of replication, promoter, foreign gene and poly(A) sequence are located between the two DNA sequences, and wherein said vector contains an E1A gene region deletion.

U.S. Pat. No. 5,820,868 discloses a live recombinant bovine adenovirus vector (BAV) wherein a part or all of the E3 multiple gene coding region is replaced by a heterolo-

13

gous nucleotide sequence encoding a foreign gene or fragment thereof. It also discloses a live recombinant bovine adenovirus vector (BAV) wherein part or all of the E3 multiple gene coding region is replaced by a heterologous nucleotide sequence encoding a foreign gene or fragment thereof and wherein said heterologous nucleotide sequence is optionally under the control of a promoter not normally associated with either said foreign gene or the bovine adenovirus genome.

U.S. Pat. No. 5,856,152 discloses a hybrid viral vector comprising: (a) adenovirus sequences comprising the adenovirus 5' and 3' cis-elements necessary for replication and virion encapsidation; and (b) adeno-associated virus sequences comprising the 5' and 3' ITRs of an adeno-associated virus, said adeno-associated virus sequences flanked by the adenoviral sequences of (a); and (c) a selected gene operatively linked to regulatory sequences which direct its expression in a target cell, said gene and regulatory sequences flanked by the adeno-associated virus sequences of (b).

U.S. Pat. No. 5,981,225 discloses a gene transfer vector consisting essentially of, in 5' to 3' orientation, the following elements: (i) a first adenovirus inverted terminal repeat, (ii) an adenoviral VAI gene and/or VAI gene, (iii) a gene foreign to adenovirus, wherein said gene is operably linked to a promoter functional in adenovirus target cells, and (iv) a second adenovirus inverted terminal repeat, wherein the order of elements (ii) and (iii) may be reversed; and wherein one or both of element (i) and element (iv) additionally comprise an adenovirus packaging signal, and wherein said vector is incapable of producing, in vitro, recombinant adenovirus virus particles which have encapsidated therein said vector unless said vector is co-transfected or co-infected into adenovirus host cells with adenovirus genomic DNA or adenovirus particles containing adenovirus genomic DNA, respectively.

In another preferred embodiment, cells containing a nucleic acid encoding a fluorophore operatively linked to the promoter of the gene are delivered to the organism. More preferably, the cells are delivered to the organism via a surgical procedure such as direct implantation by surgical orthotopic implantation (SOI) at a desired site (see e.g., Chang et al., *Anticancer Res.*, 19(5B):4199 (1999); and An et al., *Prostate*, 34(3):169-74 (1998)).

It will be understood, that by introducing a nucleic acid molecule wherein a promoter is coupled to a nucleotide sequence encoding a fluorescent reporter gene, the introduced nucleic acid molecule can be used as a surrogate for the endogenous promoter. Thus, if the endogenous gene is over-expressed or under-expressed in the context of a particular condition, the behavior of the introduced construct will mimic that of the endogenous promoter. It is not necessary that the reporter-encoding nucleotide sequence be operably linked only to a promoter; the nucleotide sequence encoding reporter may be introduced into the nucleotide sequence encoding the protein normally under control of the promoter or coupled to another protein. Any method of operably linking the nucleotide sequence encoding reporter to the control sequences for the gene whose expression is to be monitored falls within the scope of the invention.

It will be seen that there are a number of ways to introduce this construct. First, the nucleic acid comprising the reporter encoding nucleotide sequence operably linked to the control sequences/promoter of interest can be introduced to the multicellular organism by direct injection, but preferably using a viral vector, such as a adenoviral vector or a antiviral

14

vector. Since the introduced construct is not endogenous, the expression of this construct essentially functions as a surrogate for the endogenous gene. That is, the same influences which influence the endogenous gene will also influence the introduced construct. Thus, the conclusions reached by observing the expression of the construct, including the effects of various treatments on such expression, can be extrapolated to, and are equally valid for, the counterpart endogenous gene.

Second, the reporter encoding nucleotide sequence could be introduced into the cells of a particular tissue by targeting to the promoter to be studied and inserted using position-specific techniques, such as homologous recombination. When this method is used, the expression of the endogenous promoter can be observed directly as well as can the effect of various treatments thereon.

Third, a construct such as those described for the first method can be provided to embryonic tissue to obtain transgenic organisms where the reporter construct is itself endogenous, see, for example, Fukumura, D., et al., *Cell* (1998) 94:715-725, incorporated herein by reference, which describes transgenic mice which use GFP as a reporter for VEGF promoter activity.

Techniques for all three methods are well known in the art.

2. Fluorophores

Any fluorophores known in the art can be used in the present methods. In a preferred embodiment, the fluorophore operatively linked to the promoter of a gene is a humanized fluorophore. Also preferably, the fluorophore is a green fluorescent protein (GFP), a blue fluorescent protein (BFP) and a red fluorescent protein (RFP). More preferably, the GFP is the humanized hGFP-S65T.

The native gene encoding GFP has been cloned from the bioluminescent jellyfish *Aequorea victoria* (Morin et al., *J. Cell Physiol.*, 77:313-318 (1972)). The availability of the gene has made it possible to use GFP as a marker for gene expression. GFP itself is a 283 amino acid protein with a molecular weight of 27 kD. It requires no additional proteins from its native source nor does it require substrates or cofactors available only in its native source in order to fluoresce (Prasher et al., *Gene*, 111:229-233 (1992); Yang et al., *Nature Biotechnol.*, 14:1252-1256 (1996); and Cody et al., *Biochemistry*, 32:1212-1218 (1993)). Mutants of the GFP gene have been found useful to enhance expression and to modify excitation and fluorescence. GFP-S65T (wherein serine at 65 is replaced with threonine) is particularly useful in the invention method and has a single excitation peak at 490 nm. (Heim et al., *Nature*, 373:663-664 (1995)); and U.S. Pat. No. 5,625,048). Other mutants have also been disclosed by Delagrange et al., *Biotechnology*, 13:151-154 (1995); Cormack et al., *Gene*, 173:33-38 (1996); and Cramer et al. *Nature Biotechnol.*, 14:315-319 (1996). Additional mutants are also disclosed in U.S. Pat. No. 5,625,048. By suitable modification, the spectrum of light emitted by the GFP can be altered. Thus, although the term "GFP" is used in the present application, the proteins included within this definition are not necessarily green in appearance. Various forms of GFP exhibit colors other than green and these, too, are included within the definition of "GFP" and are useful in the methods and materials of the invention. In addition, it is noted that green fluorescent proteins falling within the definition of "GFP" herein have been isolated from other organisms, such as the sea pansy, *Renilla reniformis*. Any suitable and convenient form of the GFP gene can be used in the invention. Techniques for labeling cells in general using GFP are disclosed in U.S. Pat. No. 5,491,084 (supra).

Exhibit 2
23

15

Other GFP, BFP and RFP can be used in the present methods. For instances, the green fluorescent proteins encoded by nucleic acids with the following GenBank accession Nos. can be used: U47949 (AGP1); U43284; AF007834 (GFPuv); U89686 (*Saccharomyces cerevisiae* synthetic green fluorescent protein (cox3::GFPm-3) gene); U89685 (*Saccharomyces cerevisiae* synthetic green fluorescent protein (cox3::GFPm) gene); U87974 (Synthetic construct modified green fluorescent protein GFP5-ER (mgfp5-ER)); U87973 (Synthetic construct modified green fluorescent protein GFP5 (mgfp5)); U87625 (Synthetic construct modified green fluorescent protein GFP-ER (mgfp4-ER)); U87624 (Synthetic construct green fluorescent protein (mgfp4) mRNA); U73901 (*Aequorea victoria* mutant 3); U50963 (Synthetic); U70495 (soluble-modified green fluorescent protein (smGFP)); U57609 (enhanced green fluorescent protein gene); U57608 (enhanced green fluorescent protein gene); U57607 (enhanced green fluorescent protein gene); U57606 (enhanced green fluorescent protein gene); U55763 (enhanced green fluorescent protein (egfp)); U55762 (enhanced green fluorescent protein (egfp)); U55761 (enhanced green fluorescent protein (egfp)); U54830 (Synthetic *E. coli* Tn3-derived transposon green fluorescent protein (GF); U36202; U36201; U19282; U19279; U19277; U19276; U19281; U19280; U19278; L29345 (*Aequorea victoria*); M62654 (*Aequorea victoria*); M62653 (*Aequorea victoria*); AAB47853 ((U87625) synthetic construct modified green fluorescent protein (GFP-ER)); AAB47852 ((U87624) synthetic construct green fluorescent protein).

Similarly, the blue fluorescent proteins encoded by nucleic acids with the following GenBank accession Nos. can be used: U70497 (soluble-modified blue fluorescent protein (smBFP)); 1BFP (blue variant of green fluorescent protein); AAB16959 (soluble-modified blue fluorescent protein).

Also similarly, the red fluorescent proteins encoded by nucleic acids with the following GenBank accession Nos. can be used: U70496 (soluble-modified red-shifted green fluorescent protein (smRSGFP); AAB16958 (U70496) soluble-modified red-shifted green fluorescent protein).

A fluorophore that changes color with time is reported by Teiskikh, A., et al., *Science* (2000) 290:1585-1588, incorporated herein by reference. This permits tracing time dependent expression.

3. Multi-Cellular Organisms

The present methods can be used in monitoring gene expression in any suitable multi-cellular organisms. In a preferred embodiment, the multi-cellular organism to be analyzed is a plant or an animal, including a transgenic animal. More preferably, the animal is a mammal including a human. Animals that can be analyzed with the present monitoring methods include, but are not limited to, mice, rats, rabbits, cats, dogs, pigs, cows, ox, sheep, goats, horses, monkeys and other non-human primates.

4. Tissue or Organ Specific Gene Expression

The present methods can be used in monitoring expression of genes that are expressed in a tissue or organ specific manner. The present methods can be used in monitoring health and/or functionality of tissues and/or organs if expression pattern of certain genes are associated with health

16

and/or functionality of these tissues and organs. Preferably, the gene to be monitored is expressed in connective, epithelium, muscle or nerve tissue. Also preferably, the gene to be monitored is expressed in an accessory organ of the eye, annulospiral organ, auditory organ, Chievitz organ, circumventricular organ, Corti organ, critical organ, enamel organ, end organ, external female genital organ, external male genital organ, floating organ, flower-spray organ of Ruffini, genital organ, Golgi tendon organ, gustatory organ, organ of hearing, internal female genital organ, internal male genital organ, intromittent organ, Jacobson organ, neurohemal organ, neurotendinous organ, olfactory organ, otolith organ, otic organ, organ of Rosenmüller, sense organ, organ of smell, spiral organ, subcommissural organ, subforaminal organ, supernumerary organ, tactile organ, target organ, organ of taste, organ of touch, urinary organ, vascular organ of lamina terminalis, vestibular organ, vestibulocochlear organ, vestigial organ, organ of vision, visual organ, vomeronasal organ, wandering organ, Weber organ and organ of Zuckerkandl. More preferably, the gene to be monitored is expressed in an internal animal organ such as brain, lung, liver, spleen, bone marrow, thymus, heart, lymph, blood, bone, cartilage, pancreas, kidney, gall bladder, stomach, intestine, testis, ovary, uterus, rectum, nervous system, gland, internal blood vessels, etc.

In other embodiments, the fluorophore, e.g., GFP, BFP or RFP, can be operatively linked to the following animal transcriptional control regions that exhibit tissue specificity to monitor these tissue specific gene expressions in animals: elastase I gene control region which is active in pancreatic acinar cells (Swift et al., *Cell* 38:639-646 (1984); Ornitz et al., *Cold Spring Harbor Symp. Quant. Biol.* 50:399-409 (1986); MacDonald, *Hepatology* 7:425-515 (1987)); insulin gene control region which is active in pancreatic beta cells (Hanahan et al., *Nature* 315:115-122 (1985)), immunoglobulin gene control region which is active in lymphoid cells (Grosschedl et al., *Cell* 38:647-658 (1984); Adams et al., *Nature* 318:533-538 (1985); Alexander et al., *Mol. Cell Biol.* 7:1436-1444 (1987)), mouse mammary tumor virus control region which is active in testicular, breast, lymphoid and mast cells (Leder et al., *Cell* 45:485-495 (1986)), albumin gene control region which is active in liver (Pinckert et al., *Genes and Devel.* 1:268-276 (1987)), alpha-fetoprotein gene control region which is active in liver (Krumlauf et al., *Mol. Cell Biol.* 5:1639-1648 (1985); Hammer et al., *Science* 235:53-58 (1987)), alpha-1 antitrypsin gene control region which is active in liver (Kelsey et al., *Genes and Devel.* 1:161-171 (1987)), beta globin gene control region which is active in myeloid cells (Mogam et al., *Nature* 315:338-340 (1985); Kollias et al., *Cell* 46:89-94 (1986)), myelin basic protein gene control region which is active in oligodendrocyte cells of the brain (Readhead et al., *Cell* 48:703-712 (1987)), myosin light chain-2 gene control region which is active in skeletal muscle (Sani, *Nature* 314:283-286 (1985)), and gonadotrophic releasing hormone gene control region which is active in gonadotrophs of the hypothalamus (Mason et al., *Science* 234:1372-1378 (1986)).

5. Tumor or Cancer Associated Gene Expression

The present methods can be used in monitoring expression of genes that are specifically expressed in tumors or cancers. Preferably, the gene to be analyzed is a tumor or cancer associated gene such as an oncogene or a tumor suppressor gene. For instance, the expression of the oncogenes listed in the following Table 1 can be monitored by the present methods.

Exhibit 2
24

TABLE 1

<u>Oncogenes and tumor viruses</u>				
Acronym	Virus	Species	Tumor origin	Comments
abl	Abelson leukemia	Mouse	Chronic myelogenous leukemia	TyrPK(src)
erbA	Erythroblastosis	Chicken		Homology to human glucocorticoid receptor
erbB	Erythroblastosis	Chicken		TryPK EGF/TGFC receptor
ets	E26 myeloblastosis	Chicken		Nuclear
fes (fps) ^a	Snyder-Thellen sarcoma	Cat		TryPK(src)
	Gardner-Arnstein sarcoma			
fgr	Gardner-Rasheed sarcoma	Cat		TyrPK(src)
fms	McDonough sarcoma	Cat		TyrPK CSF-1 receptor
fps (fes) ^a	Fujinami sarcoma	Chicken		TyrPK(src)
fos	FBJ osteosarcoma	Mouse		Nuclear, TR
hst	NVT	Human	Stomach tumor	FGF homologue
int1	NVT	Mouse	MMTV-induced carcinoma	Nuclear, TR
int2	NVT	Mouse	MMTV-induced carcinoma	FGF homologue
jun	ASV17 sarcoma	Chicken		Nuclear, TR
hil	Hardy-Zuckerman 4 sarcoma	Cat		TyrPK GFR L
B-lym	NVT	Chicken	Bursal lymphoma	
mas	NVT	Human	Epidermoid carcinoma	Potentiates response to angiotensin II
met	NVT	Mouse	Osteosarcoma	TyrPK GFR L
mil (raf) ^b	Mill Hill 2 acute leukemia	Chicken		Ser/ThrPK
mos	Moloney sarcoma	Mouse		Ser/ThrPK
myb	Myeloblastosis	Chicken	Leukemia	Nuclear, TR
myc	MC29	Chicken	Lymphomas	Nuclear TR
	myelocytomatosis			
N-myc	NVT	Human	Neuroblastomas	Nuclear
neu (ErbB2)	NVT	Rat	Neuroblastoma	TryPK GFR L
ral (mil) ^b	3611 sarcoma	Mouse		Ser/ThrPK
Ha-ras	Harvey murine sarcoma	Rat	Bladder, mammary and skin carcinomas	GTP-binding
Ki-ras	Kirsten murine sarcoma	Rat	Lung, colon carcinomas	GTP-binding
N-ras	NVT	Human	Neuroblastomas leukaemias	GTP-binding
rel	Reticuloendotheliosis	Turkey		
ros	UR2	Chicken		TyrPK GFR L
sis	Simian sarcoma	Monkey		One chain of PDGF
src	Rous sarcoma	Chicken		TyrPK
ski	SKV770	Chicken		Nuclear
trk	NVT	Human	Colon carcinoma	TyrPK GFR L
yes	Y73, Esh sarcoma	Chicken		TyrPK(src)

Exhibit 2

25

Similarly, the expression of the following tumor suppressor genes can be monitored by the present methods: p16, p21, p27, p53, RB, WT-1, DCC, NF-1 and APC.

Since abnormally high level of oncogene expression and abnormally low expression of tumor suppressor gene are often good indicators of oncogenesis, the present methods can be used in prognosis or diagnosis of cancer, in monitoring the development of oncogenesis and in evaluating the efficacy of the cancer therapy.

C. Methods to Evaluate a Candidate Protocol or Drug for Treating Disease or Disorder

Since the method of the invention evaluates gene expression with regard to particular control sequences, the effect of various compounds, treatments (such as irradiation) or other perturbations of the genetic environment can be evaluated for their effect on expression using the methods of the invention. Thus, gene toxic agents, for example, can be identified.

In a specific embodiment, a method to evaluate a candidate protocol or drug for treating a disease or disorder is provide herein, which method comprises: a) administering

said protocol or drug to a non-human mammalian subject which expresses a fluorophore under the direction of a promoter of a gene associated with a disease or disorder, and determining the expression of said promoter via observing the presence, absence or intensity of the fluorescence generated by said fluorophore at various locations in said mammalian subject by whole-body external fluorescent optical imaging; b) determining the expression of said promoter, via observing the presence, absence or intensity of the fluorescence generated by said fluorophore at various locations in said mammalian subject by whole-body external fluorescent optical imaging, in a control non-human mammalian subject which expresses said fluorophore under the direction of said promoter of said gene; and c) comparing the expression of said promoter determined in steps a) and b), wherein the expression determined in step a) is different from that in step b) identifies said protocol or drug as effective in treating the disease or disorder.

In a preferred embodiment, overexpression of the gene is associated with the disease or disorder and the expression determined in step a) is lower than that in step b) identifies said protocol or drug as effective in treating the disease or disorder.

In another preferred embodiment, underexpression of the gene is associated with the disease or disorder and the expression determined in step a) is higher than that in step b) identifies said protocol or drug as effective in treating the infection.

In still another preferred embodiment, the non-human mammalian subject which expresses a fluorophore under the direction of a promoter of a gene associated with a disease or disorder is produced by delivering a nucleic acid encoding the fluorophore operatively linked to the promoter, or a cell containing the nucleic acid, to the non-human mammalian subject (see Section B supra).

Any non-human mammalian subject can be used in the present screening methods. Preferably, the non-human mammalian subject used in the screening is a well established laboratory animal such as a mice, a rabbit or a non-human primate. Also preferably, the non-human mammalian subject used in the screening is an infectious disease animal model. Still preferably, the non-human mammalian subject used in the screen is a transgenic animal.

Any fluorophores known in the art, including the ones described in Section B, can be used in the present screening methods. In a preferred embodiment, the fluorophore used in the screening is a green fluorescent protein (GFP), a blue fluorescent protein (BFP) or a red fluorescent protein (RFP).

The present methods can be used to screen candidate protocols or drugs for treating any known diseases or disorders. In a preferred embodiment, the diseases or disorders to be screened against are cancers, immune system diseases or disorders, metabolism diseases or disorders, muscle and bone diseases or disorders, nervous system diseases or disorders, signal diseases or disorders and transporter diseases or disorders.

In yet another preferred embodiment, the non-human mammalian subject expresses a fluorophore under the direction of a promoter of an infectious organism and the expression determined in step a) is lower than that in step b) identifies said protocol or drug as effective in treating infection caused by the infectious organism.

The non-human mammalian subject used in the screening may be an infectious disease animal model.

The infectious organism screened against may be a fungus such as a yeast, a bacterium such as an eubacteria or an archaeobacteria, or a virus such as a Class I virus, a Class II virus, a Class III virus, a Class IV virus, a Class V virus or a Class VI virus.

Any substances can be screened using the present screening methods for finding drug candidates for treating infection. In a preferred embodiment, a combinatorial library is used in the screening assays. Methods for synthesizing combinatorial libraries and characteristics of such combinatorial libraries are known in the art (See generally, *Combinatorial Libraries: Synthesis, Screening and Application Potential* (Cortese Ed.) Walter de Gruyter, Inc., 1995; Tietze and Lieb, *Curr. Opin. Chem. Biol.*, 2(3):363-71 (1998); Lam, *Anticancer Drug Des.*, 12(3):145-67 (1997); Blaney and Martin, *Curr. Opin. Chem. Biol.*, 1(1):54-9 (1997); and Schultz and Schultz, *Biotechnol. Prog.*, 12(6):729-43 (1996)).

If the infection is caused by bacteria, known antibiotics can be screened using the present screening methods for finding a suitable drug candidate. Preferably, the antibiotics to be screened are aminoglycosides (e.g., streptomycin, gentamicin, sisomicin, tobramycin, amikacin), ansamycins (e.g., rifamycin), antimycotics polyenes (e.g., nystatin, pimaricin, amphotericin B., pecilocin), benzofuran deriva-

tives (e.g., griseofulvin), β -lactam antibiotics penicillins (e.g., penicillin G and its derivatives, oral penicillins, penicillinase-fixed penicillin broad-spectrum penicillins, penicillins active against *Proteus* and *Pseudomonas*), cephalosporins (e.g., cephalothin, cephaloridine, cephalixin, cefazolin, cefotaxime), chloramphenicol group (e.g., chloramphenicol, thiamphenicol, azidamphenicol), imidazole fluconazole, itraconazole, linosamides (e.g., lincomycin, clindamycin), macrolides (e.g., azithromycin, erythromycin, oleandomycin, spiramycin, clarithromycin), peptides, peptolides, polypeptides (e.g., polymyxin B and E, bacitracin, tyrothricin, capreomycin, vancomycin), quinolones (e.g., nalidixic acid, ofloxacin, ciprofloxacin, norfloxacin), tetracyclines (e.g., tetracycline, oxytetracycline, minocycline, doxycycline) and other antibiotics (e.g., phosphomycin, fusidic acid).

D. Methods to Screen for Gene Expression Modulators and Regulators

The above-described screening methods can also be used to identify gene expression modulators, i.e., trans-acting substances that modulate the expression of a target gene in a multi-cellular organism, or regulators, i.e., cis-acting genes of a multi-cellular organism that regulate the expression of the target gene. Besides for identifying disease or disorder treatment protocols or drugs, the screening methods described herein have wide applications in industrial, agricultural, environmental protection and many other fields. For example, transgenic animals such as transgenic cows are commercially used. It is desirable to find a suitable substance that increases the expression of the transgene and such substance can be added to the animal feed. Similarly, it is desirable to find and modify gene(s) within the transgenic cow that enhances the expression of the target transgene.

Once it is decided that alteration of the expression level of a target gene is desirable, a fluorophore can be operatively linked to the promoter, or other transcriptional control region, of the target gene and be expressed in a multi-cellular organism. Then, the multi-cellular organism expressing the fluorophore can be treated with a test substance to identify which substance modulates the fluorophore expression. Alternatively, the multi-cellular organism expressing the fluorophore itself can be mutagenized to identify genes within itself that alter the fluorophore expression. These screening principles have long been used to identify cis- or trans-acting regulators of gene expression in unicellular organisms such as bacteria or yeast. However, due to the lack of quick and simple screening methods, such screening are impractical for multi-cellular organisms such as plants and animals. The whole-body external optical imaging of gene expression disclosed herein makes such screening or mutant-haunt practical for multi-cellular organisms.

In a specific embodiment, a method to screen for a modulator of the expression of a gene in a multi-cellular organism is provided herein, which method comprises: a) administering a test substance to a non-human multi-cellular organism which expresses a fluorophore under the direction of a promoter of a gene, and determining the expression of said promoter via observing the presence, absence or intensity of the fluorescence generated by said fluorophore at various locations in said multi-cellular organism by whole-body external fluorescent optical imaging; b) determining the expression of said promoter, via observing the presence, absence or intensity of the fluorescence generated by said fluorophore at various locations by whole-body external fluorescent optical imaging, in a control multi-cellular organism which expresses said fluorophore under the direc-

21

tion of said promoter of said gene; and c) comparing the expression of said promoter determined in steps a) and b), wherein the expression determined in step a) is different from that in step b) identifies said test substance as a modulator of said gene expression. Preferably, the promoter is an endogenous promoter of the multi-cellular organism.

In another specific embodiment, a method to screen for a multi-cellular organism that expresses a gene at an altered level is provided herein, which method comprises: a) administering a mutation-inducing agent or treatment to a non-human multi-cellular organism which expresses a fluorophore under the direction of a promoter of a gene, and determining the expression of said promoter via observing the presence, absence or intensity of the fluorescence generated by said fluorophore at various locations in said multi-cellular organism by whole-body external fluorescent optical imaging; b) determining the expression of said promoter, via observing the presence, absence or intensity of the fluorescence generated by said fluorophore at various locations by whole-body external fluorescent optical imaging, in an untreated control multi-cellular organism which expresses said fluorophore under the direction of said promoter of said gene; and c) comparing the expression of said promoter determined in steps a) and b), wherein the expression determined in step a) is different from that in step b) identifies a multi-cellular organism that expresses said gene at said altered level. Preferably, the mutation-inducing agent or treatment causes a mutation in germ-line cells of the multi-cellular organism so that the desired mutation is stably-transferable to offspring of the multi-cellular organism.

In addition, the various protocols described in the art for "Big Blue" transgenic mice can be utilized in the system of the invention.

The following examples are included for illustrative purposes only and are not intended to limit the scope of the invention.

EXAMPLE 1

Visualization of Gene Expression in Various Tissues using Adenovirus

Four six-week-old male of female nude/nude, nude/+, or C57BL/6 mice were used. All animal studies were conducted in accordance with the principles and procedures outlined in the National Institute of Health Guide for the Care and Use of Animals under assurance number A3873-1. Mice were fed with autoclaved laboratory rodent diet (Teklad LM-485, Western Research Products, Orange, Calif.).

The vector employed was adenoviral (vAd) vector AdCMV5GFP AE1/AE3 [vAd-green fluorescent protein (GFP)] (Quantum, Montreal, Canada), which expresses enhanced GFP and the ampicillin resistance gene.

This vector was provided to various tissues to visualize expression of the CMV promoter in these tissues. Expression of reporter under control of any desired promoter can be visualized by suitable modification of this vector, as described above.

Liver: After exposure of the portal vein following an upper midline abdominal incision, total volume of 100 μ l (8×10^{10} pfu/ml) vAd-GFP per mouse were injected in the portal vein using a 1 ml 39G1 latex-free syringe (Becton Dickinson, Franklin Lakes, N.J.). The puncture hole of portal vein was pressed for about 10 seconds with sterile cotton to stop any bleeding. The incision in the abdominal

22

wall was closed with a 7-0 surgical suture in one layer. The animals were kept under Ketamine anesthesia during surgery. All procedures of the operation described above were performed with a 7x magnification microscope (Leica MZ6, Nussloch, Germany). Animals were kept in a barrier facility under HEPA filtration.

Brain: The parietal bone of the skull was exposed after an upper midline scalp incision. Twenty microliters containing 8×10^{10} plaque-forming units (pfu)/ml vAd-GFP per mouse was injected in the brain by using a 1-ml 27G1/2 latex-free syringe (Becton Dickinson). The puncture hole in the skull was plugged with bone wax. The incision in the scalp was closed with a 7-0 surgical suture in one layer. The animals were kept under isoflurane anesthesia during surgery.

Pancreas: The pancreas was exposed after an upper midline abdominal incision. One-hundred microliters containing 8×10^{10} pfu/ml vAd-GFP per mouse was injected in the pancreas by using a 1-ml 30G_{1/2} latex-free syringe (Becton Dickinson). The puncture hole was pressed for about 10 sec with sterile cotton for hemostasis. The incision was closed with a 7-0 surgical suture in one layer. The animals were kept under Kersel anesthesia during surgery. All procedures of the operation described above were performed with a $\times 7$ magnification stereo microscope.

Prostate: The bladder and prostate were exposed after a lower midline abdominal incision. Thirty microliters containing 8×10^{10} pfu/ml vAd-GFP per mouse was injected in the prostate by using a 1-ml 30G_{1/2} latex-free syringe (Becton Dickinson). The puncture hole in the prostate was pressed for about 10 sec with sterile cotton for hemostasis. The incision in the abdominal wall was closed with a 6-0 surgical suture in one layer. The animals were kept under isoflurane anesthesia during surgery. All procedures of the operation described above were performed with a $\times 7$ magnification stereo microscope.

Bone Marrow: For bone marrow injection, animals were anesthetized by inhalation of isoflurane. The skin on the hind leg was opened with a 1-cm incision to expose the tibia. A 27-gauge needle with latex-free syringe (Becton Dickinson) then was inserted in the bone marrow cavity. A total volume of 20 μ l (8×10^{10} pfu/ml) vAd-GFP per mouse was injected into the bone marrow cavity. The puncture hole in the bone was plugged with bone wax, and the incision was closed with a 6-0 surgical suture.

Visualization: For visualization at high magnification, Leica fluorescence stereo microscope, model LZ12, equipped with a 50-W mercury lamp, was used. Selective excitation of GFP was produced through a D425/60 band-pass filter and 470 DCXR dichroic mirror. Emitted fluorescence was collected through a long-pass filter GG475 (Chroma Technology, Brattleboro, Vt.) on a Hamamatsu C5810—3-chip cooled color charge-coupled device camera (Hamamatsu Photonics Systems, Bridgewater, N.J.). Images were processed for contrast and brightness and analyzed with the use of IMAGE PRO PLUS 3.1 software (Media Cybernetics, Silver Springs, Md.). Images of 1,024 \times 724 pixels were captured directly on an IBM PC or continuously through video output on a high-resolution Sony VCR model SLV-R-1000 (Sony, Tokyo).

Imaging at lower magnification that visualized the entire animal was carried out in a light box illuminated by blue light fiber optics (Lighttools Research, Encinitas, Calif.) and imaged by using the thermoelectrically cooled color charge-coupled device camera, as described above.

Quantitation: The intensity of GFP fluorescence is measured to account for variations in the exciting illumination

Exhibit 2
27

23

with time and across the imaging area. These factors are corrected for by using the intrinsic red fluorescence of mouse skin as a base line to correct the increase over intrinsic green fluorescence caused by GFP. This can be done because there is relatively little red luminance in the GFP radiance. Consequently, the green fluorescence was calculated relative to red based on red and green channel composition in the skin image. A ratio (γ) of green to red channels was determined for each pixel in the image of skin without and with GFP. Values of γ for mouse skin throughout the image in the absence of GFP were fairly constant, varying between 0.7 and 1.0. The contribution of GFP fluorescence from within the animal increased the green component relative to red, which was reflected in higher γ values. The total amount of GFP fluorescence was approximated by multiplying the number of pixels in which value γ was higher than 1 times the γ value of each pixel. Such a product roughly corresponds to the integral GFP fluorescence [Γ_{GFP}] above the maximum value of γ for skin without GFP. The number of pixels in mouse skin images with γ value >1.0 without GFP was less than 0.02% and increased with GFP expression. The value of [Γ_{GFP}] is shown as a function of time after virus injection in FIGS. 1A and 1B for brain and liver respectively.

Images of the various organs were compared when taken at high magnification on live intact animals or similar organs viewed directly after death and dissection. The images show the distribution of gene expression in the various organs. In all cases, the images made externally are similar to those of the exposed organs.

When the live animal was viewed in a light box, it was also possible to monitor the expression of the gene, thus permitting a real time observation of the living animal and expression as it occurs in this animal. For example, a light box determination of expression of the GFP in nude mouse liver taken at 72 hours clearly shows this result. Similar results are observed in the nude mouse brain 24 hours after gene delivery. The method is quite sensitive in that the intensity of GFP fluorescence in the mouse liver at a depth of 0.8 mm under the skin was about 25% of that of the exposed organ. Gene expression is externally measurable if the average fluorescence of the GFP expressing organs is at least 20% above the average fluorescence of the surrounding skin, and at maximal level of GFP expression, the intensity in the liver exceeded more than 100 times the back dorsal and abdominal skin fluorescence.

EXAMPLE 2

Visualization of Genes Using Lentiviral Vectors

Lentiviral vectors have been shown to transduce a broad spectrum of non-dividing cells in vitro, such as neurons, retina, liver, muscle and hematopoietic stem cells (see, for example, Naldini, L. et al., *Science* (1996) 272:263-267; Kafri T. et al., *Nat. Genet* (1997) 17:314-317; Takahashi, M. et al., *J. Virol* (1999) 73:7812-7816; Miyoshi, H. et al. *Science* (1999) 283:682-686). Although it has been reported that hepatocytes are refractory to lentiviral transduction unless they progress into the cell cycle (Park, F. et al. *Nat. Genet* (2000) 24:49-52), it is shown below that lentiviral gene delivery to the liver for expression visualization is practical.

A lentiviral vector based on HIV1 designated GFP-LV was used. This vector contains a self-inactivating mutation in the U-3 region, a post-transcriptional element, and an internal CMV promoter. It also contains cppt, the central

24

polypurine tract derived from HIV-pol and a woodchuck hepatitis virus post-transcriptional element (WPRE). A diagram of this vector is shown in FIG. 2A.

The vector GHP-LV at 1×10^9 IU was injected into the portal vein of nude mice; (Hsd:asymic nude-nu). Six (6) days after injection green fluorescence was testable in the liver using in-vivo fluorescence optical imaging, as shown in FIG. 2B. At day 21, all lobes of the liver of the mice injected with this vector exhibited a homogeneous green fluorescence.

GHP-LV at 1×10^9 IU was also injected intraperitoneally and this method also resulted in a high level of transduction of liver and spleen.

Western Blot demonstrated dose dependence of GFP expression in the range of 0.5 – 2.5×10^9 IU. Vector integration in the liver 3 weeks after injection was demonstrated by PCR.

Confirmation that the transduced cells were not rapidly dividing was achieved by administering 5' bromo-2' deoxyuridine (BrdU) 15 mgs/kg by daily IP injections in order to label dividing cells. While the cells in the duodenum showed high labelling, only about 3% of liver cells were BrdU positive in either control or lentiviral-treated livers.

EXAMPLE 3

Additional Applications

In addition to the procedures exemplified in Examples 1 and 2, the methods of the invention may be used to monitor expression of control sequences that are regulated by the unfolded protein response (UPR) as described, for example, by Niwa, M., et al., *Cell* (1999) 99:691-702, the contents of which are incorporated herein by reference. Another suitable target for study is the circadian rhythm controlling genes which were studied using less convenient techniques by Yamaguchi, S., et al, *Nature* (2001) 409:684, incorporated herein by reference.

Since modifications will be apparent to those of skill in this art, it is intended that this invention be limited only by the scope of the appended claims.

What is claimed is:

1. A method to monitor the ability of a promoter to promote expression in an animal of an endogenous gene that is controlled by said promoter, which method comprises:

a) delivering, to an animal, cells containing a nucleic acid encoding a fluorophore operatively linked to the promoter of said endogenous gene whose ability to promote expression is to be analyzed; and

b) observing the presence, absence or intensity of the fluorescence generated by said fluorophore at various locations in said animal by whole-body external fluorescent optical imaging,

whereby the ability of said promoter to promote expression is monitored, and

wherein said fluorophore is a protein that is autofluorescent such that no substrates or cofactors are needed for it to fluoresce.

2. The method of claim 1, wherein the cells are delivered to the animal via a surgical procedure.

3. The method of claim 2, wherein the cells are delivered to the animal via direct implantation by surgical orthotopic implantation (SOI) at a desired site.

4. The method of claim 1, wherein the animal is a human and the fluorophore is a humanized fluorophore.

Exhibit 2
28

25

5. The method of claim 1, wherein the fluorophore is selected from the group consisting of a green fluorescent protein (GFP), a blue fluorescent protein (BFP) and a red fluorescent protein (RFP).

6. The method of claim 5, wherein the animal is a human and the GFP is the humanized hGFP-S65T.

7. The method of claim 1, wherein the animal is a mammal.

8. The method of claim 7, wherein the mammal is selected from the group consisting of a mouse, a rat, a rabbit, a cat, a dog, a pig, a cow, an ox, a sheep, a goat, a horse, a monkey and a non-human primate.

9. The method of claim 1, wherein the endogenous gene is normally expressed in a tissue or organ specific manner.

26

10. The method of claim 9, wherein the tissue is selected from the group consisting of connective, epithelium, muscle and nerve tissues.

11. The method of claim 9, wherein the organ is selected from the group consisting of brain, lung, liver, spleen, bone marrow, thymus, heart, lymph, blood, bone, cartilage, pancreas, kidney, gall bladder, stomach, intestine, testis, ovary, uterus, rectum, nervous system, gland, and internal blood vessels.

12. The method of claim 1, wherein the endogenous gene is an endogenous tumor or cancer associated gene.

13. The method of claim 12, wherein the tumor or cancer associated gene is an oncogene or a tumor suppressor gene.

* * * * *

Exhibit 2
29

EXHIBIT 3

Exhibit 3
30

EXHIBIT 3



detect and identify

Search

Bioanalytic

Home

Contact

Products

Applications

News

[Home](#) > [Bioanalytic](#) > [Products](#) > NightOWL

NightOWL II LB 983

In vivo imaging in general allows a non-invasive insight into living organisms and helps to understand metabolic processes and disease related changes. Especially bioluminescence imaging (BLI) and biofluorescence imaging (BFI) enable monitoring of gene expression or disease progression in living organisms due to outstanding sensitivity.

In 1989 Berthold Technologies introduced its first low light imaging instrument – the LB 980 Luminograph. The first in-vivo gene expression experiments in plants and animals performed on this instrument date back to the year 1993.

BLI utilizes light emitted by luciferase enzymes. Today bioluminescence markers can be tailored to any gene, enabling detailed research of gene function. BFI utilizes proteins, which fluoresce under illumination, either applied as exogenous reagents or endogenously expressed. Both BLI and BFI have contributed to the understanding of disease mechanisms and the development of new treatments.

Cameras

Today's generation of low light imagers from Berthold Technologies, the LB 983 NightOWL II, is equipped with cooled slow scan CCD cameras:

- Front-illuminated NC 320
is best suited for fluorescence applications with 3 million pixels for high resolution. Micro-lenticular array on top of CCD chip enhance light collection to maximum quantum efficiency of 85 %
- Back-illuminated NC 100
with high full well capacity for large dynamic range is best suited for luminescence applications. Midband coating enhances the quantum efficiency in the spectral range between 440 to 770 nm (80% QE) ideally to luciferase and GFP emissions. Efficient Peltier cooling keeps chip temperatures low, reducing the dark current and thereby enhancing the signal to noise ratio.

Applications*

Whole animals and plants can be imaged as well as blots, gels, microplates, cell culture dishes and arrays regardless luminescent or fluorescent markers are used. Optical calibration ensures the comparability of all images captured with the NightOWL.

Detection of weak light signals with CCD cameras can be extraordinarily achieved with high quantum efficiency and extremely low noise levels to enable long exposure times. The camera and cabinet design are the key to superior imaging performance, complemented by scientific evaluation software for quantification.

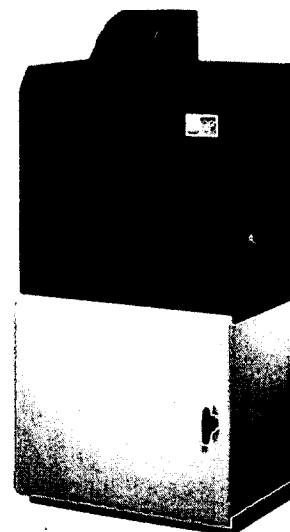
Cabinet

The NightOWL cabinet is extremely light-tight preventing any interferences from ambient light. NightOWL is the first imager with a motor-driven camera inside the cabinet. Positioning is reproducible with +/- 100 µm allowing very precise height correction. Optimum resolution and focus of the sample is achieved by automatic positioning of the camera according to the actual sample size.

The NightOWL cabinet has enough space to install special light sources or to place transilluminators, heaters, coolers etc. These devices may even be switched on and off through the software and the built-in sockets. The flange option provides light-tight access to the inner part for tubings and cables.

Fluorescence excitation unit

The unique optical system from the LB 940 Mithras Multimode Reader has been integrated in the NightOWL II model. The light beam is kept constant for each fluorescent measurement, which is ideal with the ringlight epi illumination. If the ringlight is always set at the same height, the excitation energy on the sample will always be the same. The lamp energy can be set by a lamp factor in the software. This allows calibration of the imaging system for each fluorophor. Comparison of the amounts of different fluorophors in one sample becomes very easy.



- [Callback Request](#)
- [Download of Brochure NightOWL NC 100](#)
- [Download of Brochure NightOWL NC 320](#)
- [Applications](#)
- [Application video on JovE](#)
- [indiGo Software](#)
- [Multimodality](#)
- [3D-Imaging](#)
- [Gas Anaesthesia Unit](#)
- [More Accessories](#)
- [Literature](#)
- [Gallery of Molecular Imaging](#)
- [Useful Links for Molecular Imaging](#)
- [Reporter Gene Vectors from Plasmid Factory](#)

Link to User:

- [Institut Pasteur, Paris, France](#)
- [IRCM, Montpellier, France](#)
- [Rudolf-Virchow-Centre, University of Würzburg, Germany](#)
- [ProQinase GmbH, Freiburg, Germany](#)

Exhibit 3
31

Fluorescence illumination

can be mounted in the cabinet for fluorescence applications. Different illumination systems such as gooseneck fibre optics or ringlights are available with the corresponding filters ranging from 300 nm up to 1100 nm. Tungsten halogen lamp (340-700 nm) is used for illumination.

Filter

Berthold Technologies offers a complete range of filters between 340nm up to 1100nm. Filters have to be used in fluorescence and as well BRET or FRET applications. If a transilluminator is used only an emission filter is needed. Berthold Technologies offers filter pairs for NightOWL for following standard dyes amongst others:

Filter Recommendations

	Excitation	Order No.	Emission	Order No.
GFP	475/20 nm	53183	520/10 nm	39805
Cy5	630/20 nm	50097	680/30 nm	49180
Cy5.5	630/20 nm	50097	700/20 nm	50479
Cy7	700/20 nm	50475	780/20 nm	50476
ICG	740/30 nm	50480	820/30 nm	50481
dsRed	530/20 nm	38536	600/20 nm	50477
Qdot700®	630/20 nm	50097	700/20 nm	50479
Qdot800®	630/20 nm	50097	820/30 nm	50481
mCherry	550/10 nm	39796	620/10 nm	40540

*Some techniques for generating and/or detecting light in biological subjects are patented and may require licences from third parties. Users are advised to independently determine for themselves whether their activities infringe any valid patent.

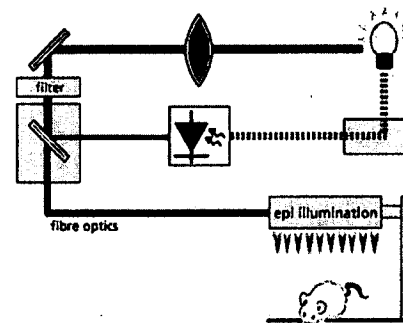


EXHIBIT 4

Exhibit 4
33

EXHIBIT 4



detect and identify

Search

Bioanalytic

[Home](#)[Contact](#)[Products](#)[Applications](#)[Home](#) > [Bioanalytic](#) > In-vivo Imaging Instruments

In vivo Imaging Instruments

Gene expression can be monitored in living organisms with ultra sensitive imaging systems.

BERTHOLD TECHNOLOGIES contributed a major breakthrough of this technology with its Luminograph LB 980 introduced in 1989.

Today, the third generation of low-light imagers is available, the NightOWL II LB 983. The researcher can choose the camera according to his individual application.

As the NightOWL is the first imaging instrument, where the camera is moved inside the cabinet, a lot of special applications can be done easily like close-up imaging, plant imaging or animal imaging in specific animal beds for multimodal imaging. Orthogonal 3D-imaging for approximate volume calculation is available.

Additionally NightOWL II offers quantitative fluorescence because the unique optical system from the Mithras multimode reader has been integrated.

Based on the experiences with the NightOWL in vivo imager BERTHOLD TECHNOLOGIES has developed the new NightSHADE imaging system with plant research in mind.

Some techniques for generating and/or detecting light in biological subjects are patented and may require licences from third parties. Users are advised to independently determine for themselves whether their activities infringe any valid patent.

NightOWL LB 983 in vivo Imaging System

NightSHADE LB 985 in vivo plant imaging system

CCD Camera LB 982



Download of Glossary Optical Digital Imaging

© 2008 BERTHOLD TECHNOLOGIES GmbH & Co. KG

Legal Notices Print Version

Exhibit 4**34**

EXHIBIT 5

Exhibit 5
35

EXHIBIT 5



NightOWL II LB 983

In vivo imaging in general allows a non-invasive insight into living organisms and helps to understand metabolic processes and disease related changes. Especially bioluminescence imaging (BLI) and biofluorescence imaging (BFI) enable monitoring of gene expression or disease progression in living organisms due to outstanding sensitivity.

In 1989 Berthold Technologies introduced its first low light imaging instrument – the LB 980 Luminograph. The first in-vivo gene expression experiments in plants and animals performed on this instrument date back to the year 1993.

BLI utilizes light emitted by luciferase enzymes. Today bioluminescence markers can be tailored to any gene, enabling detailed research of gene function. BFI utilizes proteins, which fluoresce under illumination, either applied as exogenous reagents or endogenously expressed. Both BLI and BFI have contributed to the understanding of disease mechanisms and the development of new treatments.

Cameras

Today's generation of low light imagers from Berthold Technologies, the LB 983 NightOWL II, is equipped with cooled slow scan CCD cameras:

- Front-illuminated NC 320
is best suited for fluorescence applications with 3 million pixels for high resolution. Micro-lenticular array on top of CCD chip enhance light collection to maximum quantum efficiency of 85 %
- Back-illuminated NC 100
with high full well capacity for large dynamic range is best suited for luminescence applications. Midband coating enhances the quantum efficiency in the spectral range between 440 to 770 nm (80% QE) ideally to luciferase and GFP emissions. Efficient Peltier cooling keeps chip temperatures low, reducing the dark current and thereby enhancing the signal to noise ratio.

Applications*

Whole animals and plants can be imaged as well as blots, gels, microplates, cell culture dishes and arrays regardless luminescent or fluorescent markers are used. Optical calibration ensures the comparability of all images captured with the NightOWL.

Detection of weak light signals with CCD cameras can be extraordinarily achieved with high quantum efficiency and extremely low noise levels to enable long exposure times. The camera and cabinet design are the key to superior imaging performance, complemented by scientific evaluation software for quantification.

Cabinet

The NightOWL cabinet is extremely light-tight preventing any interferences from ambient light. NightOWL is the first imager with an motor-driven camera inside the cabinet. Positioning is reproducible with +/- 100 µm allowing very precise height correction. Optimum resolution and focus of the sample is achieved by automatic positioning of the camera according to the actual sample size. The NightOWL cabinet has enough space to install special light sources or to place transilluminators, heaters, coolers etc. These devices may even be switched on and off through the software and the built-in sockets. The flange option provides light-tight access to the inner part for tubings and cables.

Fluorescence excitation unit

The unique optical system from the LB 940 Mithras Multimode Reader has been integrated in the

Exhibit 5
36

NightOWL II model. The light beam is not constant for each fluorescent measurement which is ideal with the ringlight epi illumination. If the ringlight is always set at the same height, the excitation energy on the sample will always be the same. The lamp energy can be set by a lamp factor in the software. This allows calibration of the imaging system for each fluorophor. Comparison of the amounts of different fluorophors in one sample becomes very easy.

Fluorescence illumination

can be mounted in the cabinet for fluorescence applications. Different illumination systems such as gooseneck fibre optics or ringlights are available with the corresponding filters ranging from 300 nm up to 1100 nm. Tungsten halogen lamp (340-700 nm) is used for illumination.

Filter

Berthold Technologies offers a complete range of filters between 340nm up to 1100nm. Filters have to be used in fluorescence and as well BRET or FRET applications. If a transilluminator is used only an emission filter is needed. Berthold Technologies offers filter pairs for NightOWL for following standard dyes amongst others:

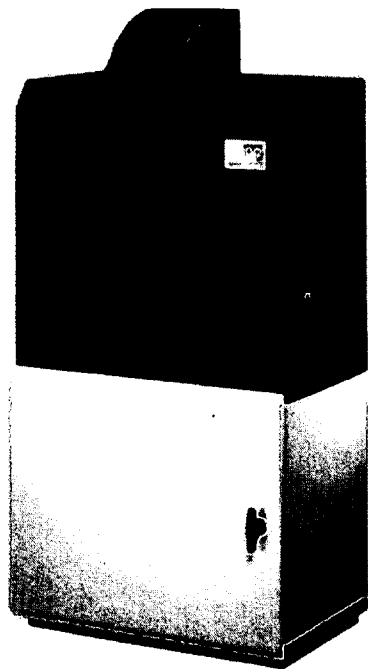
Filter Recommendations















	Excitation	Order No.	Emission	Order No.
GFP	475/20 nm	53183	520/10 nm	39805
Cy5	630/20 nm	50097	680/30 nm	49180
Cy5.5	630/20 nm	50097	700/20 nm	50479
Cy7	700/20 nm	50475	780/20 nm	50476
ICG	740/30 nm	50480	820/30 nm	50481
dsRed	530/20 nm	38536	600/20 nm	50477
Qdot700®	630/20 nm	50097	700/20 nm	50479
Qdot800®	630/20 nm	50097	820/30 nm	50481
mCherry	550/10 nm	39796	620/10 nm	40540

*Some techniques for generating and/or detecting light in biological subjects are patented and may require licences from third parties. Users are advised to independently determine for themselves whether their activities infringe any valid patent.

Exhibit 5

37

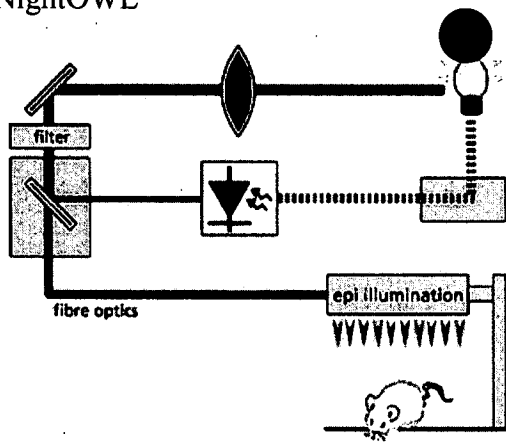


-  [Callback Request](#)
-  [Download of Brochure NightOWL NC 100](#)
-  [Download of Brochure NightOWL NC 320](#)
-  [Applications](#)
-  [Application video on JovE](#)
-  [indiGo Software](#)
-  [Multimodality](#)
-  [3D-Imaging](#)
-  [Gas Anaesthesia Unit](#)
-  [More Accessories](#)
-  [Literature](#)
-  [Gallery of Molecular Imaging](#)
-  [Useful Links for Molecular Imaging](#)
-  [Reporter Gene Vectors from Plasmid Factory](#)

Link to User:

-  [IRCM, Montpellier, France](#)
-  [Rudolf-Virchow-Centre, University of Würzburg, Germany](#)
-  [ProQinase GmbH, Freiburg, Germany](#)

Exhibit 5
38



© 2008 BERTHOLD TECHNOLOGIES GmbH & Co. KG

Exhibit 5
39

EXHIBIT 6

Exhibit 6
40

EXHIBIT 6

Luciferin bioavailability in mice during in-vivo imaging

Arnaud Pillon¹, Philippe Gauthier², Mathieu Seimandi¹, André Pèlegri², Françoise Vignon¹, Patrick Balaguer¹, Jean-Claude Nicolas¹, Wolfgang Schäfer³ and Manfred Hennecke³

Introduction

Reporter genes are widely used for monitoring gene expression in *in vitro* and *in vivo* assays. This technology enables non-invasive visualization of gene expression in intact animals. Bioluminescent models based on luciferase gene expression have become useful tools for evaluating cancer treatment efficiencies and the role of receptors in invasion and proliferation.

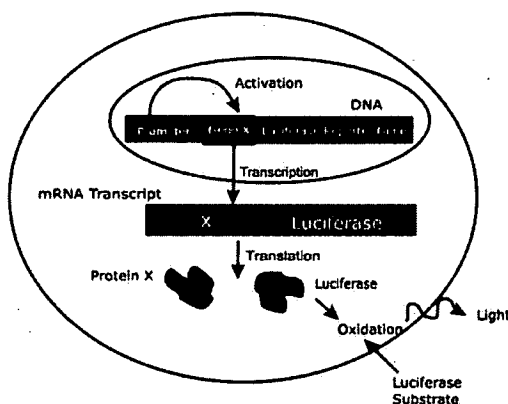


Figure 1: Principle of Reporter Gene Assays. The promoter activates the transcription of gene x and the close luciferase reporter in the cell nucleus. After translation the luciferase enzyme will catalyse the reaction of Luciferin (luciferase substrate) and ATP to oxyluciferin and light.

The light resulting from the bioluminescent oxidation of luciferin in the presence of ATP, magnesium and oxygen can be easily detected and quantified with a cooled charge-coupled device (CCD) camera, like the NightOWL LB 981 NC 100 system from BERTHOLD TECHNOLOGIES.

Exhibit 6

41

¹ INSERM Unité 540, UM I, Endocrinologie Moléculaire et Cellulaire de Cancers, Montpellier, France

² INSERM EMI 0227 - CRLC Val d'Aurelle - Paul Lamarque, 34298 Montpellier, France

³ BERTHOLD TECHNOLOGIES GmbH & Co. KG, 75312 Bad Wildbad, Germany

The advantages of a luciferase assay are the high sensitivity, the absence of luciferase activity inside most of the cell types, the wide dynamic range, rapidity and low costs. The most versatile and common reporter gene is the luciferase of the North American firefly *Photinus pyralis* with the highest quantum efficiency of the light reaction. The protein requires no posttranslational modification for enzyme activity. At the concentrations used for bioluminescence imaging, D-luciferin is non-toxic and non-immunogenic, and so serial imaging examinations can be performed with the same mouse. D-luciferin crosses cell membranes and penetrates the intact blood-brain barrier in addition to placental barriers after injection in mice, allowing this reporter protein to be imaged in any anatomic site. As the technique does not harm the animals, multiple sequential imaging studies in the same animal are possible.

Experimental Procedure

Usually luciferase expression is analyzed after intraperitoneal luciferin injection. Concentrations of D-Luciferin used for *in vivo* imaging are between 120 mg/kg up to 225 mg/kg bodyweight in mice. Since the magnitude of bioluminescence measured *in vivo* varies with time after luciferin injection, as well as with dose, time after injection and dose of D-luciferin have to be kept constant in the sequential imaging experiences with the same animals (Burgos et al.). Only under constant conditions comparison of the quantitative results are possible.

To determine the optimal luciferase activity detection time, time course experiments were performed. Serial pictures were taken at different time intervals following luciferin injection (125 mg/kg bodyweight) roughly every 2 min. (Fig. 2). Maximal bioluminescent signal was obtained about 10 min after injection and remained stable during 10 more minutes.

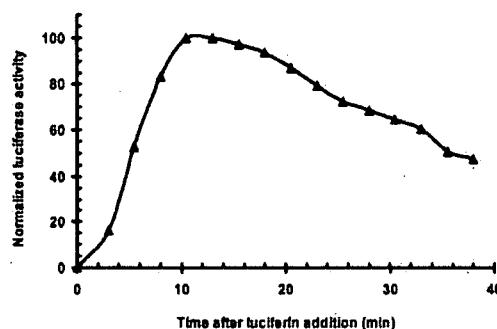


Figure 2: Time course of *in vivo* light emission from luciferin-treated LSCL*N cells. Data were obtained after subcutaneous implantation of LSCL*N cells in female Swiss nude mice. Mice were anesthetized and luciferin was ip injected. After 2 min imaging with CCD camera, data were extracted using WinLight software (BERTHOLD TECHNOLOGIES). The curve represents the normalized light units at each point measured by taking maximum value as 100.

Exhibit 6
42

To perform further studies with several mice simultaneously, NightOWL LB 981 NC 100 system (BERTHOLD TECHNOLOGIES) was coupled with an anaesthesia system from TEM (Bordeaux) that allow mice imaging in combination with a temperature controlled mice holder in the inner of the instrument (Fig.3).

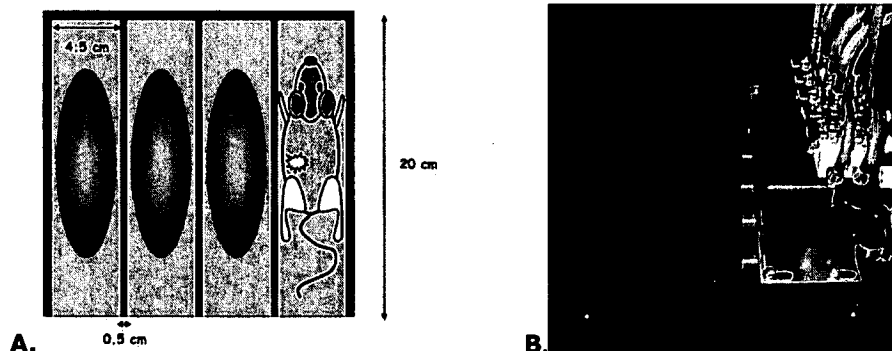


Figure 3: NightOWL NC 100 mice holder. Schematic view (A) of the mice holder was made by INSERM U 540, Montpellier, France and the realization of the final product was achieved by BERTHOLD TECHNOLOGIES engineers (B).

This anesthesia system allowed us to perform kinetic of luciferine distribution within 1 to 4 mice simultaneously. For this purpose, we used the sequence acquisition mode of WinLight software to follow the apparition of the bioluminescent signal as shown in figure 4.

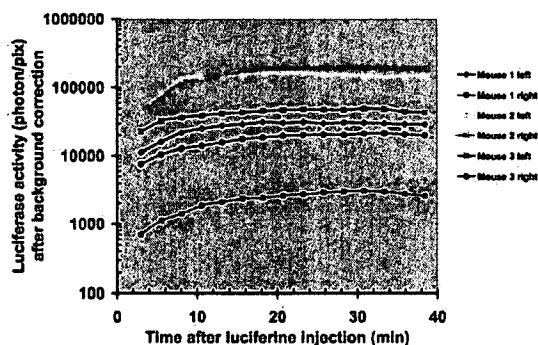


Figure 4: Time course of in vivo light emission from luciferin-treated mice. Data were obtained after subcutaneous implantation of bioluminescent cells in female Swiss nude mice (two implantations per mice: left flank and right flank). Mice were anesthetized and luciferin was subcutaneously injected. Mice were imaged using acquisition mode within a 2 min period and data were extracted using WinLight software (BERTHOLD TECHNOLOGIES).

Most of the time kinetic was similar but we have noted some variation mostly due to luciferin distribution that depends on injection (either intraperitoneal or subcutaneous injection). Figure 5 showed three different kinetic often obtained.

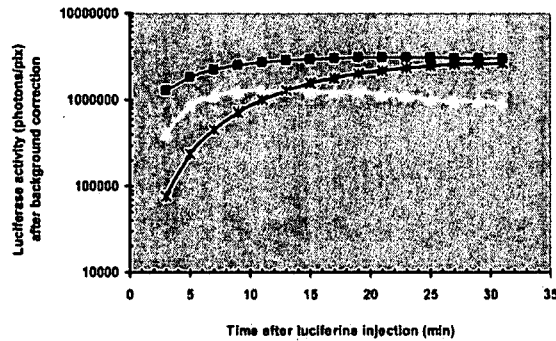


Figure 5: Three different time courses of *in vivo* light emission from luciferin-treated mice. Data were obtained after subcutaneous implantation of bioluminescent cells nude mice. Mice were anesthetized and luciferin was subcutaneously injected. Mice were imaged using acquisition mode within a 2 min period and data were extracted using WinLight software (BERTHOLD TECHNOLOGIES).

Those three patterns were very different. The yellow curve in which the maximal bioluminescent signal was obtained about 10 min after injection and remained stable during 10 more minutes and when decreased, was the more often obtained. But sometimes, the signal remained stable during more than 30 minutes (red curve) or it took more than 30 minutes to reach the maximum luciferase activity (blue curve). This experiment point out the necessity to perform time courses using the sequence acquisition mode to reduce signal variability of *in vivo* measurements. The bioavailability of luciferin within the animal could be different from an experiment to another. To avoid this problem, we have used constitutive luciferase expressing cells as an internal standard. Mice were subcutaneously double grafted (right and left flanks) as shown in figure 7.

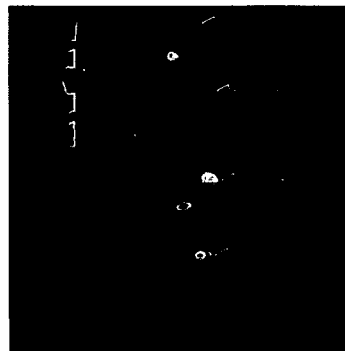


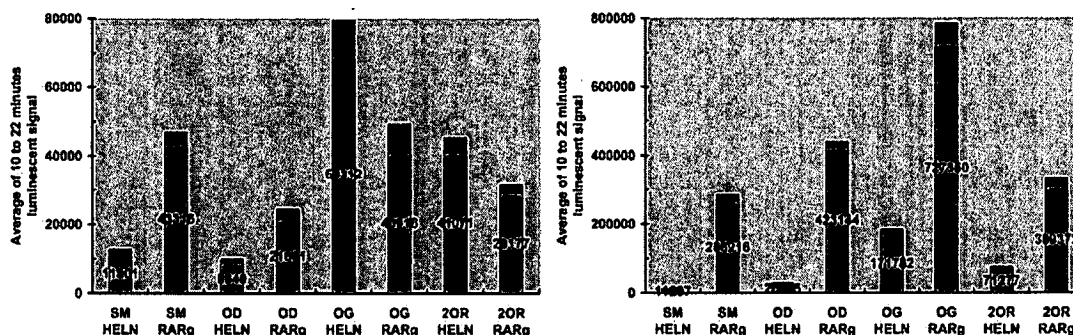
Figure 6: Implantation of inducible and constitutive cells as an internal standard. Four mice subcutaneously double grafted with cells expressing a constitutive luminescent signal (HELN cells) on their left flank (red arrows) and with cell expressing a retinoid inducible luminescent signal (RAR γ) on their right flank (green arrows).

Mice were imaged using the sequential mode before and after 16 hours induction by a ligand of the inducible cells (retinoid agonist) administered orally. Averages of luminescent signal between 10 and 22 minutes were calculated for each tumor and reported in figure 7 and table below.

Exhibit 6

44

Application Note



	Cells	Basal luminescent values (photon/pix)	Induced luminescent values (photon/pix)	Induction simple	Induction corrected
Mouse 1 (SM)	Constitutive (HELN)	11801	11207	0.95	6.47
	Inducible (RARy)	43316	266216	6.15	
Mouse 2 (OD)	Constitutive (HELN)	8840	26655	3.02	6.48
	Inducible (RARy)	21661	423144	19.53	
Mouse 3 (OG)	Constitutive (HELN)	69312	171782	2.48	7.17
	Inducible (RARy)	40916	727350	17.78	
Mouse 4 (2OR)	Constitutive (HELN)	41071	71277	1.74	6.11
	Inducible (RARy)	29177	309372	10.60	

Figure 7: Averages of luminescent signal. Four mice were imaged using the sequential mode before and after 16 hours induction by a ligand of the inducible cells (retinoid agonist) administered orally. Averages of luminescent signal between 10 and 22 minutes were calculated. HELN were constitutive luciferase expressing cells and RARy were retinoid luciferase inducible cells. Induction factor were calculated with or without constitutive cells correction.

Without any correction, fold induction of retinoid inducible cells were 6.15, 19.53, 17.78 and 10.60 for the four mice. Those results were very heterogeneous and could be due to variability of luciferin injection and its bioavailability as well as cell proliferation. Using the internal standard correction, fold induction were 6.47, 6.48, 7.17 and 6.11, respectively. This homogeneity allows us to determine the real fold induction of this experiment: 6.56 ± 0.44 .

Literature

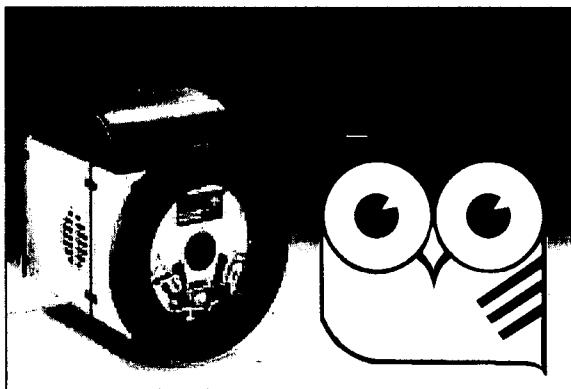
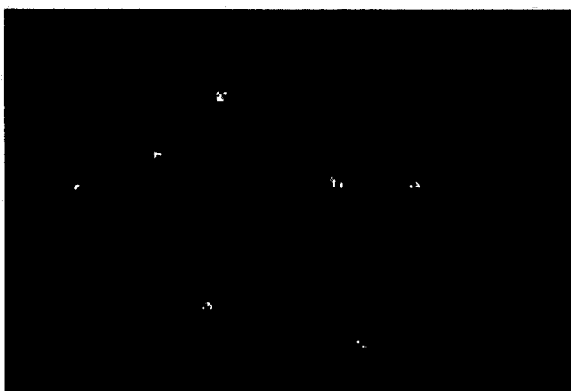
Burgos, J.S., M. Rosol, R.A. Moats, V. Khankaldyyan, D.B. Kohn, M.D. Jr. Nelson, and W.E. Laug. 2003. Time course of bioluminescent signal in orthotopic and heterotopic brain tumors in nude mice. *Biotechniques* 34:1184-8.

EXHIBIT 7

EXHIBIT 7

Exhibit 7
46

detect and identify



Glossary

Optical Digital Imaging

Exhibit 7
47

2-Year Factory Warranty on all Berthold Instruments.

Glossary Optical Digital Imaging

edited by Manfred Hennecke, BERTHOLD TECHNOLOGIES, Bad Wildbad, Germany

A

A/D conversion

see → **Bit Depth of Camera Data**

Animal bed

is needed to fix and anesthetize an animal in such a way to perform → **multimodality imaging** in different scanners.

Aperture

see → **f-stop**

B

Back-thinned or back-illuminated CCD chips

are a rather expensive and delicate type of chips for high-end scientific-grade → **slow scan CCD**, → **ICCD** and → **ebCCD** cameras. By etching down to about 10 - 15 µm the illuminated back is thinned so that it becomes transparent. These sensors have a substantially improved sensitivity over the entire spectral range as compared to standard or front-illuminated CCD chips. Between 450 and 650 nm the quantum efficiency may exceed 90 %.

A substantial downside of this chip type is a readout noise that is usually considerably higher than that of standard chips even at slow digitization speed. The dark noise can be higher in cases as well.

Bandpass filters

transmit with high efficiency a particular wavelength band while rejecting by absorption or reflection the out-of-band energy. They are the simplest and most cost-effective way to transmit a well-defined band of light. Compared with a grating monochromatic system, the cost of bandpass filters is usually significantly lower, and performance is comparable, if not better, in terms of in-band transmission and out-of-band rejection.

Binning

is the combination of neighbouring CCD pixels during readout. The result is an increased signal and thus an improved sensitivity and a better signal-to-noise ratio, however, at the cost of loss in spatial resolution. The binning factor is adjustable and usually square (2x2, 4x4...) to avoid image distortion.

BLI

stands for **BioLuminescence Imaging**, where the reaction is catalyzed by luciferases, an enzyme class, which can be coexpressed in a reporter gene assay. In contrast chemiluminescence are those reactions which are catalyzed by a chemical reaction.

BFI

stands for **BioFluorescence Imaging** and uses the natural occurring fluorescence proteins like GFP, eGFP or YFP, which can be coexpressed in a reporter gene assay. In contrast chemifluorescence is done with all the non-protein labels (see also → **fluorescence reflectance imaging**).

Blooming

occurs, if the illumination exceeds the → **full-well capacity** of the photodiodes in bright areas of the image. Excess charges will overflow into adjacent wells and erroneously cause high intensities of the corresponding image pixels. This is a clear hint that the image is overexposed.

Bit Depth of Camera Data

refers to the digitization of the analog light signal by the analog-to-digital (A/D) converter of the camera, which is the binary range of the possible grayscale values of the produced images. Common bit depths are 8 to 16 bit, which equals $2^8 = 256$ to $2^{16} = 65536$ gray levels.

The human scotopic vision (night vision) can distinguish in the order of 50 gray scales. Computer monitors are able to display 8 bit digital grayscale images. 16 bit images are reduced to 8 bit upon display.

Bit Depth of Digital Images

gives the number of possible gray scales (intensities) an image file format allows. An 8 bit number comprises 8 digits that are either "0" or "1". Up to 256 different gray values can be listed with 8 bit numbers because with each bit having one of the two values there are $2^8 = 256$ possibilities. In the decimal system they represent the values 0 - 255. Similarly, in 16 bit format $2^{16} = 65536$ different gray values can be stored.

Exhibit 7

48

C

Camera Resolution

is obviously an important parameter for the selection of a CCD camera. Digital images consist of → **pixels**, which represent miniature photodiodes on the CCD chip. Each photodiode integrates the intensity of its area. It is easy to understand that the image resolution depends on the total number of pixels it is composed of and corresponds to the number of photodiodes on a CCD chip of a certain size.

It should be noted very clear, that even if small CCD pixels improve the resolution, they also reduce the → **dynamic range** of the device, because the → **full-well capacity** depends also on the size of the photodiodes.

Furthermore, the average signal per pixel is directly dependent on the size (area) of the pixels. This is the reason why luminescence and fluorescence applications can not be optimized with one type of CCD camera, since big pixels are best for luminescence, small pixels best for fluorescence.

Camera Noise

comprises → **dark noise** and → **readout noise**.

CCD

stands for "charge-coupled device".

CCD Chip Types

are manufactured nowadays in a broad variety for different purposes and applications, see therefore

- **Back-thinned CCD chips**
- **Full-frame CCD chips**
- **Frame-transfer CCD chips**
- **Interline-transfer CCD chips**
- **Electron Multiplying CCD (emCCD) chips**

CCD Chip Size

is often given in an inch measure: 1/2" chip, 2/3" chip, etc. This does not refer to the chip diagonal in inch but has historical reasons. It relates the field-of-view of the camera to that of former tube cameras.

CMOS Chips (APS)

In an (Active Pixel Sensor) **Complimentary Metal Oxide Semiconductor** chip each photodiode (pixel) is coupled to an individual amplifier. Also there is one A/D converter for each column of pixels so that the data of a row of amplifiers can be read out in parallel. The individual amplifiers lead to an overall reduction of noise, however, fixed pattern noise artefacts are induced, at least in early generation CMOS sensors, because of variations in amplifier gain and offset across the chip.

Advantages of these devices are the possibility of pixel-wise gain manipulation and true region-of-interest readout. A fundamental difference to CCD

chips is further that here incoming photons remove electrons from charged capacitors instead of creating electrons in empty ones. A consequence is relatively high noise at low light levels which is one of the reasons for which CMOS cameras are not widespread in this field.

C-mount

is a mechanical adapter between camera and lens. The mechanical definition of a C-mount is a 1 inch hole with 32 TPI (turns per inch) threading, female on the camera side, male on the microscope side. The optical definition of a C-mount is that the image reaches the → **focal plane** of the CCD at 17.5 mm beyond the shoulder of mounting ring.

Each microscope needs a special C-mount male adapter piece offered by the manufacturer. Cameras are always equipped with the same female adapter port for easy exchange.

Color Images

produced by computer monitors and TV screens are generated by pixelwise mixing of the three primary colors red (R), green (G) and blue (B).

This is called additive mixing of light. Digital images where the color information is encoded by intensities of the primary colors are commonly referred to as RGB images. The three light components are called color channels.

Contrast

is the variation of signal intensity relative to the average intensity ($\Delta I/I$). Together with resolution it is the most important factor determining the quality of an image. Contrast and resolution are linked by the Contrast Transfer Function.

Conversion Factor

The A/D converter divides the electronic charges of the CCD pixels that are readout from the chip by a certain factor, the conversion factor, thus delivering a digital signal measured in counts (or gray levels). The maximum possible conversion factor would be the full-well capacity divided by the bit depth. However, often the conversion factor is somewhat lower than this.

Some cameras provide the option to reduce the conversion factor for low light level experiments, referred as change of gain. This way saturation is reached faster while the light-to-gray scale digitization is finer (fewer electrons per count) and the resulting intrascene dynamic range of the image is improved.

An example: A 12 bit camera with a full-well capacity of 18,000 electrons might have a standard conversion factor of 4. That means, saturation (4095 counts) is reached with 16,380 electrons; this would be the effective full-well capacity.

With a conversion factor of 2 the limit would be 8190 electrons, or half the signal. Consider an image with a background intensity of 1000 electrons and a maximum signal of 5000 electrons. With a conversion factor of 4 the resulting image would have an intensity spectrum of 1000 gray levels after background subtraction but 2000 if the factor is 2. The intrascene dynamic range would be twice as high.

CW fluorescence intensity

stands for Continuous Wave (CW) fluorescence intensity, sometimes referred as multi wavelength fluorescence imaging, but is identical with → **fluorescence reflectance imaging**.

D

Dark Noise (Thermal Noise)

is caused by current fluctuations on the photodiodes, in the absence of light arising from thermally generated electrons. The dark noise is the geometric mean of dark current and integration time. It is temperature dependent, this is why many CCD cameras are actively cooled, for example by Peltier elements. Roughly, a 6-8 °C decrease in temperature reduces the dark current by about half.

Data Readout Rate

is usually the rate limiting step in analog-to-digital signal conversion. The conversion rate ranges somewhere between 1 and 20 MHz (pixels per second) for 10 - 16 bit converters (16 bit data) in most cameras. For very low → **readout noise**, the data readout rate is sometimes set to 100 kHz.

Depth of Field or Depth of Focus (DOF)

is defined as the difference between the closest and farthest distances an object may be shifted before an unacceptable blur is observed. DOF should not be confused with → **working distance**.

Digital Image files

are based on tables that list the intensities, or "counts", of all pixels. The values are stored in the binary system as 8 or 16 bit numbers; see also → **Bit Depth**. Which pixel count gets which gray value or color in the image display assigned, is defined in look-up tables that are edited upon changing the contrast or blanking out background etc.

Displaying Digital Images

The on-screen appearance of digital images, the way the data is displayed normally, is defined by the display palette or look-up table. It relates the different gray scales or colors to the range of pixel intensities that occur in the image.

Most image processing programs offer an autoscale function which adjusts the gray scale palette so that the darkest pixel of an image is set to black and brightest to white. The contrast of the image display can further be optimized by changing the slope of the gradient or any background intensity be blanked out by shifting the black threshold upwards.

Monochrome images can also be displayed in pseudo-colors, for example in order to appear as observed through the eyepiece of a microscope. Instead of a black and white palette, for example a black and green palette can be used.

Often false color palettes are used because of the increased contrast they offer. This is due to the ability of the human eye to better distinguish colors than gray scales. A popular such palette is the black-blue-green-red pseudo-rainbow. Note that with the same slope of the gradient as above, the weaker details of the image are better visible.

Distortion

is an optical error (aberration) in the lens that causes a difference in magnification at different points, within the image.

Dynamic Range

of a CCD camera (DR) is the maximum signal (which is directly related to the → **full-well capacity (FWC)**) divided by the → **camera noise (CN)**, the combination of the dark and readout noises: $DR = FWC/CN$. The higher the dynamic range the more reliable is the quantification of differences between the dimmest and the brightest intensities of an taken image.

The dynamic range is sometimes measured in decibels (dB) ($DR = 20 \times \log (FWC/CN)$).

The dynamic range of acquired image data is maximum intensity divided by total noise. At high light levels it is practically limited by the signal noise, that is the square root of the maximum signal of the image (prior to digitization).

The intrascene dynamic range of an image (intensity range, difference between brightest and dimmest pixel) is determined by camera gain, exposure time, sample staining, microscope settings, background intensity, display palette and more variabls and can be represented by the intensity histogram.

Exhibit 7

50

E

Electron-bombarded CCD (ebCCD) cameras

is a type of intensified cameras that is kind of an intermediate between CCD and ICCD cameras. Like ICCDs they contain a photocathode to generate photoelectrons but do not feature an MCP.

The photoelectrons are accelerated by a high voltage gradient (1.5 - 2 kV) before "bombarding" a back-thinned CCD chip. Unlike photons, which, depending on the QE, are converted into one electron at the most when collected by a photodiode of a CCD chip, the impact of an accelerated electron generates up to several hundred new charges.

This is only a modest gain if compared with ICCDs but in general ebCCDs have a higher spatial resolution and a better signal-to-noise ratio.

Electron Multiplying CCD (emCCD) cameras

This is a new on-chip gain technique that can be applied to all current chip types. Such chips feature an additional gain register inserted between shift register and output amplifier through which all electrons are moved serially upon data readout.

In each charge, transfer step electron multiplication occurs upon impact ionization caused by electrodes with higher voltage amplitude than is necessary for the transfer alone. While the multiplication factor per step might be low, the huge number of steps during serial readout leads to a significant gain.

For example, 0.5% gain per step leads to a 165-fold signal increase for 1024 pixels per line. Besides voltage and number of transfer steps, the gain factor is also dependent on the chip temperature. The lower the temperature the more probable is the generation of secondary electrons.

The fundamental difference to intensified CCDs is that the photoelectrons are multiplied prior to reaching the CCD chip, while here the gain is achieved on-chip. Because it is done before readout the read noise is not affected and consequently the signal-to-noise ratio enhanced significantly.

On the other hand, dark charges are multiplied together with the photoelectrons, however, the cooling of the CCD keeps this factor low. A certain additional noise factor arises from the probabilistic nature of the secondary electron generation and the uncertainty that goes along.

An advantage over intensified CCDs is that there is no risk of hardware damage due to overexposure. The spatial resolution is the same as for an analogous standard CCD and is not reduced by a photocathode or MCP.

Entocentric Lenses

are designed to enhance perspective, i.e. close objects appear larger than distant objects.

F

Field of View

is the area of the object that will be viewed on the monitor.

Fill Factor

is a measure of the space between the pixels, which are not photon-sensitive. Today's full-frame chips are close to 100 percent, which means there is nearly no "empty space" between the diodes and no incoming photons are lost.

Filters

are often used in imaging for different purposes and applications. Refer therefore for

→ **Bandpass filters**

→ **IR-cut off filters**

FireWire

see → **IEEE-1394**

Fluorescence Molecular Tomography (FMT)

FMT, supported by the company VisEn, images the animal, collects data sets from multiple points of view and captures on the order of 50,000-100,000 source-detector pair measurements within a scan time on the order of 2-4 minutes. Due to such data set the light source is reconstructed by software showing the size and the depth of the light source.

Fluorescence Reflectance Imaging

is the typical set of illumination to excite the sample from above. The signals which are emitted from the sample are measured by a camera also positioned above the sample. The proper set of filters have to be chosen to excite the fluorophore and measure its emission.

F-mount

is another mechanical adapter between camera and lens. The mechanical definition of a F-mount is that of Nikon lenses. The optical definition of a F-mount is that the image reaches the focal plane of the CCD like in Nikon SLR-cameras beyond the shoulder of mounting bajonett.

Focal length

is defined as the distance between lens and focal plane when the lens is set to infinity.

Focal plane

is the distance between shoulder of mounting ring and CCD chip. There are a variety of mechanical adapters or → **Optical Interfaces**.

Frame-transfer CCD chips

use two-part chips in which one half is exposed and collects photons while the other is used for temporary data storage only and masked to protect it from incoming light. During the exposure of an image, the

data of the previous image are readout from the storage array via the serial shift register through an output amplifier and A/D converter.

Once exposure and readout are completed the newly accumulated charges are very rapidly moved from the light sensitive half to the emptied storage array; this is termed the "frame transfer". Afterwards the cycle can be repeated and the next image acquired. A disadvantage of this principle is the possibility of charge smearing during the parallel transfer if the light influx is continuous throughout.

F-stop (f/#)

also called → **aperture**, is a measure of the light gathering ability of a lens, which is the diameter of lens divided by the focal length. The smaller the f/#, the "faster" the lens. The smallest f/# and the → **focal length** specifies a lens.

Full-frame CCD chips

consist of a high-density array of photodiodes that convert the incoming photons into electrical potentials. The → **fill factor** is close to 100 percent, which means there is nearly no "empty space" between the diodes and no incoming photons are lost. After image exposure the data readout is performed by shifting the charges in a parallel fashion one row at a time to the serial register.

The serial register then shifts each row of information sequentially to an output amplifier before it is directed to an A/D signal converter.

Unless mechanical shutters or synchronized illumination is used for exposure, smearing artifacts occur because the photodiodes are being continuously illuminated during parallel register readout.

Full-Well Capacity

is the maximum amount of charges (electrons) the photodiodes of a CCD chip can accommodate. It is also called well depth and usually ranges from about 10,000 to 350,000.

The linear full-well capacity is the point where the linear relationship between the amount of incident light and the charges it originates is lost, i.e., when the pixel well nears saturation resulting in a degradation of the signal.

Gray scale

refers to the number of possible intensities (gray values) an image file format allows. With an 8 bit A/D conversion the gray scale include values between 0-255, because with each bit having one of the two values there are $2^8 = 256$ possibilities. Similarly, in 16 bit format $2^{16} = 65536$ different gray values can be stored.

The human scotopic vision (night vision) can distinguish in the order of 50 gray scales. Computer monitors are able to display 8 bit digital grayscale images. 16 bit images are reduced to 8 bit upon display.

H

Histogram

A histogram is the graphical version of a table which shows what proportion of cases fall into each of several or many specified categories.

The categories are usually specified as non overlapping intervals of some variable.

I

IEEE-1394

also called FireWire, is a modern plug-and-play interface between PC and camera and allows the connection of several cameras to one board without the need of a frame grabber. It is sort of a high-speed serial memory bus capable of operating at 400 Mbit/s. 1394 refers to the total bus bandwidth.

The bandwidth being 30 times larger than that of USB makes it more suitable for the high-speed data transfer desirable for digital imaging.

Image File Formats

There is a vast variety of data formats, some of which are relatively universal, others are specific for certain software programs or operating systems. The most widespread format may be the "tagged image file format" or TIFF (*.tif). There are many derivatives of this format which quite often causes the problem that a software is unable to open a file that was created with a different program.

Other common formats are bitmap (*.bmp) and windows metafile (*.wmf). Postscript (*.ps) is a page description format with the necessary information for printers. Encapsulated postscript (*.eps) may contain CMYK, gray scale, vector or compression data and consists of a postscript code that is independent from the type of output device. Such files can be read by many programs but often not further processed.

Certain formats (*.gif, *.jpg, *.png) are used to compress images in order to reduce storage space and download time for use in the world wide web. These formats employ different algorithms to store sequences of pixels with repeating patterns as one piece of information instead of pixel by pixel as in the uncompressing formats.

The "graphic interchange format" (GIF) can render the entire color range of 24 bit RGB images but one image may only contain 256 colors at the most (8 bit). Otherwise the compression occurs without information loss. It is most useful for graphics with sharp contours. A useful feature is that one color can be set transparent. The format was invented for the online service CompuServe and there are patent issues to be considered.

The JPEG format ("joint photographers expert group") changes the colors of the individual pixels assuming that the eye is unable to resolve certain details anyway. The compressing factor is adjustable so that the user has direct influence on the quality of the image - and on the data size. Transparency of colors is not possible.

Many consumer cameras offer this format as an option. The compression is very effective but because of the loss of information this file type is not useful for quantitative imaging but probably serves best for standard photography.

The "portable network graphic" (PNG) was developed especially for the use in websites as a patent free alternative to GIF. PNG supports not only truecolor and reyscale images (like JPEG) but also palettized images (similar to GIF). This means that an individual 8 bit palette is stored along with the image and each pixel refers to one of the colors in this palette.

Thus not each pixel has to carry three-channel information and the overall amount of data is reduced. Shades of transparency can be achieved via storage of an additional alpha channel whereas GIF supports only binary transparency.

The compression is without loss of information for truecolor images which however renders it less effective with respect to data reduction as compared to the "lossy" JPEG compression.

This is especially the case for landscape photography, for example, while for graphics and rather uniform images the compression factor tends to be higher.

The "fts" format was developed by NASA to save more information with the image. Since there is no editor to manipulate the pictures, this file-format is very save due to GLP.

Intensified CCD Cameras

are divided in two general types of cameras used for image intensification. In the most common intensified CCD cameras, the ICCDs, an intensifier unit is optically coupled to a CCD chip via relay lenses or fiber-optic tapered bundles.

The second type are the → **electron-bombarded CCD cameras (ebCCD)** where the photoelectrons are merely accelerated (but not multiplied) before reaching the CCD chip. ICCD cameras are basically full-performance CCD cameras optically coupled in two possible ways (see below) to an intensifier.

A so-called proximity-focused intensifier (or wafer tube) consists of an entrance window, a photocathode, a microchannel plate (MCP) electron multiplier and a phosphorescent output screen. The photocathode converts the photons into electrons via the photoelectric effect.

The quantum efficiency of the conversion is an important parameter and depends on the coating material which differs in the different generations of intensifiers (see below). The photoelectrons are driven to the MCP which is set under a field of several hundred volts. The MCP contains millions of parallel channels with a diameter of about six micrometers in the newest generations.

The channels are coated with a secondary electron emitter which generates more electrons when hit by passing electrons. The intensification gain caused by the avalanche effect of multiple collisions is adjustable over a wide range up to several 10,000. The electrons are accelerated by a voltage of several kV upon exiting the MCP before reaching the phosphor screen where they are converted back into photons with an additional multiplication factor. The screen output light is then relayed to the CCD chip either by a lens or fiber-optic coupling.

The advantage of relay lens coupling is the possibility of constructing removable intensifiers that enable to easily convert the ICCD camera reversibly into a standard CCD camera or retrofit an existing camera. However, the → **light efficiency** is limited and causes a significant loss of signal and a reduced signal-to-noise ratio.

A much more efficient method to optically couple intensifier and CCD chip is through a fiber-optic taper which, however, requires a far more sophisticated manufacturing process.

Such a taper is a bundle of microscopic fibers (2 - 3 microns in diameter) that guides the light from the fluorescent screen to the CCD chip. There are up to nine fibers per pixel usually machined directly onto the diode array. Each microfiber has a cladding to maximize light transmission and a stray-light absorbing coating to contain leakage and prevent the resulting contrast reduction.

The signal-to-noise ratio of ICCD cameras is usually lower than that of standard CCD cameras because thermal noise from the photocathode and multiplication noise from the MCP are additional contributions to the overall camera noise.

The low light detection abilities of intensified cameras also allow a very high time resolution. This is due to the fact that the devices can be switched on and off very fast. This so called gating is necessary to provide the time needed to move the data off the CCD chip while the influx of photoelectrons is temporarily stopped.

The switchable voltage difference between photocathode and MCP enables this. If the voltage at the MCP is more positive than accelerated at the

photocathode, the photoelectrons are toward the MCP; if the MCP is more negative, the electron influx is stopped and the intensifier is gated off.

The relatively high resistance of the photocathode material does not allow gating faster than about 25-50 ns.

For gating faster than 2 ns, a nickel underlayer can be deployed to reduce the resistance, which, however, lowers the transmission and consequently reduces the QE significantly. With high-performance fiber-coupled ICCDs, single photon detection is possible. At higher light levels the gain can be adjusted to increase the dynamic range.

Main disadvantages of intensified cameras are the lower → **quantum efficiency** of the photocathode as compared to that of the CCD chip alone. Another disadvantage is increased noise and a limited intrascene dynamic range of the images because the wells fill much faster upon intensification due to the electron multiplication. ICCD cameras furthermore have a reduced spatial resolution caused by the microchannel plate.

Interline-transfer CCD chips

On interline-transfer chips each column of individual photodiodes has a light-shielded (masked) vertical transfer shift register directly adjacent to it. The parallel photodiode registers and interline masks are separated by transfer gates.

Similarly to frame-transfer CCDs, there are cycles of simultaneous photodiode exposure and charge transfer channel readout followed by very rapid interline charge transfer from the photodiodes to the emptied shift registers.

Interline-transfer chips are usually equipped with microlense arrays. There is a lens for every pixel to collect photons that would otherwise remain undetected by hitting the interline masks or transfer gates. These lenslet arrays increase the so-called photodiode fill factor by more than a factor of three.

These devices also include an "electron drain" to prevent electron overflow into neighbouring pixels by overexposure and the resulting blooming artifacts in the images. Furthermore, electronic shuttering is possible by switching the photodiodes voltage in order to prevent photoelectrons that are generated during off-times from reaching the transfer registers.

IR-cutoff filters

are used to cut autofluorescence of plastics e. g. in the range of 800 nm.

L

Lenses

project optically the image onto the front of a parallel CCD array.

Lenslets

see → **Microlenses** (on chip)

Light efficiency

is a function of transmission and inversely of the square of → **magnification** and → **lens f-stop**.

Look-up table (LUT)

By use of a Look-Up Table (LUT), image values are mapped to greyscale. The top of the LUT is initialized to white and the bottom to black, with greyscale linearly distributed in between.

M

MACU

stands for **Multimodal Animal Carrier Unit**, a special → **animal bed**

Magnification (System)

is the total magnification from the object to the image on the monitor, which is the product of the → **primary magnification** and the camera-to-monitor magnification (the ratio between the monitor size and the sensor size).

Microlenses (on chip)

also called lenslets, are tiny little lenses above each pixel to collect photons that would otherwise remain undetected by hitting the interline masks or transfer gates. These lenslet arrays increase the so-called photodiode fill factor by more than a factor of three.

Multimodality imaging

is widely considered to involve the incorporation of two or more imaging technologies (modalities), for example, optical and nuclear medicine reporter agents or by performing on the same objekt optical imaging together with MRI, PET, SPECT or x-ray CT.

Exhibit 7

54

N

Noise

of a digital image consists of the → **signal noise** and the camera noise which again comprises → **dark noise** and → **readout noise**. The dark noise is usually very low and comparable in size with the readout noise only in uncooled cameras.

In case of Peltier-cooled cameras its contribution can be ignored even for very long exposure times. In general, the dominating noise factor in most experiments is the unavoidable signal noise, only for very low light intensities does the camera noise significantly influence the image quality.

O

Object Distance

also called working distance, is the measurement from objective lens to the object.

Optical Imaging

is used for those methods where a lens for imaging is needed, in contrast to MRI, PET, SPECT, CT or ultrasonic.

Optical Interface

describe the mechanical adaptation between camera and lens. The mechanical definition is various, but the optical definition is always connected with the → **focal plane**. Optical interfaces are standardized nowadays:

- **C-Mount**: 1-32UN2A
- NF-Mount: M 17x0,5
- L-Mount: M 39x1/26"
- **F-Mount** (Nikon lens bayonet)
- U-Mount (M42x1)

P

Perspective Errors

also called parallax, is a phenomenon in conventional or → **entocentric lenses**, which causes a change in magnification as it moves in and out from best focus. Closer objects appear larger than objects further away. → **Telecentric lenses** optically correct for this occurrence.

Pixels

or picture elements are tiny squares on the CCD chip. Each pixel represents an area of the image and its intensity is linearly dependent on the charges generated by the incident photons in the corresponding photodiode of the parallel shift array of the CCD chip.

The more pixels in a given image area the higher the resolution of the image is. If a digital image is increasingly enlarged there will come a point, when the individual elements can be seen as separate dots – similar to graining in a silver halide photography – and the more pixels an image contains per area, the more it can be enlarged, before the separate pixels start to show.

The size of the image can be described by its dimensions in numbers of pixels, for example, 1024 x 1024 pixels.

Primary Magnification

is defined as the ratio between the sensor size and the → **Field of View** (FOV), which is correlated with the focal length of the lens and object distance.

Q

Quantum Efficiency (QE) of the camera

is a measure that describes the ability of the CCD to convert the photons that are collected by the photodiodes of the chip into electronic charges, usually given in percent. The QE is a function of the wavelength. Current high resolution chips peak around 550 nm (yellow-green) with about 85% QE equipped with → **lenslets** (on chip microlenses). Back-illuminated chips even top this with more than 90 %.

Quantum Efficiency (QE) of the reaction

The efficiency of a bioluminescent reaction is also described by the quantum efficiency. In this case the ability is meant to convert substrate molecules into photons, given in percent. The bioluminescent reaction of American firefly luciferase and luciferin has a quantum efficiency of 91%, where as bacterial luciferases can have as less as 15%.

Quantum Efficiency (Total)

is defined as the multiplication of → **quantum efficiency of the reaction** and → **quantum efficiency of the camera**.

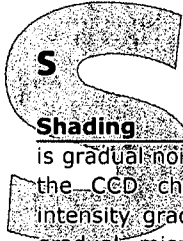
R

Readout Noise

is the noise caused by the camera electronics, mostly by the on-chip preamplifier, upon quantification of the signal but also dependent on the A/D conversion rate. It is of significance only in low light applications.

Resolution (Total)

of an image is a function of → **camera resolution**,
→ **focal length** and → **working distance**.



Shading

is gradual noise and/or sensitivity variations across the CCD chip and the corresponding inherent intensity gradients in the images. The cause is a gradual mismatch of photodiodes and on-chip microlenses.

Signal Noise (Photon Noise, Shot Noise)

Light has an inherent noise that derives from the stochastic nature of the photon flux and equals the square root of the intensity. For a signal of 100 photons a noise of 10 photons or 10% results, while for 10,000 photons it is only 1% (100 photons).

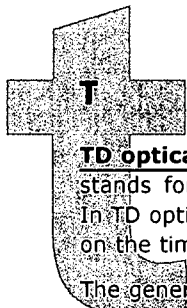
Since this noise is caused by the natural statistical variation of the light, it is not influenced by the camera design. Binning reduces the signal noise.

Slow-Scan CCD Cameras

CCD cameras are often termed slow-scan cameras because their standard frame rate is usually less than that of a video camera. The "scan" derives from the fact that the data readout is performed pixel row by pixel row.

System Magnification

is the total magnification from the object to the image on the monitor, which is the product of the → **primary magnification** and the camera-to-monitor magnification (the ratio between the monitor size and the sensor size).



TD optical molecular imaging

stands for Time Domain (TD) optical technology. In TD optical imaging, photons are classified based on the time at which they emerge from the tissue.

The generated time-of-flight distribution (generally referred to as a TPSF or temporal-point-spread-function) can be thought of as a statistical distribution of all possible photon paths between the point of illumination and the point where the light exits the tissue. This distribution can be used to recover the optical characteristics of the specimen and thus discriminate scattering from absorption.

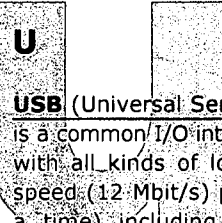
Telecentric Lenses

are parallax-free, that is, the size of an object in the image does not vary with its distance from the lens. For this reason, telecentric lenses find ready application in inspection systems for gauging measurements of objects which may be positioned at variable positions from the camera.

The only difference in the appearance of objects will be how far they are in or out of focus, depending on the depth of focus currently set. Telecentric lenses always have a fixed working distance and field of view.

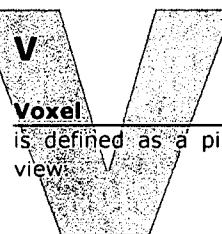
TWAIN

The TWAIN Working Group is a not-for-profit organization which represents the imaging industry. TWAIN's purpose is to provide and foster a universal public standard which links applications and image acquisition devices.



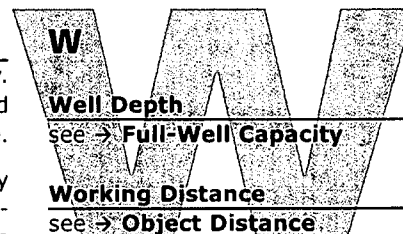
USB (Universal Serial Bus)

is a common I/O interface used to connect computers with all kinds of low-speed (1.5 Mbit/s) and full-speed (12 Mbit/s) peripheral devices (up to 127 at a time), including many cameras. However, for applications requiring high-speed data transfer such as fast imaging it is inferior to the IEEE-1394 (FireWire) standard. The new version 2.0 with 480 Mbit/s (high-speed) is 40 times as fast as USB 1.1.



Voxel

is defined as a picture element in 3-dimensional view.



Well Depth

see → **Full-Well Capacity**

Working Distance

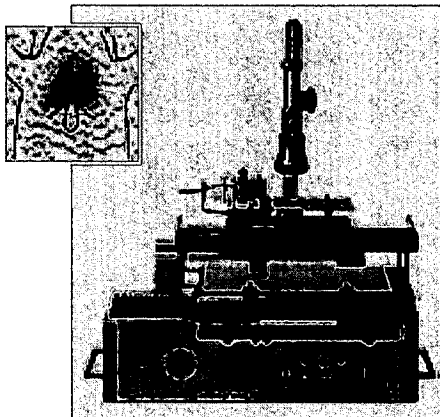
see → **Object Distance**

Exhibit 7

56

BERTHOLD TECHNOLOGIES, one of the pioneers of Molecular Imaging

BERTHOLD TECHNOLOGIES GmbH & Co. KG is located in Bad Wildbad, Germany. The company was founded in 1949 by Prof. Dr. Rudolf Berthold and was named "Laboratorium Prof. Dr. Rudolf Berthold". At the end of the 70ies BERTHOLD developed an animal imager based on a TLC scanner. The results are very rough due to poor resolution.



Since Siemens, Germany, developed a high sensitive intensified CCD camera, and Prof. Szalay became aware of it, the idea was born to monitor non-invasively gene expression in living organisms.

BERTHOLD developed a cabinet for such a camera and the imaging software. In 1989 BERTHOLD introduced its first low light imaging instrument - the LB 980 Luminograph. The first in-vivo gene expression experiments in plants and animals performed on this instrument date back to the year 1993.

It turned out, that intensified CCD cameras had major problems in linearity and dynamic range, so, BERTHOLD introduced slow scan CCD cameras. NightOWL was launched in 1996 as the most sensitive molecular imaging system known for a long time. With NightOWL BERTHOLD made a substantial contribution to the breakthrough of this technology.

Today, a new generation of slow scan CCD cameras is developed based on enhanced sensitive chips. Furthermore, based on the microplate reader technology of BERTHOLD, in LB 983 NightOWL II fluorescence can be performed much better and easily due to high sophisticated lamp and beam control and automated filter changing.



2-Year Factory Warranty on all Berthold Instruments.



BERTHOLD TECHNOLOGIES USA, LLC
99 Midway Lane
Oak Ridge TN 37830

Exhibit 7
57

Phone: 865-483-1488
Fax: 865-425-4309
E-mail: Berthold-US@berthold.com
Internet: <http://www.Berthold-US.com>

EXHIBIT 8

EXHIBIT 8

Exhibit 8
58

detect and identify



NightOWL II LB 983

Superiority in
Molecular Imaging

Exhibit 8
59

2-Year Factory Warranty on all Berthold Instruments.

NightOWL II LB 983

Superiority in Molecular Imaging

Bioluminescence imaging (BLI) and biofluorescence imaging (BFI) make monitoring of gene expression in living organisms possible.



In 1989 BERTHOLD TECHNOLOGIES introduced its first low light imaging instrument – the LB 980 Luminograph. The first in-vivo gene expression experiments in plants and animals were performed on this instrument before 1993.

BLI utilizes light emitted by luciferase enzymes. Today bioluminescence markers can be tailored to any gene, enabling detailed research of gene function. BFI utilizes proteins, which fluoresce under illumination, either applied as exogenous reagents or endogenously expressed. Both BLI and BFI have contributed to the understanding of disease mechanisms and the development of new treatments.

Cameras

Today's generation of low light imagers from BERTHOLD TECHNOLOGIES, the LB 983 NightOWL II, is equipped with cooled slow scan CCD cameras:

- Front-illuminated NC 320 is ideal for fluorescence applications with 3.2 million pixels for high resolution. Micro-lenticular arrays on top of the CCD chip enhance light collection to maximum quantum efficiency of 85 %.
- Back-illuminated NC 100 with high full well capacity for large dynamic range is the appropriate model for luminescence applications. Broadband coating enhances the quantum efficiency in the spectral range between 500 to 750 nm ideally suited for luciferase and GFP emissions. The efficient Peltier cooling keeps the chip temperature low, reducing the dark current and thereby enhancing sensitivity.

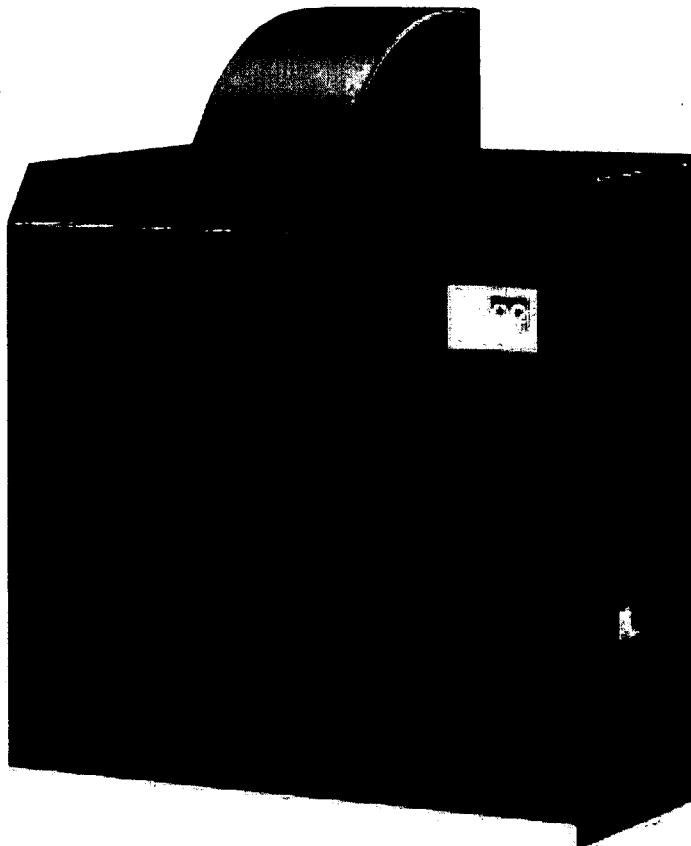
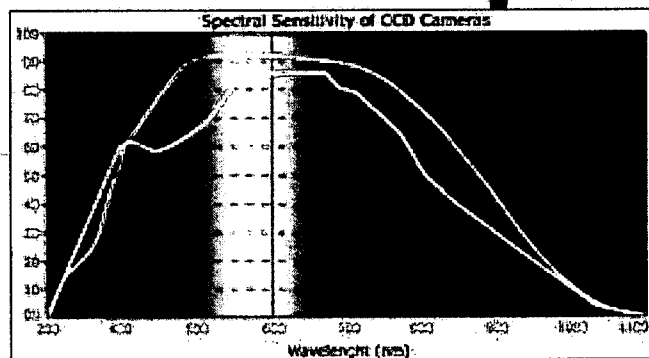


Exhibit 8
60



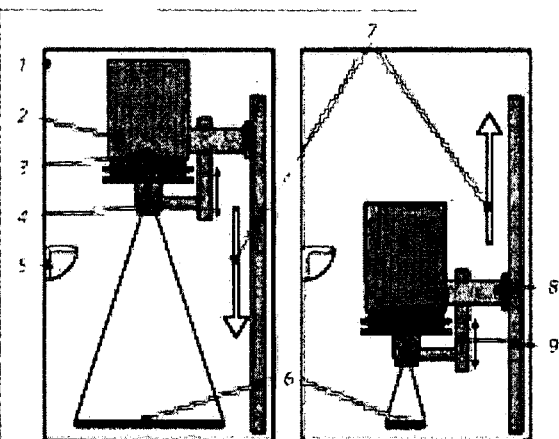
— Camera NC 100

--- Camera NC 320

Cabinet

The NightOWL cabinet is extremely light-tight preventing any interferences from ambient light.

NightOWL is the only imager with a motor-driven camera inside the cabinet. Optimum resolution and focus of the sample is achieved by automatic positioning of the camera according to the actual sample size.



NightOWL dark cabinet

Light-tight housing (1) containing the Peltier cooled CCD camera (2) with a motor-driven vertical adjustment of magnification (7,8), CCD chip (3), the lens (4) with a second vertical precision drive for focus adjustment (9), a fluorescence light source (5) with exchangeable filters, the sample table (6) supporting 2D and 3D objects from 35 (right drawing) to 260 mm (left drawing).

The camera can be moved from a height of 35 mm to 725 mm allowing focussing on every sample size up to 260 mm. For close-ups a macro table can be used.

The camera is set up with flat field and height correction. This calibration eliminates non-uniformities caused by variations in the optical path due to height, illumination or lens effects.

The NightOWL cabinet has enough space to install special light sources or to place transilluminators, heaters, coolers etc. These devices may even be switched on and off through the software and the built-in sockets.

The flange option provides light-tight access to the inner part for tubings and cables.

Fluorescence Reflectance Imaging (FRI)

requires a range of illumination devices to excite the sample from above. As the camera is positioned directly with view to the sample it can easily measure the signals emitted. To excite the fluorophors and measuring its emission, the proper illumination and set of filters have to be chosen.

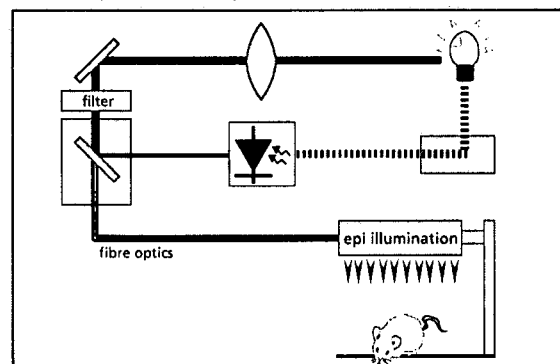
Excitation & Emission Filters

Software-driven filter carriers provide quick change of emission and excitation filters within one reading sequence especially important for all applications with a ratiometric readout. Measurement at different wavelengths at one time can be carried out due to the flexible protocol definition software.

The time for changing the adjacent emission filters is less than 500 ms, much faster than the camera readout. Selected high quality interference filters are mounted in the required positions and additional filters can easily be added by the user.

Optics and lamp control

The unique optical system from the LB 940 Mithras Multimode Reader has been integrated in the NightOWL II model. The light beam is kept constant for each fluorescent measurement, which is ideal with the ring-light epi illumination. If the ring-light is always set at the same height, the excitation energy on the sample will always be the same.



The lamp energy can be set by a lamp factor in the software. This allows calibration of the imaging system for each fluorophor. Comparison of the amounts of different fluorophors in one sample becomes very easy.

detect and identify

indiGO™ Software

The new easy-to-use indiGO™ software has been developed together with users. Well organized menus and dialogue boxes guide the user through camera set-up, image processing and image analysis.



Some techniques for generating and/or detecting light in biological subjects are patented and may require licences from third parties. Users are advised to independently determine for themselves whether their activities infringe any valid patent.

- quantitative analysis
- display of luminescence, fluorescence or photographic images in black & white or pseudocolour
- contrast and image enhancement tools
- colour overlay e.g. photographic image with luminescence image, e.g. fluorescent gel with the hybridization signal, or of various fluorescent images
- line plot function
- surface plot function
- zoom function (up to 5-fold)
- definition of areas of insert and evaluation
- geometrical analysis
- arithmetic functions
- data export into spreadsheet
- raw data and processed data are filed separately (according to GLP rules)
- individual exposures or image sequences
- macro function to automate image processing steps
- image import and export (16-bit TIF file generated by indiGO™ can easily be processed by further software packages, e.g. for multimodality or co-registration)
- printing on any Windows printer via software

Versatility and flexibility

The conditions to image living organisms can be very different. Gas anaesthesia e.g. is nowadays used for small animals but never used in plant imaging. In that case controlling of light, temperature or humidity is more important.

In the field of infectious diseases or food processing the growth of bacteria will be the aim of interest. In dermatology and material science the very faint luminescence of radical oxygen species (ROS) is measured. In live science, quality control or forensic studies you need a very sensitive instrument for Western, Southern and Northern blots.

To cover all these applications an imaging system has to be very flexible. BERTHOLD TECHNOLOGIES ensures such flexibility with the NightOWL itself and provides a huge variety of accessories (please refer to brochure Accessories for NightOWL).

Moving of camera inside the cabinet	✓
Height correction in each position	✓
Enough space inside the cabinet	✓
Easy exchange of camera	✓
Microscope and plant chamber adaption	✓
Power sockets inside the cabinet	✓
Control of interface inside the cabinet	✓
Positioning plates	✓
Macro table	✓
Flange	✓
Gas anaesthesia unit	✓
Workstation	✓
Fluorescence Reflectance Imaging	✓
Ring-light epi illumination	✓
Dual line epi illumination	✓
Gooseneck spot illumination	✓
Transilluminators	✓
Orthogonal 3D-Imaging option	✓
Animal beds for multimodality imaging	✓

EXHIBIT 9

EXHIBIT 9

Exhibit 9
63

detect and identify

Applications*

Whole animals and plants can be imaged as well as blots, gels, microplates, cell culture dishes and arrays regardless of the luminescent or fluorescent markers used. Optical calibration ensures the comparability of all images captured with the NightOWL.

Detection of weak light signals with CCD cameras can be achieved with high quantum efficiencies and extremely low noise levels to enable long exposure times. The camera and cabinet design are the key to superior imaging performance, complemented by scientific evaluation software for quantification.

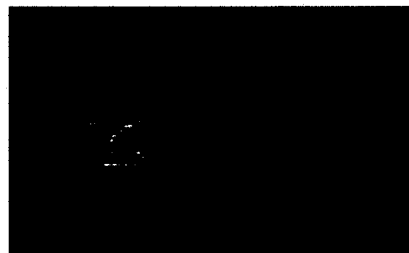
Applications	NC 100	NC 320
Biochip	+	+
Bioluminescence	+++	++
Blot documentation	++	++
Chemiluminescence	+++	++
Colony counting	++	++
Fluorescence	++	+++
Gel documentation	++	++
In vivo Imaging	+++	++
Microplates	+	+
Microscopy	++	+++
Multi-label measurements	+++	++

- In-vivo visualization of reporter gene expression in prokaryotic and eucaryotic cells, in living transgenic animals and plant.



- Visualization of bacterial growth in food
- In-vivo visualization of skin diseases in dermatology
- Research and product optimization in varnish, paint and pigment production
- Imaging of chemiluminescence of solid polymers
- Detection of ROS (reactive oxygen species)
- Forensic Science
- Imaging of microplates: immunoassays, reporter genes detection, gene probes and phagocytosis

- In-vivo visualization of fluorophors, e.g.



Oxazines bound to beta-amyloid deposits as present in Alzheimer's disease.

- In-vivo visualization of infectious diseases



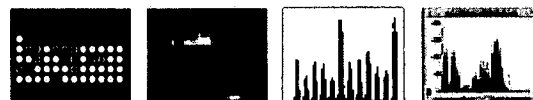
Intraperitoneally inoculated with *Salmonella enteritidis* carrying a lux Operon of *Xenorhabdus luminescens*; exposure time: 60 sec. (Courtesy: P. Hill, Nottingham, UK).

- Study of circadian rhythms via reporter genes in living transgenic plants.



The time-course follows the rhythm of transcription from the CAB2 promoter over 48 hours.

- Gels and blots: imaging and measuring of chemiluminescent stained Southern, Northern and dot blots as well as Western blots.



* Some techniques for generating and/or detecting light in biological subjects are patented and may require licences from third parties. Users are advised to independently determine for themselves whether their activities infringe any valid patent.

NightOWL II LB 983

Technical Specification and Order Information

CCD Cameras	for more information refer also to the brochure of NightOWLcam LB 982
NC 100	back illuminated, 1024 x 1024 pixel, quantum efficiency 90 % at 620 nm, sensitive from 300 to 1050 nm, dynamic range of 82 dB, cooling performance of > -90 °C
NC 320	front illuminated, 2184 x 1472 pixel, quantum efficiency 85% at 600 nm, sensitive from 300 to 1050 nm, dynamic range of 73 dB, cooling performance of > -60 °C
Exposure times	from 30 milliseconds to hours
Pixel binning	variable in x and y to increase sensitivity
Filters	4 excitation filters per slide 4 emission filters per wheel user selectable frame 340 nm up to 1100 nm additional filter slides/wheels available
Light Source	75 W tungsten lamp
Working distance	automated positioning of the camera allows working distances between 35 mm and 725 mm. For working distances below 35 mm the macro table has to be used. Connection to a microscope changes field of view also.
Interfaces	to place transilluminators, heaters, coolers, light sources etc.
Dimensions	122 x 60 x 40 cm (HxWxD)
Weight	85 kg



Order Information	Order Number
NightOWL II LB 983 NC 100 complete incl. Software	40508-10
NightOWL II LB 983 NC 320 complete incl. Software	40508-20

The new indiGO™ software will be available in Q2/2008.

For a huge variety of accessories please see separate brochure. For further information of available filters please see filter data sheet.

Recommended minimum data system:
Pentium 200 MHz, 32 MB RAM, 2 GB hard disk,
true Colour 22" display

BERTHOLD TECHNOLOGIES reserves the right to implement technical improvements and/or design changes without prior notice. NightOWL and indiGO are trademarks of BERTHOLD TECHNOLOGIES.

2-Year Factory Warranty on all Berthold Instruments.

Exhibit 9
65

BERTHOLD
TECHNOLOGIES

BERTHOLD TECHNOLOGIES U.S.A., LLC

99 Midway Lane
Oak Ridge TN 37830

Phone: 865-483-1488
Fax: 865-425-4309
E-mail: Berthold-US@berthold.com
Internet: <http://www.Berthold-US.com>

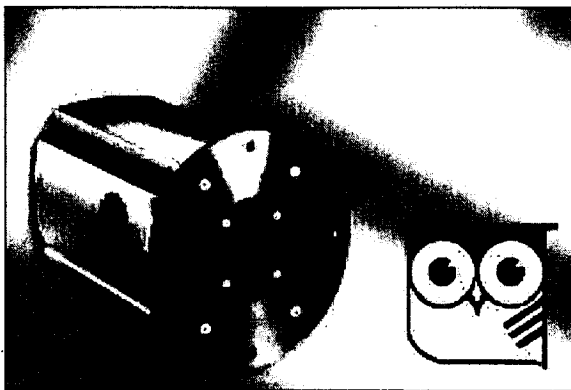
NightOWL II LB 983 · 11-2007 · 3000 · Id.Nr. 40508PR2 Rev. 01

EXHIBIT 10

EXHIBIT 10

Exhibit 10
66

detect and identify



NightOWL II
LB 983 NC 100

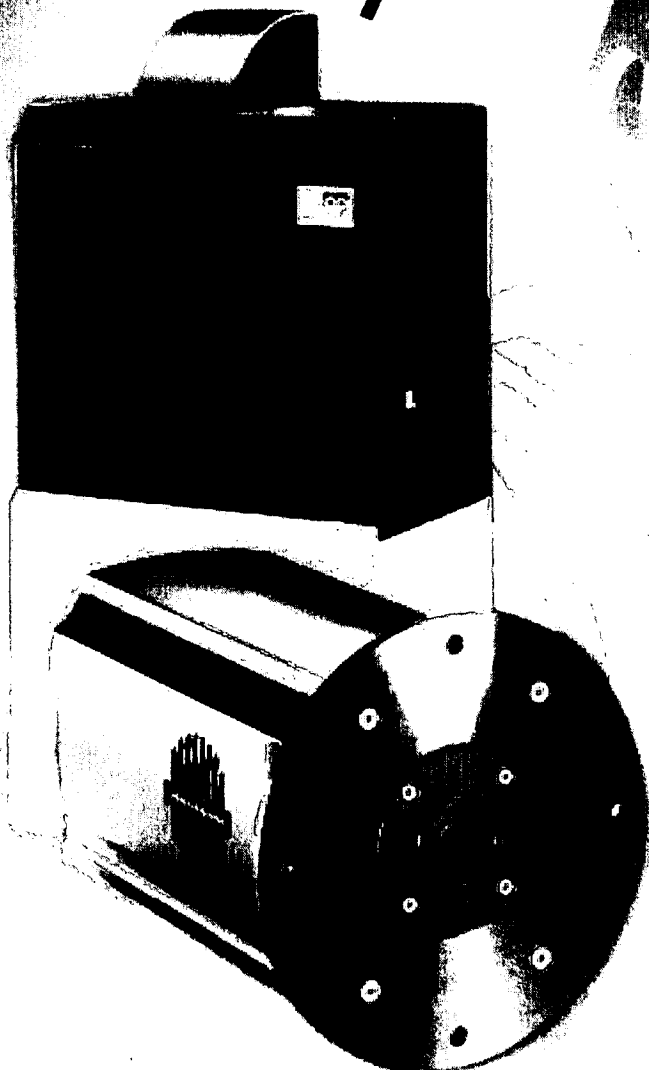
Exhibit 10

67

NightOWL II LB 983 NC 100

Superiority in Molecular Optical Imaging

*Inspired
by nature*



Bioluminescence imaging (BLI) and biofluorescence imaging (BFI) allow monitoring of gene expression in living organisms.



In 1989 BERTHOLD TECHNOLOGIES introduced its first low light imaging instrument – the LB 980 Luminograph. The first in-vivo gene expression experiments in plants and animals were performed on this instrument before 1993.

BLI utilizes light emitted by luciferase enzymes. Today bioluminescence markers can be tailored to any gene, enabling detailed research of gene function. BFI utilizes proteins, which fluoresce under illumination, either applied as exogenous reagents or endogenously expressed. Both BLI and BFI have contributed to the understanding of disease mechanisms and the development of new treatments.

Exhibit 10
68

detect and identify

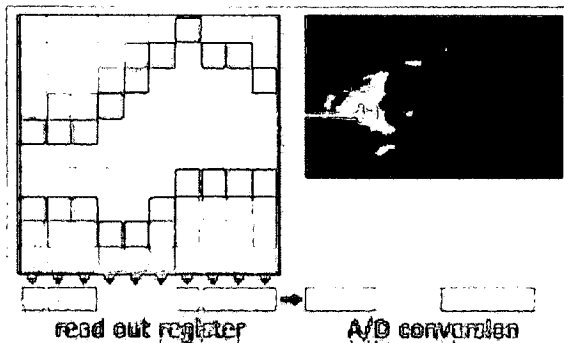


NightOWL II LB 983 NC 100

Superiority in Molecular Optical Imaging

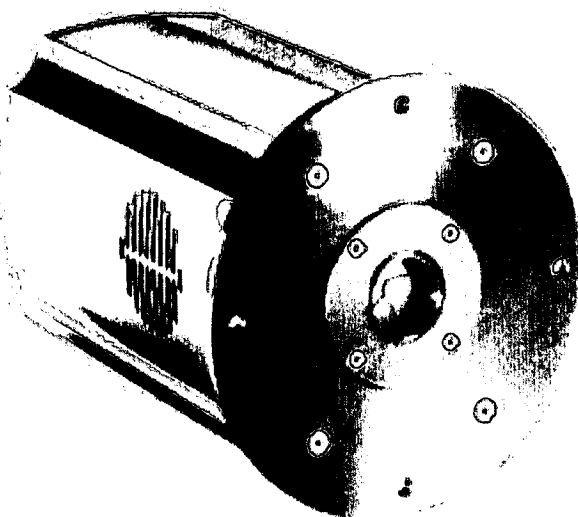
Full-frame CCD cameras

Images are optically projected onto the front of a parallel array acting as the image plane. The array takes the image information and partitions the image into discrete elements. Those elements are defined by the number of pixels thus "quantizing" the image. The resulting rows of image information are then shifted in a parallel fashion to the readout register that subsequently shifts the row of information to the output as a serial stream of data. The process repeats until all rows are transferred off chip.



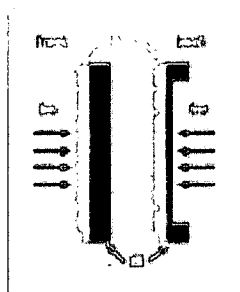
The image is reconstructed as dictated by the system. Since the parallel register is used for both image detection and readout, a mechanical shutter must be used to preserve image integrity.

This technology allows reliable image quantification, which is vital for comparative research.



NightOWLcam NC 100

is an ultra sensitive back-illuminated (or backlit) CCD camera with midband coating enhancing the quantum efficiency up to 90% in the spectral range between 500 – 660 nm, which is optimal for firefly luciferase, GFP and its derivatives.



Back-illumination refers to a method of preparing the CCD sensor in a way that the photons directly strike the light-sensitive thinned back surface, in contrast to conventional CCDs where photons pass through non-light sensitive elements on the front of the CCD with a resulting loss of efficiency.

Today, these systems also have very low noise, and long exposures can therefore be used to integrate the signal over time and to obtain a usable signal.

Noise of a digital image consists of the signal noise and the camera noise which again comprises readout noise and dark noise, which is directly linked to the temperature. Efficient cooling of the array (absolute -80 to -90°C depending on the room temperature) ensures lowest light detection.

Camera	NC 100
CCD array type	back-illuminated
Grade	1
Sensitive area	13.3 x 13.3 mm
Pixel size	13 x 13 μ m
Pixel resolution	1024 x 1024
Spectral range from	300 to 1100 nm
Max. quantum efficiency	90% at 620 nm
80 % quantum efficiency	460-770 nm
Full well capacity	100.000 e-/pix
Readout noise	<3 e- rms

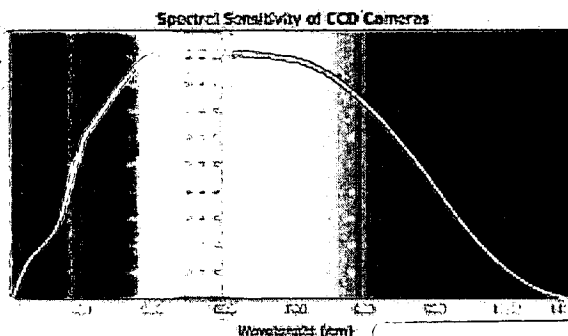
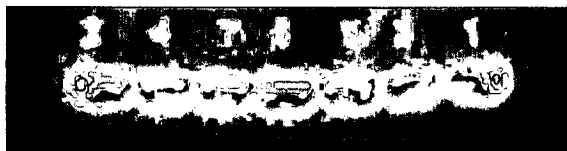


Exhibit 10
70

Versatility and flexibility

The conditions required to image living organisms can be very different. For example, today gas anaesthesia is used for small animals but is never used in plant imaging. For plants control of light, temperature or humidity are of more importance.

In the field of infectious diseases or food processing the study of bacterial growth is the objective. In dermatology and material science the very faint luminescence from free radical oxygen species (ROS) is measured. In life science, quality control or forensic studies you need a very sensitive instrument for Western, Southern and Northern blots.



To cover all these applications BERTHOLD TECHNOLOGIES provides the very flexible low light luminescence and fluorescence imaging system NightOWL and a wide variety of accessories:

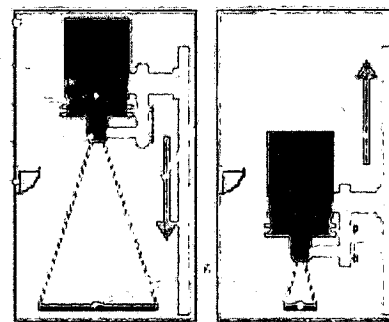
Moving of camera inside the cabinet	✓
Height correction in each position	✓
Large space inside the cabinet	✓
Easy exchange of camera	✓
Microscope and plant chamber adaption	✓
Power sockets inside the cabinet	✓
Control of interface inside the cabinet	✓
Positioning plates	✓
Macro table	✓
Flange	✓
Gas anaesthesia unit	✓
Workstation	✓
Fluorescence Reflectance Imaging	✓
Ring-light epi illumination	✓
Dual Line epi illumination	✓
Gooseneck spot illumination	✓
Transilluminators	✓
Orthogonal 3D-Imaging option	✓
Animal beds for multimodality imaging	✓



Cabinet

The NightOWL cabinet is extremely light-tight preventing any interferences from ambient light.

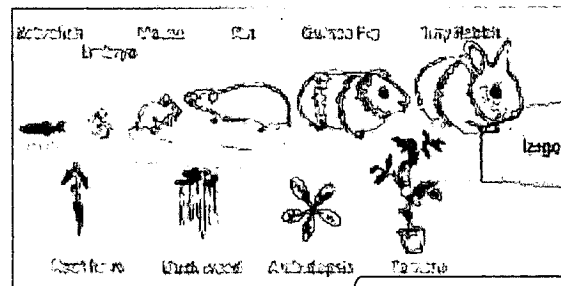
NightOWL is the first imager with a motor-driven camera inside the cabinet. Optimum resolution and focus of the sample is achieved by automatic positioning of the camera according to the actual sample size.



NightOWL dark cabinet

Light-tight housing (1) containing the Peltier cooled CCD camera (2) with a motor-driven vertical adjustment of magnification (7.8), CCD chip (3), the lens (4) with a second vertical precision drive for focus adjustment (9), a fluorescence light source (5) with exchangeable filters, the sample table (6) supporting 2D and 3D objects from 35 (right drawing) to 260 mm (left drawing).

The camera can be moved from a height of 50 mm to 725 mm allowing focussing on every sample size up to 250 mm. For close-ups a macro table can be used. The camera is set up with flat field and height correction. This calibration eliminates non-uniformities caused by variations in the optical path due to height, illumination or lens effects.



NightOWL II LB 983 NC 100

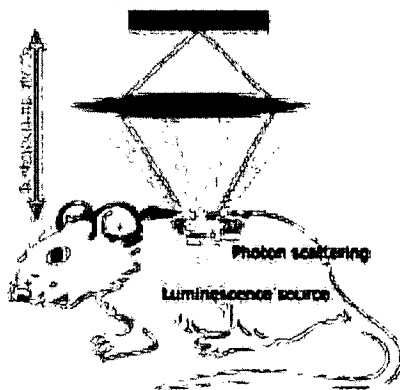
Superiority in Molecular Optical Imaging

Resolution

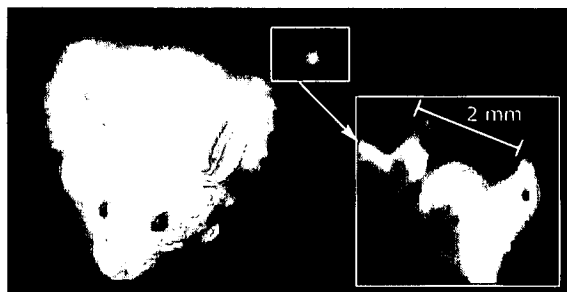
The resolution of an image is a function of camera resolution, focal length and working distance. The NightOWL II allows easy setting of the focal length. Once the sample is positioned, the resolution is automatically calculated. The resolutions are given in the following examples:

Sample size	Resolution
20 cm	200 μ m
10 cm	100 μ m
5 cm	50 μ m
With macro table	
2 cm	20 μ m
1 cm	10 μ m

The closer the camera to the sample the more photons can be collected due to the spherical angle of the lens.



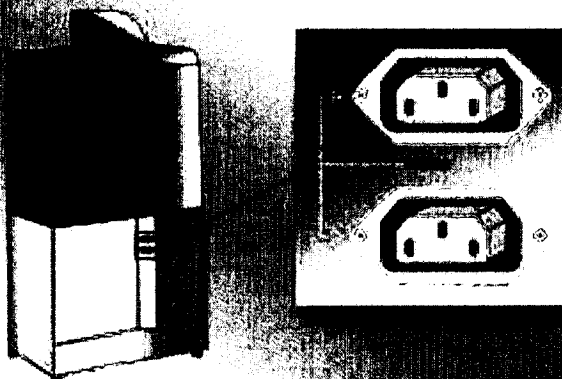
Sometimes small objects have to be acquired. With the macro table the magnification goes up to 5 fold. With another 5-fold digital zoom the overall magnification up to 25-fold can be possible.



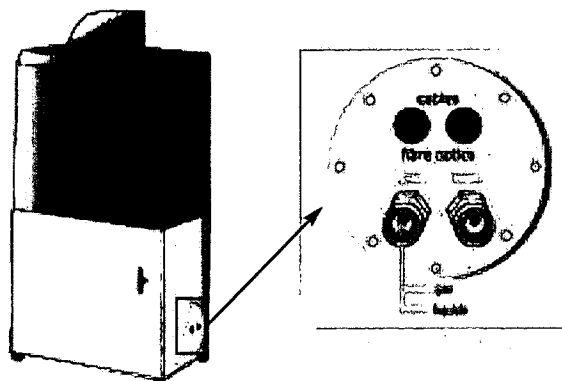
The left hind leg of the anaesthetised mouse is imaged with the gooseneck spot illumination. Only with the macro table it is possible to image the leg between camera and sample. The distance between camera and object was only 2.5 cm (dsRed excitation at 525 nm and emission 605 nm; 3-fold digital magnification of the mouse claw).

Additional features

The NightOWL cabinet has enough space to install special light sources or to place transilluminators, heaters, coolers etc. These devices may even be switched on and off through the software and the built-in sockets. This possibility enables the researcher to add more features into the cabinet. Plant researchers often use special lamps or flash lights in their experiments. Researchers in material science sometimes need special heating devices. The transilluminators are also connected with mains.



The flange option provides light-tight access to the inner part for tubings, cables or even fibre optics, e. g. for special illumination of plants. Such modifications of the flange can be of course customized for special purpose. BERTHOLD TECHNOLOGIES will be pleased to quote for customized flanges.



NightOWL II is equipped with a telescopic table top for easier sample handling. It is very convenient to position and check the samples outside the cabinet and then to slide them inside for acquisition.

Exhibit 10
72

detect and identify

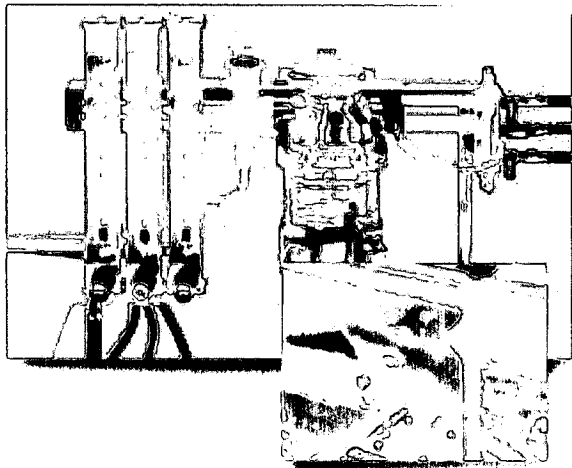
Gas anaesthesia units

During the luminescence or fluorescence image acquisition rodents have to be anaesthetized. In principle, there are two ways: intraperitoneal injection of a liquid mixture of anaesthesia (e. g. ketamine / xylazine or tribromoethanol) or anaesthesia by gaseous isoflurane.

One of the benefits of gas anaesthesia is an increased luminescent signal in rodents by a factor of two compared to tribromoethanol anaesthesia. Breathing is normal, blood pressure and ATP levels are more stable. Gas anaesthesia is less harmful, so rodents can be anaesthetized for longer periods and more often per day, which is an important advantage.

Unit for five rodents

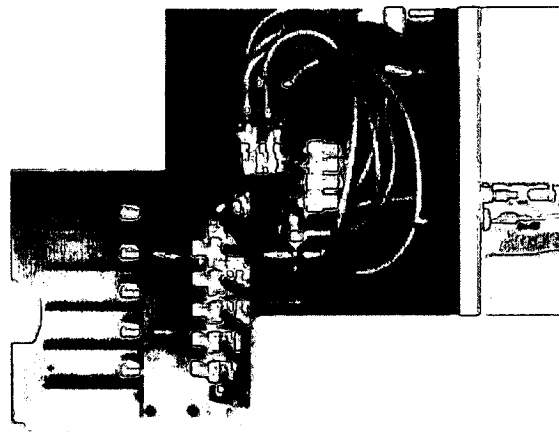
The TEM gas anaesthesia system has been adapted to the NightOWL. The vaporizer system works with low pressure and low flow making sure no gas is leaking from the nozzles and reducing the throughput of isoflurane. A yearly calibration of the vaporizer ensures proper functioning.



The induction box can be used for both mice and rats. In collaboration with INSERM Unité 540, Montpellier, France, a special mouse tray has been developed. Up to five mice can be anaesthetized in parallel in this tray.

The tray is temperature controlled to ensure that body temperature is kept stable during imaging. To prevent crosstalk of light emission from one rodent to the other removable barriers separate five compartments.

The anaesthesia system comes complete, but if pressured air, oxygen line or scavenging line are installed in the lab, the anaesthesia system can be modified accordingly. If any gas anaesthesia unit is already present in the lab, only the inner tray has to be ordered.



Order information

Complete unit for 5 rodents, 220 Volt	41930
Complete unit for 5 rodents, 110 Volt	46238
Inner tray	45941

Single unit

The macro table for LB 983 is covered with a magnetic foil. A magnetic anaesthesia gas nozzle can be mounted in any direction for optimal mouse arrangement under the camera. This single gas nozzle is connected in the same way as the unit for 5 rodents, as is the induction box. Rats can be measured directly on the table since their body temperature is more stable.

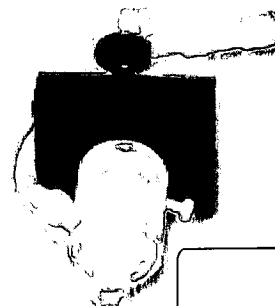


Exhibit 10
73

Order information

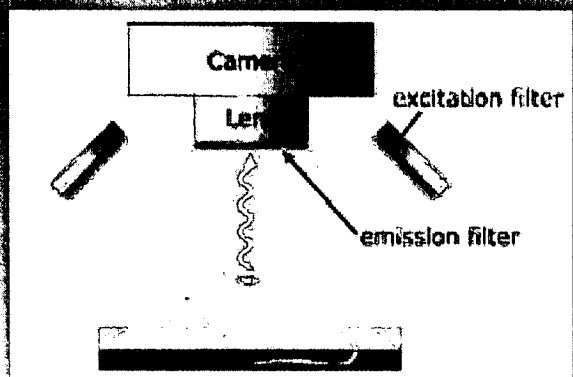
Macro table with temperature control for mice	51578
Single gas nozzle for mice	53192
Single gas nozzle for rats	on request

NightOWL II LB 983 NC 100

Superiority in Molecular Optical Imaging

Fluorescence Reflectance Imaging (FRI)*

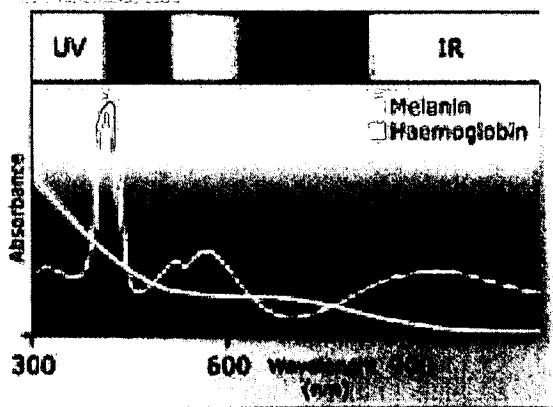
Fluorescence Reflectance Imaging (FRI) is a technique that uses illumination devices to excite the fluorescent source. The signals emitted are detected by the camera. To excite the fluorescent source, the proper wavelength of the excitation light has to be chosen. The emission range of the fluorescent source has to be taken into account.



Schematic set-up of FRI

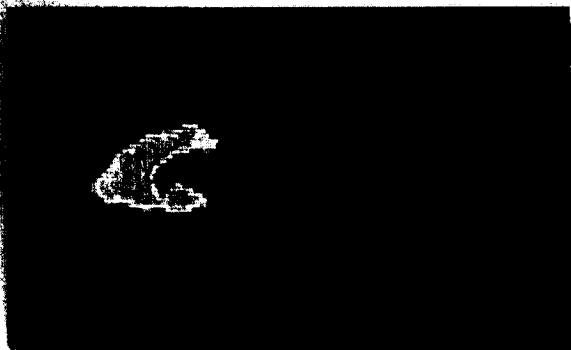
The fluorescence under illumination is either applied as exogenous agent or will be endogenously expressed.

In biofluorescence imaging (BFI) GFP and its derivatives YFP and dsRED are used. The excitation and emission optimum of these dyes are between 470, 500 or 550 nm for excitation and 530 up to 580 nm for emission. In this spectral region melanin in skin and haemoglobin in the blood vessels absorb very strong in animals. Therefore the signal intensity will decrease rapidly the deeper the fluorescent source is in the animal.



Spectral response of Melanin and Haemoglobin

The best spectral range for penetrating an animal is between 600 nm and 900 nm. Therefore near infrared (NIR) fluorescence is a promising technique to get better signals from deep inside the animal. Researchers are developing different dyes for this application. For example Novartis in Switzerland showed the ability to bind oxazines to beta-amyloid deposits present in Alzheimer's disease. Excitation of such dyes is done at 680 nm, emission is in the range of 720 nm.



Oxazine fluorescence in an animal model

Another example of successful application is the use of Quantum Dots® 700 or 800 nm. The shift of these lanthanide complexes are between 470 nm to 700 / 800 nm, additionally, the emission is long (400 ns - 400 ms).



Four different concentrations of Quantum Dots® subcutaneous injected

Another advantage of the IR-region is the low amount of autofluorescence. Other false positive signals can be detected, if too much chlorophyll (strong phosphorescent substance) is in the food. Teeth also often glow due to incorporated phosphorus, as does paper, if treated with phosphate. If plastic devices are used e. g. Petri dishes, osmotic pumps etc. a special IR cut-off filter has to be used to inhibit autofluorescence at around 800 nm.

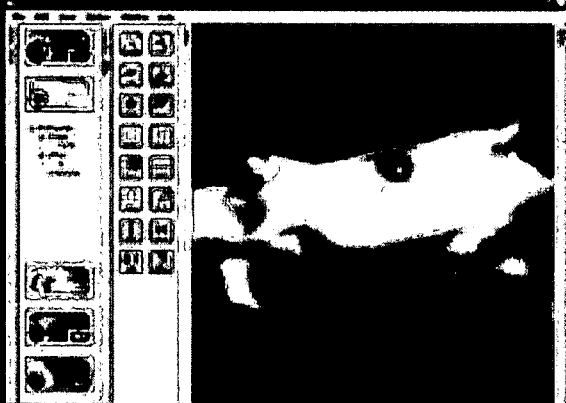
Exhibit 10

74

Exhibit 10
75

NightOWL II LB 983 NC 100

Superiority in Molecular Optical Imaging



- user defined
- quantitative analysis
- display of luminescence, fluorescence or photographic images
- contrast and image enhancement tools
- colour overlay e.g. photographic image with luminescence image, e.g. fluorescent gel with the hybridization signal, or of various fluorescent images
- line plot function
- surface plot function
- zoom function (up to 5-fold)
- definition of areas of interest and evaluation
- geometrical analysis
- arithmetic functions
- data export into spreadsheet
- raw data and processed data are filed separately (according to GLP rules)
- individual exposures or image sequences
- function to automate image processing steps
- image import and export (16-bit TIFF file generated by indiGO™ can easily be processed by further software packages, e.g. for multimodality or co-registration)
- printing on any Windows printer via software
- version can be installed at instrument and office site
- remote control via internet for service and quick assistance

Software Options

The newly developed indiGO™ software allows complete control over the hardware and offers all tools for image evaluation. There are special software needs which BERTHOLD TECHNOLOGIES offers as options, for example

DICOM option
21 CFR part 11 option
geometrical alignment option
etc. for stereo alignment option, etc.

designed for the sequential modus of operation, e.g. several animal beds for sequential imaging, for example

for the sequential modus of operation, e.g. several animal beds for sequential imaging, for example

for the sequential modus of operation, e.g. several animal beds for sequential imaging, for example

Animal bed for YAP-PET Scanner

Multimodality software

Software packages to fuse MRI, PET, SPECT and X-ray CT data are available, since all these imaging technologies offer 3D-data. BLI and FRI data are the planar or 2D, so only the z-plane can be overlaid with the same z-plane of 3D-data. In case the orthogonal 3D-option is used, 3 z-planes can be overlaid. BERTHOLD TECHNOLOGIES will develop a solution to fuse BLI or FRI images with the other imaging technologies.

In case of the software package VINCI from Max-Planck-Institut, Cologne, fts-files can be already implemented.

Exhibit 10

76

detect and identify

Applications

Whole animals and plants can be imaged as well as blots, gels, microplates, cell culture dishes and arrays regardless of the luminescent or fluorescent markers used. Optical calibration ensures the comparability of all images captured with NightOWL.

Detection of weak light signals with CCD cameras can be achieved with high quantum efficiencies and extremely low noise levels to enable long exposure times. The camera and cabinet design are the key to superior imaging performance, complemented by scientific evaluation software for quantification.

Application	NC 100
Biochip	+
Bioluminescence	+++
Blot documentation	++
Chemiluminescence	+++
Colony counting	++
Fluorescence	++
Gel documentation	++
In-vivo Imaging	+++
Microplates	+
Microscopy	++
Multi-label measurements	+++
+good performance ++superior performance +++excellent performance	

All applications and publications are presented on the web page: www.berthold.com/bio.

- In-vivo visualization of reporter gene expression in prokaryotic and eucaryotic cells, in living transgenic animals and plant.



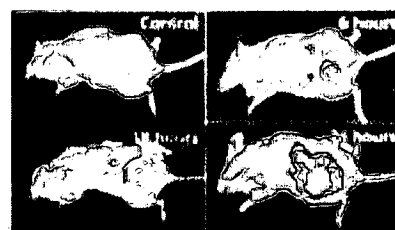
- Visualization of bacterial growth in food
- In-vivo visualization of skin diseases in dermatology
- Research and product optimisation in varnish, paint and pigment production
- Imaging of chemiluminescence of solid polymers
- Detection of ROS (reactive oxygen species)
- Forensic Science
- Imaging of microplates: immunoassays, reporter genes detection, gene probes and phagocytosis

- In-vivo visualization of fluorophors, e.g.



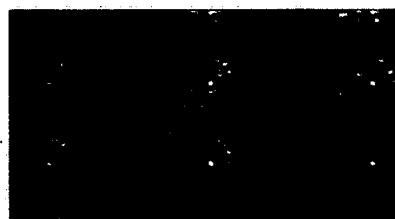
Oxazines bound to beta amyloid deposits as present in Alzheimer's disease.

- In-vivo visualization of infectious diseases



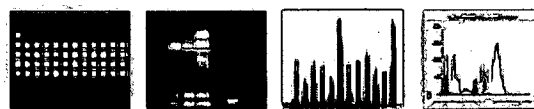
Intraperitoneally inoculated with *Salmonella enteritidis* carrying a lux Operon of *Xenorhabdus luminescens*; exposure time: 60 sec. (Courtesy: P. Hill, Nottingham, UK).

- Study of circadian rhythms via reporter genes in living transgenic plants.



The time-course follows the rhythm of transcription from the CAB2 promoter over 48 hours.

- Gels and blots: imaging and measuring of chemiluminescent stained Southern, Northern and dot blots as well as Western blots.



* Some techniques for generating and/or detecting light in biological subjects are patented and may require licences from third parties. Users are advised to independently determine for themselves whether their activities infringe any valid patent.

Exhibit 10

77

NightOWL II LB 983 NC 100

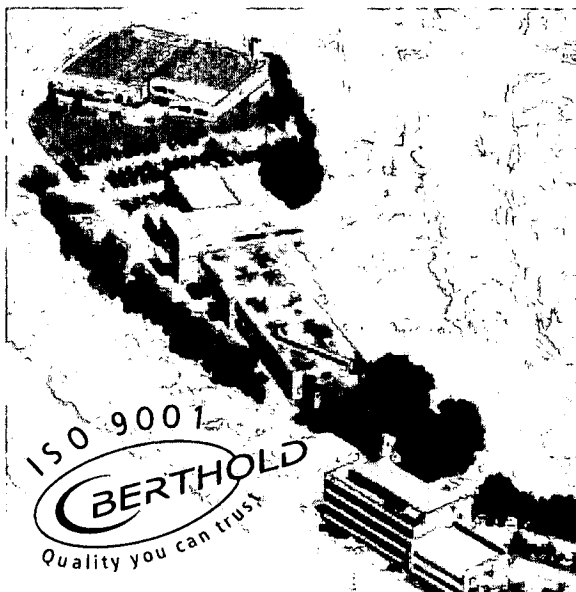
Technical Specification and Order information

NC 100	back illuminated, 1024 x 1024 pixel, quantum efficiency 90 % at 620 nm, sensitive from 300 to 1050 nm, dynamic range of 90 dB, cooling to absolute -80°C to -90°C depending on the room temperature.	
Resolution	Sample size	Resolution
	20 cm	200 µm
	10 cm	100 µm
	5 cm	50 µm
With macro table	2 cm	20 µm
	1 cm	10 µm
Exposure times	from 30 milliseconds to hours	
Pixel binning	variable to increase sensitivity	
Filters	4 excitation filters per slide 4 emission filters per wheel 340 nm up to 1100 nm additional filter slides/wheels available	
Light Source	75 W tungsten lamp	
Working distance	automated positioning of the camera allows working distances between 50 mm and 725 mm. For working distances below 50 mm the macro table has to be used. Connection to a microscope changes field of view also.	
Interfaces	to place transilluminators, heaters, coolers, light sources etc.	
Dimensions	122 x 60 x 40 cm (HxWxD)	
Weight	85 kg	
Regulations	CE, EN	

Laboratory environment	
Power Supply	110-240 V; 50/60 Hz; max 400 VA; minimum 3 sockets
Temperature Range	max 30°C
Humidity	10 - 80%, non condensing
PC Requirements	Pentium processor, 500 MHz (or better), CD ROM drive, 2 GB hard disk (or more), true colour 22" display, serial port, parallel port, free ethernet port (RJ-45 for service remote control), USB
Room	If gas anaesthesia is used room has to be ventilated; pressured air and scavenging line for surplus gas would be an asset.
Bench	stable to sustain 85 kg of the instrument; minimum size 120 x 50 cm (L x D)

Order Information	Order Number
NightOWL II LB 983 NC 100	
complete incl. software	40508-30
For accessories please see separate brochure. For further information of available filters please see filter data sheet.	

BERTHOLD TECHNOLOGIES reserves the right to implement technical improvements and/or design changes without prior notice. NightOWL and indIGO are trademarks of BERTHOLD TECHNOLOGIES. Quantum Dot is a trademark of Invitrogen.



BERTHOLD TECHNOLOGIES GmbH & Co. KG

P.O. Box 100 163
75312 Bad Wildbad
Germany

Exhibit 10
78

Phone: +49 7081 177-0
Fax: +49 7081 177-100
E-mail: Bio@Berthold.com
Internet: www.Berthold.com/Bio

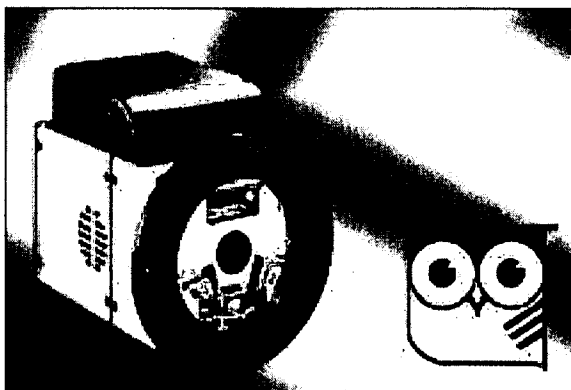
NightOWL II LB 983 NC 100 · 08-2008 · 3000 · Id-Nr. 40508PR2 Rev02

EXHIBIT 11

EXHIBIT 11

Exhibit 11
79

detect and identify



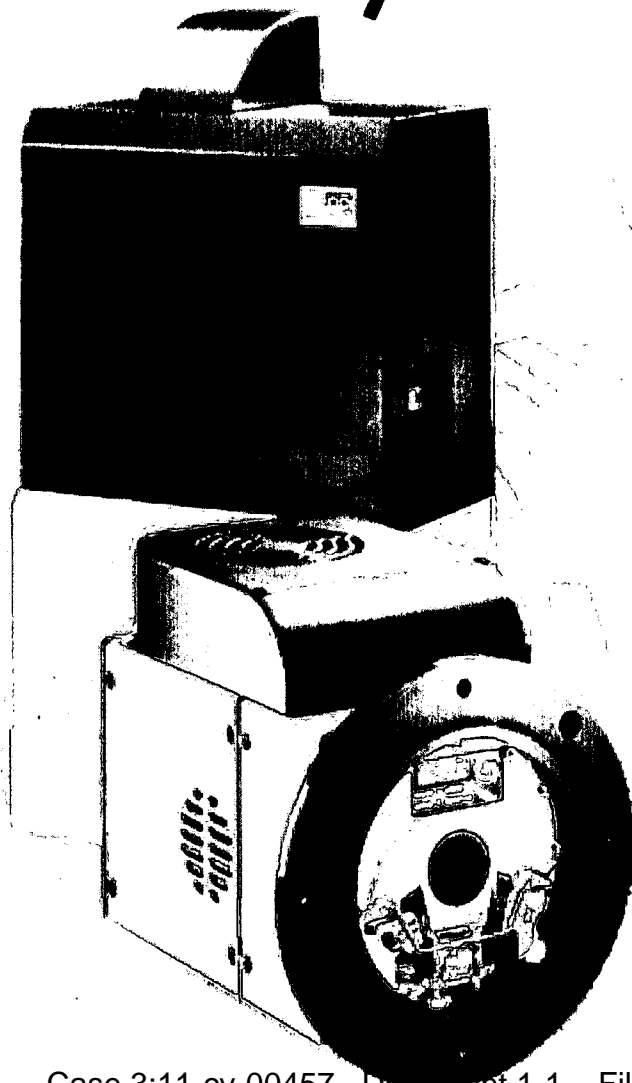
NightOWL II
LB 983 NC 320

Exhibit 11
80

NightOWL II LB 983 NC 320

Superiority in Molecular Optical Imaging

*Inspired
by nature*



Bioluminescence imaging (BLI) and biofluorescence imaging (BFI) allow monitoring of gene expression in living organisms.



In 1989 BERTHOLD TECHNOLOGIES introduced its first low light imaging instrument – the LB 980 Luminograph. The first in-vivo gene expression experiments in plants and animals were performed on this instrument before 1993.

BLI utilizes light emitted by luciferase enzymes. Today bioluminescence markers can be tailored to any gene, enabling detailed research of gene function. BFI utilizes proteins, which fluoresce under illumination, either applied as exogenous reagents or endogenously expressed. Both BLI and BFI have contributed to the understanding of disease mechanisms and the development of new treatments.

Exhibit 11

81

detect and identify

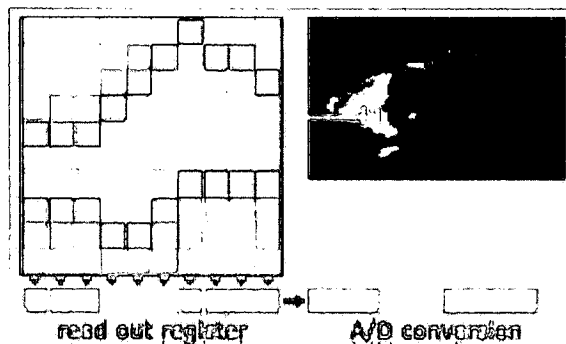


NightOWL II LB 983 NC 320

Superiority in Molecular Optical Imaging

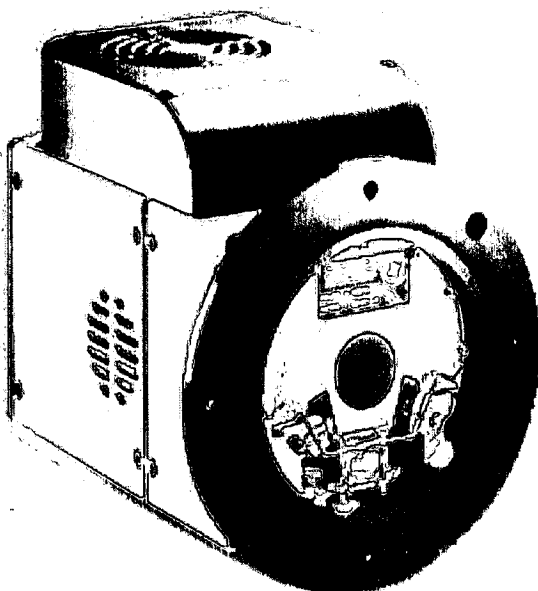
Full-frame CCD cameras

Images are optically projected onto the front of a parallel array acting as the image plane. The array takes the image information and partitions the image into discrete elements. Those elements are defined by the number of pixels thus "quantizing" the image. The resulting rows of image information are then shifted in a parallel fashion to the readout register that subsequently shifts the row of information to the output as a serial stream of data. The process repeats until all rows are transferred off chip.



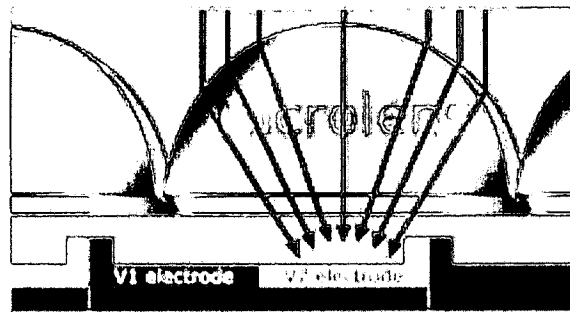
The image is then reconstructed as dictated by the system. Since the parallel register is used for both image detection and readout, a mechanical shutter must be used to preserve image integrity.

This technology allows reliable image quantification, which is vital for comparative research.



NightOWLcam NC 320

is a front-illuminated (or frontlit) CCD camera with a 3.2 Mpixel CCD chip. Such a pixel density results in high optical resolution. Cooling is performed up to 60 °C below ambient temperature, which is efficient in fluorescence.



To improve the sensitivity of the camera, microlens arrays are formed directly over each pixel. These arrays are tiny little lenses ("microlens") which act to focus the light that would normally strike the non-photosensitive areas (V1 electrode) into those regions which are sensitive (V2 electrode). This new technology results in enhancing the quantum efficiency of front-illuminated CCD up to 85%.

Camera	NC320
CCD array type	front-illuminated
Grade	1
Sensitive area	14.8 x 10.3 mm
Pixel size	6.8 x 6.8 μ m
Pixel resolution	2184 x 1472
Spectral range from	400 to 1100 nm
Max. quantum efficiency	90% at 600 nm
80 % quantum efficiency	560-700 nm
Full well capacity	55.000 e-/pix
Readout noise	<12 e- rms

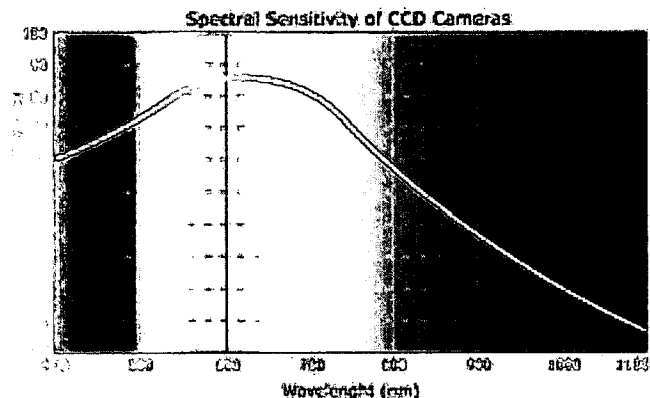


Exhibit 11
83

detect and identify

Versatility and flexibility

The conditions required to image living organisms can be very different. For example, today gas anaesthesia is used for small animals but is never used in plant imaging. For plants control of light, temperature or humidity are of more importance.

In the field of infectious diseases or food processing the study of bacterial growth is the objective. In dermatology and material science the very faint luminescence from free radical oxygen species (ROS) is measured. In life science, quality control or forensic studies you need a very sensitive instrument for Western, Southern and Northern blots.



To cover all these applications BERTHOLD TECHNOLOGIES provides the very flexible low light luminescence and fluorescence imaging system NightOWL and a wide variety of accessories:

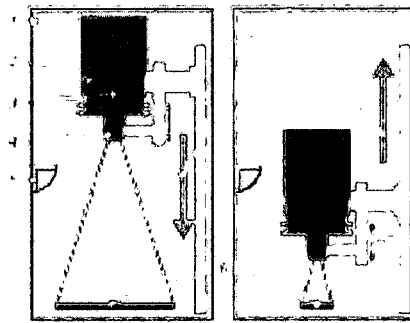
Moving of camera inside the cabinet	✓
Height correction in each position	✓
Large space inside the cabinet	✓
Easy exchange of camera	✓
Microscope and plant chamber adaption	✓
Power sockets inside the cabinet	✓
Control of interface inside the cabinet	✓
Positioning plates	✓
Macro table	✓
Flange	✓
Gas anaesthesia unit	✓
Workstation	✓
Fluorescence Reflectance Imaging	✓
Ring-light epi illumination	✓
Dual Line epi illumination	✓
Gooseneck spot illumination	✓
Transilluminators	✓
Orthogonal 3D-Imaging option	✓
Animal beds for multimodality imaging	✓



Cabinet

The NightOWL cabinet is extremely light-tight preventing any interferences from ambient light.

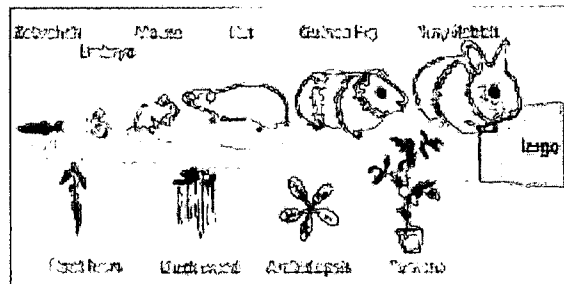
NightOWL is the first imager with a motor-driven camera inside the cabinet. Optimum resolution and focus of the sample is achieved by automatic positioning of the camera according to the actual sample size.



NightOWL dark cabinet

Light-tight housing (1) containing the Peltier cooled CCD camera (2) with a motor-driven vertical adjustment of magnification (7,8), CCD chip (3), the lens (4) with a second vertical precision drive for focus adjustment (9), a fluorescence light source (5) with exchangeable filters, the sample table (6) supporting 2D and 3D objects from 35 (right drawing) to 260 mm (left drawing).

The camera can be moved from a height of 50 mm to 725 mm allowing focussing on every sample size up to 250 mm. For close-ups a macro table can be used. The camera is set up with flat field and height correction. This calibration eliminates non-uniformities caused by variations in the optical path due to height, illumination or lens effects.



NightOWL II LB 983 NC 320

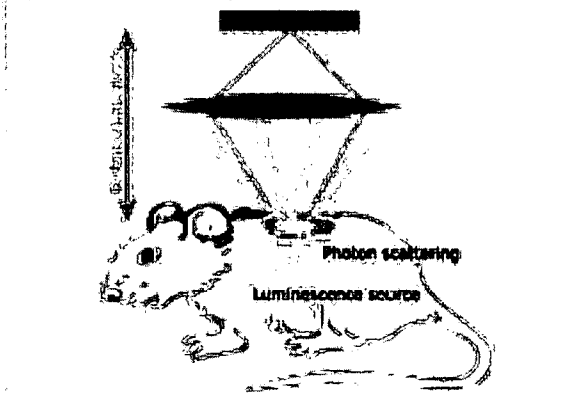
Superiority in Molecular Optical Imaging

Resolution

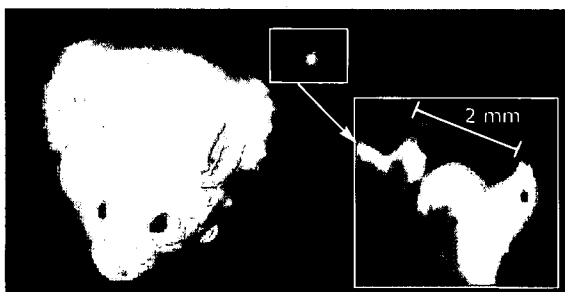
The resolution of an image is a function of camera resolution, wavelength and working distance. NightOWL II allows easy settings of resolution. Once the sample is positioned, the resolutions can be set. The resolutions are given in the following examples:

Sample size	Resolution
20 cm	90 μ m
10 cm	45 μ m
5 cm	23 μ m
With macro table	
2 cm	9 μ m
1 cm	5 μ m

The closer the camera to the sample the more photons can be collected due to the spherical angle of the lens.



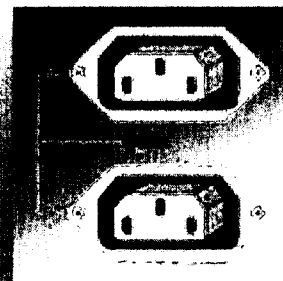
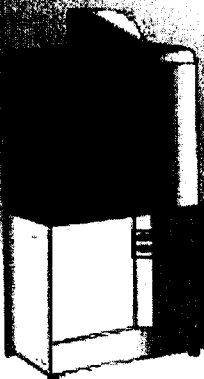
Sometimes small objects have to be acquired. With the macro table the magnification goes up to 5 fold. With another 5-fold digital zoom the overall magnification up to 25-fold can be possible.



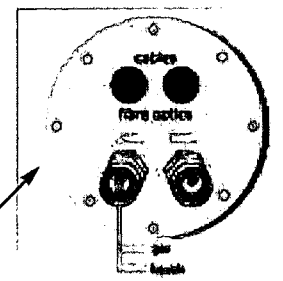
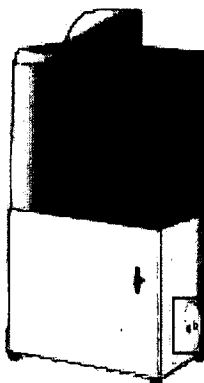
The left hind leg of the anaesthetised mouse is imaged with the gooseneck spot illumination. Only with the macro table it is possible to image the leg between macro table and camera. The distance between camera and object was only 3 cm (dsRed excitation at 525 nm and emission 605 nm; 3-fold digital magnification of the mouse claw).

Additional features

The NightOWL cabinet has enough space to install special light sources or to place transilluminators, heaters, coolers etc. These devices may even be switched on and off through the software and the built-in sockets. This possibility enables the researcher to add more features into the cabinet. Plant researchers often use special lamps or flash lights in their experiments. Researchers in material science sometimes need special heating devices. The transilluminators are also connected with mains.



The flange option provides light-tight access to the inner part for tubings, cables or even fibre optics, e. g. for special illumination of plants. Such modifications of the flange can be of course customized for special purpose. BERTHOLD TECHNOLOGIES will be pleased to quote for customized flanges.



NightOWL II is equipped with a telescopic table top for easier sample handling. It is very convenient to position and check the samples outside the cabinet and then to slide them inside for acquisition.

Exhibit 11
85

detect and identify

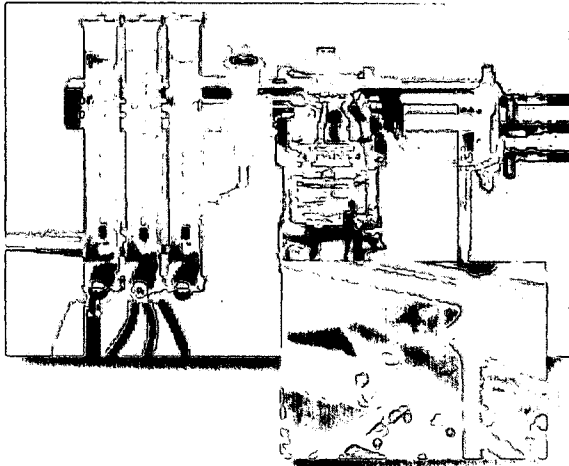
Gas anaesthesia units

During the luminescence or fluorescence image acquisition rodents have to be anaesthetized. In principle, there are two ways: intraperitoneal injection of a liquid mixture of anaesthesia (e. g. ketamine / xylazine or tribromoethanol) or anaesthesia by gaseous isoflurane.

One of the benefits of gas anaesthesia is an increased luminescent signal in rodents by a factor of two compared to tribromoethanol anaesthesia. Breathing is normal, blood pressure and ATP levels are more stable. Gas anaesthesia is less harmful, so rodents can be anaesthetized for longer periods and more often per day, which is an important advantage.

Unit for five rodents

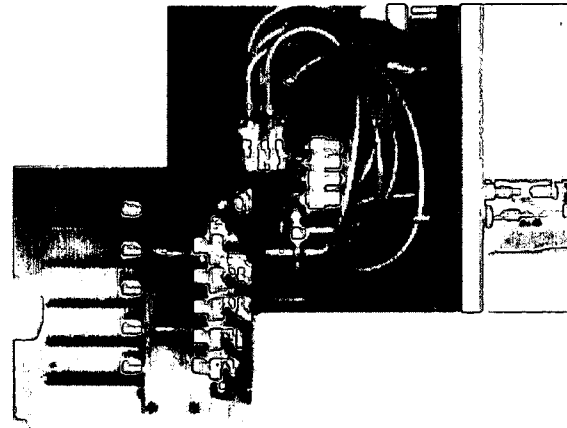
The TEM gas anaesthesia system has been adapted to the NightOWL. The vaporizer system works with low pressure and low flow making sure no gas is leaking from the nozzles and reducing the throughput of isoflurane. A yearly calibration of the vaporizer ensures proper functioning.



The induction box can be used for both mice and rats. In collaboration with INSERM Unité 540, Montpellier, France, a special mouse tray has been developed. Up to five mice can be anaesthetized in parallel in this tray.

The tray is temperature controlled to ensure that body temperature is kept stable during imaging. To prevent crosstalk of light emission from one rodent to the other removable barriers separate five compartments.

The anaesthesia system comes complete, but if pressured air, oxygen line or scavenging line are installed in the lab, the anaesthesia system can be modified accordingly. If any gas anaesthesia unit is already present in the lab, only the inner tray has to be ordered.



Order information

Complete unit for 5 rodents, 220 Volt	41930
Complete unit for 5 rodents, 110 Volt	46238
Inner tray	45941

Single unit

The macro table for LB 983 is covered with a magnetic foil. A magnetic anaesthesia gas nozzle can be mounted in any direction for optimal mouse arrangement under the camera. This single gas nozzle is connected in the same way as the unit for 5 rodents, as is the induction box. Rats can be measured directly on the table since their body temperature is more stable.



Exhibit 11
86

Order information

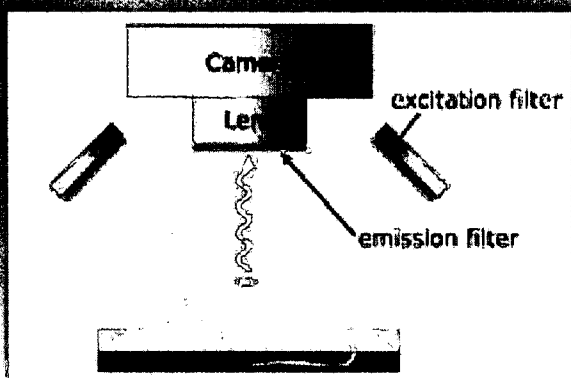
Macro table with temperature control for mice	51578
Single gas nozzle for mice	53192
Single gas nozzle for rats	on request

NightOWL II LB 983 NC 320

Superiority in Molecular Optical Imaging

Fluorescence Reflectance Imaging (FRI)*

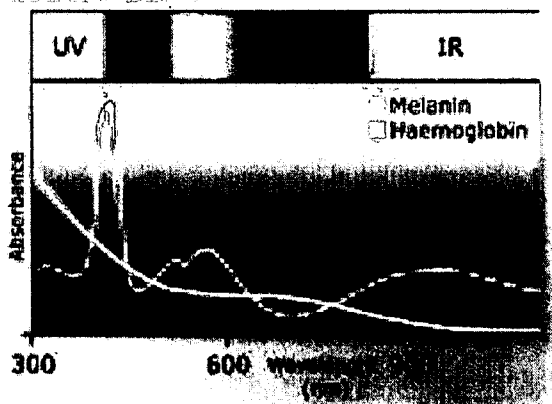
Fluorescence reflectance devices to excite the sample and detect the signals emitted are positioned above the sample. To excite the sample, the proper wavelength of the light source has to be chosen. The emission filter is used to filter the light range of the sample.



Schematic set-up of FRI

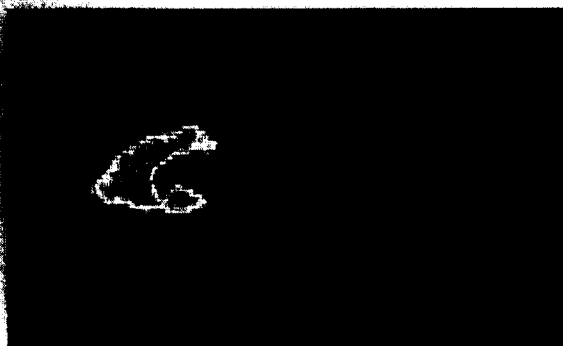
The fluorescence under illumination is either applied as exogenous agent or will be endogenously expressed.

In biofluorescence imaging (BFI) GFP and its derivatives YFP and dsRED are used. The excitation and emission optimum of these dyes are between 470, 500 or 550 nm for excitation and 530 up to 580 nm for emission. In this spectral region melanin in skin and haemoglobin in the blood vessels absorb very strong in animals. Therefore the signal intensity will decrease rapidly the deeper the fluorescent source is in the animal.



Spectral response of Melanin and Haemoglobin

The best spectral range for penetrating an animal is between 600 nm and 900 nm. Therefore near infrared (NIR) fluorescence is a promising technique to get better signals from deep inside the animal. Researchers are developing different dyes for this application. For example Novartis in Switzerland showed the ability to bind oxazines to beta-amyloid deposits present in Alzheimer's disease. Excitation of such dyes is done at 680 nm, emission is in the range of 720 nm.



Oxazine fluorescence

Another example of successful application is the use of Quantum Dots® 700. The shift of these lanthanide complexes (470 nm to 700 / 800 nm), additionally the emission is long (400 ns - 400 ms).



Four different concentrations of Quantum Dots® subcutaneous injected

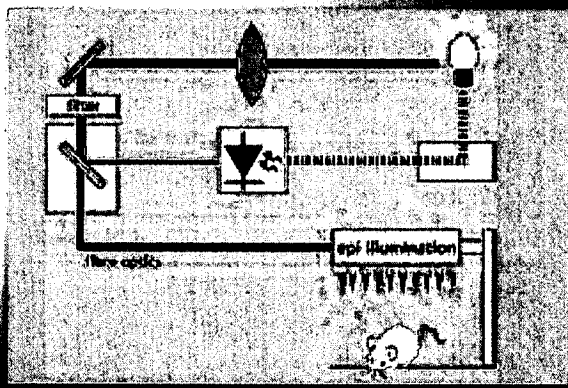
Another advantage of the IR-region is the low amount of autofluorescence. Other false positive signals can be detected, if too much chlorophyll (strong phosphorescent substance) is in the food. Teeth also often glow due to incorporated phosphorus, as does paper, if treated with phosphate. If plastic devices are used e. g. Petri dishes, osmotic pumps etc. a special IR cut-off filter has to be used to inhibit autofluorescence at around 800 nm.

Exhibit 11
87

detect and identify

Optics and illumination

The unique optical system from the LB 9830 Multimode Reader has been integrated into the NightOWL II model. The light beam is kept constant for each fluorescent measurement, which is done with the ring-light epi illumination. If the ring light is always set at the same height, the excitation energy on the sample will always be the same.



The lamp energy can be set by a lamp factor in the software. This allows calibration of the imaging system for each fluorophor. Comparison of the amounts of different fluorophors in one sample becomes possible.

Gooseneck

One of the most important features for researchers is to have a flexible and adjustable light source. The gooseneck light source from the LB 9830 is a perfect tool. It is possible to move the light source in every direction.

The gooseneck light source is a perfect combination of flexibility and stability. The space between the light source and the sample is very small, only the gooseneck can bring light onto the sample (see page 4).

Order information

29663

This document is for generating and/or detecting light in the field of view of the detector and may require licences from the relevant authorities. It is advised to independently determine for each application whether these activities infringe any valid patent.

The LB 9830 Multimode Reader is a powerful tool for the detection and identification of fluorescently labeled samples. It is designed for the detection of low concentrations of fluorescently labeled samples and is suitable for the detection of a wide range of fluorescently labeled samples. The LB 9830 Multimode Reader is a powerful tool for the detection and identification of fluorescently labeled samples. It is designed for the detection of low concentrations of fluorescently labeled samples and is suitable for the detection of a wide range of fluorescently labeled samples.

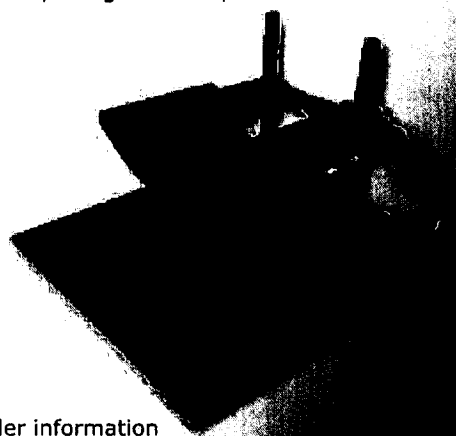
Order information

Ring-light epi illumination for LB 9830

51685

Dual Line epi illumination

This epi illumination option is another alternative for fluorescence illumination to image rats or, if close-up images are required.



Order information

Dual Line epi illumination

Dual Line epi illumination

with temperature control

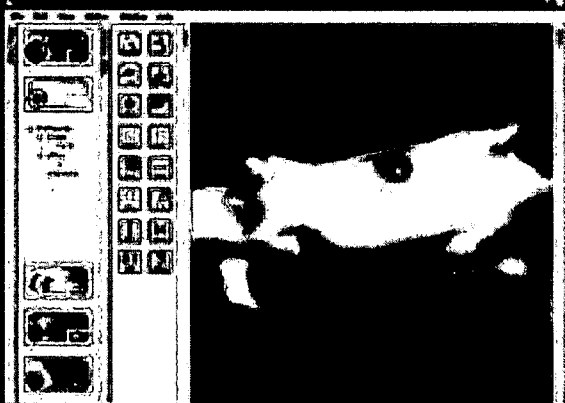
51685

Exhibit 11

88

NightOWL II LB 983 NC 320

Superiority in Molecular Optical Imaging



- user-defined
- quantitative analysis
- display of luminescence, fluorescence, or photographic images
- contrast and image enhancement tools
- colour overlay e.g. photographic image with luminescence image, e.g. fluorescent gel with the hybridization signal, or of various fluorescent images
- line plot function
- surface plot function
- zoom function (up to 5-fold)
- definition of areas of interest and evaluation
- geometrical analysis
- arithmetic functions
- data export into spreadsheet
- raw data and processed data are filed separately (according to GLP rules)
- individual exposures or image sequences
- function to automate image processing steps
- image import and export (16-bit TIFF file generated by indiGO™ can easily be processed by further software packages, e.g. for multimodality or co-registration)
- printing on any Windows printer via software
- version can be installed at instrument and office site
- remote control via Internet for service and quick assistance

Software Options

The newly developed indiGO™ software allows complete control over the hardware and offers all tools for image evaluation. There are special software needs which BERTHOLD TECHNOLOGIES offers as options, for example

- DICOM option
- 21 CFR part 11 option
- animal alignment option
- digital image alignment option, etc.

For the sequential modus of operation, several animal beds for different applications have been developed, for example

- for small animals (e.g. mice)
- for large animals (e.g. rats)
- for human patients (e.g. PET scanner)

Animal bed for YAP-PET Scanner

Multimodality software

Software packages to fuse MRI, PET, SPECT and X-ray CT data are available, since all these imaging technologies offer 3D-data. BLI and FRI data are the planar or 2D, so only the z-plane can be overlaid with the same z-plane of 3D-data. In case the orthogonal 3D-option is used, 3 z-planes can be overlaid. BERTHOLD TECHNOLOGIES will develop a solution to fuse BLI or FRI images with the other imaging technologies.

In case of the software package VINCI from Max-Planck-Institut, Cologne, fts-files can be already implemented.

Exhibit 11

89

detect and identify

Applications¹

Whole animals and plants can be imaged as well as blots, gels, microplates, cell culture dishes and arrays regardless of the luminescent or fluorescent markers used. Optical calibration ensures the comparability of all images captured with NightOWL.

Detection of weak light signals with CCD cameras can be achieved with high quantum efficiencies and extremely low noise levels to enable long exposure times. The camera and cabinet design are the key to superior imaging performance, complemented by scientific evaluation software for quantification.

Application	NC 320
Biochip	++
Bioluminescence	++
Blot documentation	++
Chemiluminescence	++
Colony counting	++
Fluorescence	+++
Gel documentation	++
In-vivo Imaging	++
Microplates	+
Microscopy	+++
Multi-label measurements	++
+good performance ++superior performance +++excellent performance	

All applications and publications are presented on the web page: www.berthold.com/bio.

- In-vivo visualization of reporter gene expression in prokaryotic and eucaryotic cells, in living transgenic animals and plant.



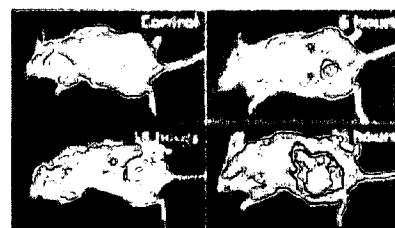
- Visualization of bacterial growth in food
- In-vivo visualization of skin diseases in dermatology
- Research and product optimisation in varnish, paint and pigment production
- Imaging of chemiluminescence of solid polymers
- Detection of ROS (reactive oxygen species)
- Forensic Science
- Imaging of microplates: immunoassays, reporter genes detection, gene probes and phagocytosis

- In-vivo visualization of fluorophors, e.g.



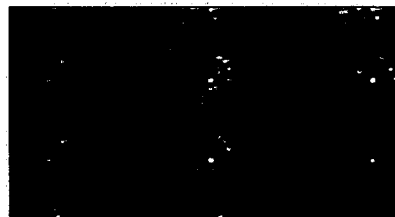
Oxazines bound to beta amyloid deposits as present in Alzheimer's disease.

- In-vivo visualization of infectious diseases



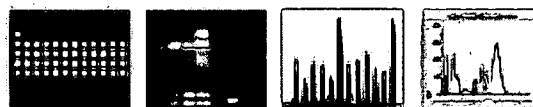
Intraperitoneally inoculated with *Salmonella enteritidis* carrying a lux Operon of *Xenorhabdus luminescens*; exposure time: 60 sec. (Courtesy: P. Hill, Nottingham, UK).

- Study of circadian rhythms via reporter genes in living transgenic plants.



The time-course follows the rhythm of transcription from the CAB2 promoter over 48 hours.

- Gels and blots: imaging and measuring of chemiluminescent stained Southern, Northern and dot blots as well as Western blots.



* Some techniques for generating and/or detecting light in biological subjects are patented and may require licences from third parties. Users are advised to independently determine for themselves whether their activities infringe any valid patent.

Exhibit 11
90

NightOWL II LB 983 NC 320

Superiority in Molecular Optical Imaging

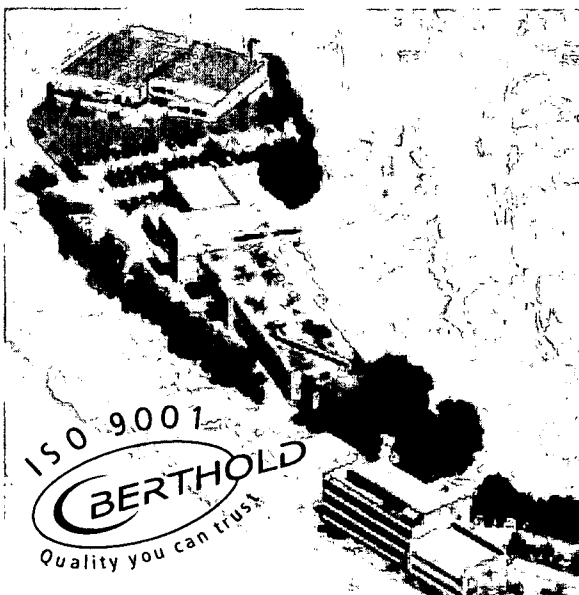
NC 320	front illuminated, 2184 x 1472 pixel, quantum efficiency 85% at 600 nm, sensitive from 300 to 1050 nm, dynamic range of 73 dB, cooling to absolute -30°C to -40°C depending on the room temperature.	
Resolution	Sample size	Resolution
	20 cm	90 µm
	10 cm	45 µm
	5 cm	23 µm
With macro table	2 cm	9 µm
	1 cm	5 µm
Exposure times	from 30 milliseconds to hours	
Pixel binning	variable to increase sensitivity	
Filters	4 excitation filters per slide	
	4 emission filters per wheel	
	340 nm up to 1100 nm	
	additional filter slides/wheels available	
Light Source	75 W tungsten lamp	
Working distance	automated positioning of the camera allows working distances between 50 mm and 725 mm. For working distances below 50 mm the macro table has to be used. Connection to a microscope changes field of view also.	
Interfaces	to place transilluminators, heaters, coolers, light sources etc.	
Dimensions	122 x 60 x 40 cm (HxWxD)	
Weight	85 kg	
Regulations	CE, EN	

Laboratory environment	
Power Supply	110-240 V; 50/60 Hz; max 400 VA; minnum 3 sockets
Temperature Range	max 30°C
Humidity	10 - 80%, non condensing
PC Requirements	Pentium processor, 500 MHz (or better), CD ROM drive, 2 GB hard disk (or more), true colour 22" display, serial port, parallel port, free ethernet port (RJ-45 for service remote control), USB
Room	if gas anaesthesia is used room has to be aerated; pressured air and scavenging line for surplus gas would be an asset.
Bench	stable to sustain 85 kg of the instrument; minimum size 120 x 50 cm (L x D)

Order Information	Order Number
NightOWL II LB 983 NC 320	
complete incl. Software	40508-20

For accessories please see separate brochure. For further information of available filters please see filter data sheet.

BERTHOLD TECHNOLOGIES reserves the right to implement technical improvements and/or design changes without prior notice. NightOWL and indigo are trademarks of BERTHOLD TECHNOLOGIES. Quantum Dot is a trademark of Invitrogen.



BERTHOLD
TECHNOLOGIES

BERTHOLD TECHNOLOGIES GmbH & Co. KG

P.O. Box 100 163
75312 Bad Wildbad
Germany

Exhibit 11
91

Phone: +49 7081 177-0
Fax: +49 7081 177-100
E-mail: Bio@Berthold.com
Internet: www.Berthold.com/Bio

NightOWL II LB 983 NC 320 - 08-2008 - 3000 - Id-Nr: 40508-20PR2 Rev00

EXHIBIT 12

EXHIBIT 12

Exhibit 12
92



detect and identify

Search

Bioanalytic

Home

[Home](#) > [Bioanalytic](#) > [Products](#) > [NightOWL](#) > Literature

Literature about Imaging with NightOWL

Contact

Products

Applications

News

BLI in vivo of pancreatic tumours: Zumsteg et al.(2010):

A bioluminescent mouse model of pancreatic β -cell carcinogenesis; *Carcinogenesis*, doi:10.1093/carcin/bgq109

BLI in vivo of lung chimeras: Zhou et al.(2010):

Chimeric mouse tumor models reveal differences in pathway activation between ERBB family- and KRAS-dependent lung adenocarcinomas; *Nature Biotechnology* 28, 71 - 78 (2010)

Bioluminescence Imaging of cells: Kimura et al.(2010):

Functional molecular imaging of ILK-mediated Akt/PKB signaling cascades and the associated role of β -parvin; *Journal of Cell Science* 123, 747-755 (2010)

BFI in vivo of tumour mice with DiD: Morille et al.(2010):

Long-circulating DNA lipid nanocapsules as new vector for passive tumor targeting; *Biomaterials*, Volume 31; Issue 2, January 2010, Pages 321-329

BLI in vivo: Le Gall (2010):

A Novel Cationic Lipophosphoramidate with Diunsaturated Lipid Chains: Synthesis, Physicochemical Properties, and Transfection Activities; *J. Med. Chem.*, DOI: 10.1021/jm900897a

Review: Leblond et al.(2010):

Pre-clinical whole-body fluorescence imaging: Review of instruments, methods and applications; *Journal of Photochemistry and Photobiology B: Biology*, Volume 98, Issue 1, 21 January 2010, Pages 77-94

BFI in vivo of tumour mice with GFP: Jiang et al.(2009):

The combined status of ATM and p53 link tumor development with therapeutic response; *Genes & Dev.* 2009. 23: 1895-1909

BFI in vivo with Quantum Dots: Higuchi et al. (2009):

Development of multifunctional quantum dots for tracing cells by fluorescence imaging in vivo; *Medical Science Digest* Vol 35 (13), 2009

BLI of retinoblastoma growth and metastasis: Ji et al.(2009):

Non-invasive visualization of retinoblastoma growth and metastasis via bioluminescence imaging; *Association for Research in Vision and Ophthalmology*, doi:10.1167/iov.08-3258

BFI in vivo of lung tumour cells: Emmrich et al(2009):

Antisense gapmers selectively suppress individual oncogenic p73 splice isoforms and inhibit tumor growth in vivo; *Molecular Cancer* 2009 :61 doi:10.1186/1476-4598-8-61

BLI of prostate tumour cells: Le Pivert et al. (2009):

Percutaneous Tumor Ablation: Microencapsulated Echo-guided Interstitial Chemotherapy Combined with Cryosurgery Increases Necrosis in Prostate Cancer; *Technology in cancer research & treatment* 2009, vol. 8, n°3, pp. 207-216

BLI ex vivo of lamb embryos: Moulton et al.(2009):

Ex vivo bioluminescence imaging of late gestation ewes following intrauterine inoculation with lux-modified *Escherichia coli*; *Comparative Immunology, Microbiology and Infectious Diseases*, Volume 32, Issue 5, September 2009, Pages 429-438

BLI in vivo of estrogen receptor in mice: Rando et al. (2009):

Differential effect of pure isoflavones and soymilk on estrogen receptor activity in mice; *Toxicology and Applied Pharmacology*, Volume 237, Issue 3, 15 June 2009, Pages 288-297

Texier & Jossier (2009): In Vivo Imaging of Quantum Dots

In Vivo Imaging of Quantum Dots; *Methods in Molecular Biology™*; Volume 544, pages 393-406

BLI in vivo of bacterial colonization and clearance: Wiles et al. (2009)

Bioluminescent Monitoring of In Vivo Colonization and Clearance Dynamics by Light-Emitting Bacteria; *Methods in Molecular Biology™*; Volume 574, pages 137-153

BLI & Qdot tumour imaging in vivo: Mulder et al.(2009):

Molecular imaging of tumor angiogenesis using $\alpha v \beta 3$ -integrin targeted multimodal quantum dots; *Angiogenesis* Volume 12, Number 1 / März 2009

BLI in vivo of tumour monitoring: Gräser et al.(2009):

Exhibit 12

93

Antimetastatic Effects of Normal Gemcitabine and Empty Liposomes in an Orthotopic Mouse Model of Pancreatic Cancer; *Pancreas*, April 2009 - Volume 38 - Issue 3 - pp 330-337

Bioluminescence imaging in vivo: Liu et al.(2009):

Peripheral Gene Transfer of Glial Cell-Derived Neurotrophic Factor Ameliorates Neuropathic Deficits in Diabetic Rats; *Human Gene Therapy*, July 2009, 20(7): 715-727

BLI in vivo: Medellin-Peña et al.(2009):

Effect of Molecules Secreted by *Lactobacillus acidophilus* Strain La-5 on *Escherichia coli* O157:H7 Colonization; *Applied and Environmental Microbiology*, February 2009, p. 1165-1172, Vol. 75, No. 4

BLI tumour monitoring in vivo + multimodality with µCT and X-ray: Strube et al.(2009):

Sagopilone Inhibits Breast Cancer Bone Metastasis and Bone Destruction Due to Simultaneous Inhibition of Both Tumor Growth and Bone Resorption; *Clinical Cancer Research* 15, 3751, June 1, 2009

BLI in vivo: Granio et al.(2009):

Improved Adenovirus Type 5 Vector-Mediated Transduction of Resistant Cells by Piggybacking on Coxsackie B-Adenovirus Receptor-Pseudotyped Baculovirus; *Journal of Virology*, June 2009, p. 6048-6066, Vol. 83, No. 12

BLI detection of Salmonella: Moza et al.(2009):

Use of bioluminescent *Salmonella enterica* serovar Enteritidis to determine penetration in tumbled and hand-tumbled marinated chicken breast fillets; *J APPL POULT RES* 2009. 18:269-273

BLI in Arabidopsis: Manzano et al.(2009):

Altered Interactions within FY/AtCPSF complexes required for *Arabidopsis* FCA-mediated chromatin silencing; *PNAS* May 26, 2009 vol. 106 no. 21 8772-8777

BLI in vivo in hyperthermic mice: Deckers et al.(2009):

Image-guided, noninvasive, spatiotemporal control of gene expression; *PNAS* January 27, 2009 vol. 106 no. 4 1175-1180

BLI in vivo with thymic electroporation: Irla et al (2008):

ZAP-70 Restoration in Mice by *In Vivo* Thymic Electroporation; *PLoS ONE* 3(4): e2059. doi:10.1371/journal.pone.0002059

BLI in brain sections: Stell et al.(2008):

Molecular Imaging Provides Novel Insights on Estrogen Receptor Activity in Mouse Brain; *Molecular Imaging* 1535-3508, Volume Number: 7, Nov-Dec.2008, pp 283-292

Imaging of biophoton emission from skin: Slawinski & Gorski (2008):

Imaging of biophoton emission from electrostimulated skin acupuncture point jg4: Effect of light enhancers; *Indian Journal of Experimental Biology* Vol 46, May 2008, pp. 340-344

BLI of liver: Chen et al(2008):

Induction of hepatic differentiation of mouse bone marrow stromal stem cells by the histone deacetylase inhibitor VPA; *Journal of Cellular and Molecular Medicine* 10.1111/j.1582-4934.2008.00471

BLI tumour monitoring in vivo: Bauerschlag et al.(2008):

SU11248 (Sunitinib) does inhibit tumor growth and angiogenesis in an ovarian cancer murine xenograft model; *Journal of Clinical Oncology*, 2008 ASCO Annual Meeting Proceedings Vol 26, No 15S (May 20 Supplement), 2008: 16557

BLI in vivo: Fritz et al.(2008):

Antitumoral Activity and Osteogenic Potential of Mesenchymal Stem Cells Expressing the Urokinase-Type Plasminogen Antagonist Amino-Terminal Fragment in a Murine Model of Osteolytic Tumor; *Stem Cells* Vol. 26 No. 11 November 2008, pp. 2981 -2990

BLI in vivo: Mukai et al.(2008):

Renal press-mediated transfection method for plasmid DNA and siRNA to the kidney; *Biochemical and biophysical research communications*, Vol. 372, No. 3. (1 August 2008), pp. 383-387

Reactive Oxygen Species: Hakoziaki et al.(2008):

Visualization and characterization of UVB-induced reactive oxygen species in a human skin equivalent model; *Archives of Dermatological Research*, Volume 300, Supplement 1, April 2008

BLI in vivo: Alajati et al.(2008):

Spheroid-based engineering of a human vasculature in mice; *Nature Methods* - 5, 439 - 445 (2008)

BLI in vivo: Wu et al.(2008):

PROFILING OF ESTROGEN RECEPTOR/SPECIFICITY PROTEIN-DEPENDENT TRANSACTIVATION; *Endocrinology*, doi:10.1210/en.2008-0720

BLI of Arabidopsis: Pien et al.(2008):

ARABIDOPSIS TRITHORAX1 Dynamically Regulates *FLOWERING LOCUS C* Activation via Histone 3 Lysine 4 Trimethylation; *The Plant Cell* 20:580-588

BLI tumour monitoring in vivo: Garcia et al.(2008):

A convenient clinically relevant model of human breast cancer bone metastasis; *Clinical and Experimental Metastasis*, Volume 25, Number 1, March 2008

Exhibit 12
94

▶ **BLI tumour monitoring in vivo: Weibel et al.(2008):**

Colonization of experimental murine breast tumours by *Escherichia coli* K-12 significantly alters the tumour microenvironment; *Cellular Microbiology*, doi:10.1111/j.1462-5822.2008.01122.x

▶ **BLI tumour monitoring in vivo: Bornmann et al. (2008):**

A new liposomal formulation of Gemcitabine is active in an orthotopic mouse model of pancreatic cancer accessible to bioluminescence imaging; *Cancer Chemotherapy and Pharmacology*, Volume 61, Number 3, March 2008

▶ **BLI in vivo and in vitro: Biserni et al.(2008):**

IN VIVO IMAGING REVEALS SELECTIVE PEROXISOME PROLIFERATOR ACTIVATED RECEPTOR MODULATOR (SPPARM) ACTIVITY OF THE SYNTHETIC LIGAND MK-886; *Molecular Pharmacology*, DOI: 10.1124/mol.107.042689

▶ **Digital spectral separation methods for BLI: Wang et al.(2008):**

Digital spectral separation methods and systems for bioluminescence imaging; *Optics Express*, Vol. 16, Issue 3, pp. 1719-1732

▶ **BLI in vivo: Henriquez et al. (2007):**

Advances in optical imaging and novel model systems for cancer metastasis research; *Clinical and Experimental Metastasis*; Volume 24, Number 8, November 2007

▶ **BLI of brain sections: Böer et al.(2007):**

CRE/CREB-Driven Up-Regulation of Gene Expression by Chronic Social Stress in CRE-Luciferase Transgenic Mice: Reversal by Antidepressant Treatment; *PLoS ONE*. 2007; 2(5): e431

▶ **BLI in vivo: Shanker et al.(2007):**

CD8 T Cell Help for Innate Antitumor Immunity; *The Journal of Immunology*, 2007, 179: 6651-6662

▶ **BLI in vivo + multimodality with PET: Ottobriani et al.(2007):**

Development of a bicistronic vector for multimodality imaging of estrogen receptor activity in a breast cancer model: preliminary application; *European Journal of Nuclear Medicine and Molecular Imaging* 10.1007/s00259-007-0578-z

▶ **BLI in vivo: Hattori et al.(2007):**

Non-viral delivery of the connexin 43 gene with histone deacetylase inhibitor to human nasopharyngeal tumor cells enhances gene expression and inhibits in vivo tumor growth; *Int J Oncol*. 2007 Jun; 30 (6):1427-39 17487363

▶ **Bioluminescence in-vivo: Hattori et al.(2007):**

Highly efficient cationic hydroxyethylated cholesterol-based nanoparticle-mediated gene transfer *in vivo* and *in vitro* in prostate carcinoma PC-3 cells; *Journal of Controlled Release* Volume 120, Issues 1-2, 13 July 2007, Pages 122-130

▶ **BLI in vivo: Stell et al.(2007):**

Multimodality imaging: novel pharmacological applications of reporter systems; *Q J Nucl Med Mol Imaging*, 2007 Jun;51(2):127-38

▶ **Review: Instrumentation for molecular imaging: Lecchi et al.(2007):**

Instrumentation and probes for molecular and cellular imaging; *Q J Nucl Med Mol Imaging*, 2007 Jun;51(2):111-26

▶ **BLI tumour monitoring in vivo: Stritzker et al. (2007):**

Tumor-specific colonization, tissue distribution, and gene induction by probiotic *Escherichia coli* Nissle 1917 in live mice; *International Journal of Medical Microbiology*, Volume 297, Issue 3, 11 June 2007, Pages 151-162

▶ **Western Blot: Tsai et al (2007):**

Injury-Induced Janus Kinase/Protein Kinase C-Dependent Phosphorylation of Growth-Associated Protein 43 and Signal Transducer and Activator of Transcription 3 for Neurite Growth in Dorsal Root Ganglion; *Journal of Neuroscience Research*, Volume 85 Issue 2, Pages 321 - 331

▶ **BLI in vivo and in vitro: Eefting et al.(2007):**

Prolonged *In Vivo* Gene Silencing by Electroporation-Mediated Plasmid Delivery of Small Interfering RNA; *Human Gene Therapy*, doi:10.1089/hum.2006.176.

▶ **BLI in vivo: Hattori et al. (2007):**

Non-viral delivery of the connexin 43 gene with histone deacetylase inhibitor to human nasopharyngeal tumor cells enhances gene expression and inhibits in vivo tumor growth; *Int J Oncol* 2007 Jun; 30 (6):1427-39

▶ **BLI in vivo of tumour cells: Hattori & Maitani (2007):**

DNA/Lipid complex incorporated with fibronectin to cell adhesion enhances transfection efficiency in prostate cancer cells and xenografts; *Biol Pharm Bull*. 2007 Mar;30(3):603-7

▶ **BLI in vivo: Houten et al. (2007):**

In vivo imaging of FXR activity reveals the ileum as the primary bile acid signaling tissue; *Molecular Endocrinology*, doi:10.1210/me.2007-0113

▶ **BLI of plant leaves: Doukhanina et al. (2007):**

Expression of Human Nuclear Receptors in Plants for the Discovery of Plant-Derived Ligands; *Journal of Biomolecular Screening*, Vol. 12, No. 3, 385-395 (2007)

▶ **BLI in vivo: Ciana et al. (2007):**

A Novel Peroxisome Proliferator-Activated Receptor Responsive Element-Luciferase Reporter Mouse Reveals Gender Specificity of Peroxisome Proliferator-Activated Receptor Activity in Liver; *Molecular Endocrinology* 21 (2): 388-400

Exhibit 12
95

- Reactive oxygen species: Shimura et al. (2006):**
Generation and distribution of reactive oxygen species in the skin of hairless mice under UVA: studies on in vivo chemiluminescent detection and tape stripping methods; *Experimental Dermatology* 15 (11), 891-899.
- BLI in vivo: Hyoudou et al. (2006):**
Analysis of in vivo NF-kappaB Activation during Liver Inflammation in Mice: Prevention by Catalase Delivery; *Molecular Pharmacology*, DOI: 10.1124/mol.106.027169
- BLI of Salmonella: Moulton et al. (2006):**
Use of glycerol as an optical clearing agent for enhancing photonic transference and detection of Salmonella typhimurium through porcine skin; *Journal of Biomedical Optics*, Volume 11, Issue 5, 054027
- Molecular Imaging - Review: Ottobri et al. (2006):**
Molecular imaging: A new way to study molecular processes in vivo; *Molecular and Cellular Endocrinology* 246 (2006) 69-75
- Circadian rhythms: Allen et al. (2006):**
Arabidopsis PHY3 Specifically Gates Phytochrome Signaling to the Circadian Clock; *The Plant Cell*, 10.1105/tpc.105.037358
- BLI tumour monitoring in vivo: Annicotte et al. (2006):**
Peroxisome Proliferator-Activated Receptor Regulates E-Cadherin Expression and Inhibits Growth and Invasion of Prostate Cancer; *Molecular and Cellular Biology*, October 2006, p. 7561-7574, Vol. 26, No. 20
- BLI in vivo monitoring of tumour cells: Hyoudou et al. (2006):**
Inhibition of adhesion and proliferation of peritoneally disseminated tumor cells by pegylated catalase; *Clinical and Experimental Metastasis*, Volume 23, Numbers 5-6, November 2006
- Circadian rhythms: Devlin et al. (2006):**
PHOTOMORPHOGENESIS IN PLANTS AND BACTERIA; *Springer Netherlands* DOI 10.1007/1-4020-3811-9
- Luminescence AHL detection in bacteria: Janssens et al. (2006):**
Synthesis of N-Acyl Homoserine Lactone Analogues Reveals Strong; *Appl Environ Microbiol.* 2007 January; 73(2): 535-544.
- Blots: Subbaiah et al. (2006):**
Mitochondrial localization and putative signaling function of sucrose synthase in maize; *J. Biol. Chem.* 10.1074/jbc.M600355200
- BLI of implanted cells: Lemaire et al. (2006):**
Identification of New Human PXR Ligands among Pesticides Using a Stable Reporter Cell System; *Toxicological Sciences*, doi:10.1093/toxsci/kfj173
- BLI in vivo of virus in salmonids: Harmache et al. (2006):**
Bioluminescence Imaging of Live Infected Salmonids Reveals that the Fin Bases Are the Major Portal of Entry for Novirhabdovirus; *Journal of Virology*, April 2006, p. 3655-3659, Vol. 80, No. 7
- Bioluminescence monitoring in vivo: Suzuki et al. (2006):**
Plasmid DNA Sequences Present in Conventional Herpes Simplex Virus Amplicon Vectors Cause Rapid Transgene Silencing by Forming Inactive Chromatin; *Journal of Virology*, April 2006, p. 3293-3300, Vol. 80, No. 7
- Reactive oxygen species: Fujimori et al. (2006):**
Orally active antioxidative copper(II) aspirinate: synthesis, structure characterization, superoxide scavenging activity, and in vitro and in vivo antioxidative evaluations; *J Biol Inorg Chem.* 2005 Dec;10(8):831-41. Epub 2005 Oct 28
- BLI in vivo: Verhaagh et al. (2006):**
Human CD46-transgenic mice in studies involving replication-incompetent adenoviral type 35 vectors; *J Gen Virol* 87 (2006), 255-265; DOI 10.1099/vir.0.81293-0
- Circadian rhythms: Li et al. (2005):**
Independent Roles for EARLY FLOWERING 3 and ZEITLUPE in the Control of Circadian Timing, Hypocotyl Length, and Flowering Time; *Plant Physiology* 139:1557-1569 (2005)
- Review: Reporter mice and drug discovery: Maggi & Ciana (2005):**
Reporter mice and drug discovery and development; *Nature Review Drug Discovery* 2005 Mar;4(3):249-55
- BLI in vivo of Leishmania in mice: Lang et al. (2005):**
Bioluminescent Leishmania expressing luciferase for rapid and high throughput screening of drugs acting on amastigote-harboring macrophages and for quantitative real-time monitoring of parasitism features in living mice; *Cellular Microbiology* Volume 7 Issue 3 Page 383-392, March 2005
- Bioluminescent Assay in Vibrio: De Keersmaecker et al. (2005):**
Chemical Synthesis of (S)-4,5-Dihydroxy-2,3-pentanedione, a Bacterial Signal Molecule Precursor, and Validation of Its Activity in Salmonella typhimurium; *J. Biol. Chem.*, Vol. 280, Issue 20, 19563-19568, May 20, 2005
- BLI in vivo: Ciana et al. (2005):**
Estrogenic Activities in Rodent Estrogen-Free Diets; *Endocrinology* Vol. 146, No. 12 5144-5150
- Reactive oxygen species: Sakurai et al. (2005):**

Exhibit 12
96

Detection of reactive oxygen species in the skin of live mice and rats exposed to UVA: a research review on chemiluminescence and trials for UVA protection; *Photochem. Photobiol. Sci.*, 2005, 4, 715 - 720, DOI: 10.1039/b417319h

▶ **BLI in vivo of estrogen-responsive cells in tumours: Pillon et al. (2005):**

In vivo bioluminescence imaging to evaluate estrogenic activities of endocrine disrupters; *Analytical Biochemistry*, Volume 340, Issue 2, 15 May 2005, Pages 295-302

▶ **Bioluminescent imaging of gene expression and tumor progression - review: Löwik et al. (2005):**

Noninvasive Real-Time In Vivo Bioluminescent Imaging of Gene Expression and of Tumor Progression and Metastasis; *Molecular Imaging*, Volume 49, pages 193-227

▶ **Bioluminescent AHL detection in Pseudomonas: Aendekerk et al. (2005):**

The MexGHI-OpmD multidrug efflux pump controls growth, antibiotic susceptibility and virulence in *Pseudomonas aeruginosa* via 4-quinolone-dependent cell-to-cell communication; *Microbiology* 151 (2005), 1113-1125; DOI 10.1099/mic.0.27631-0

▶ **Circadian rhythms: Kim et al. (2005):**

Independent Roles for EARLY FLOWERING 3 and ZEITLUPE in the Control of Circadian Timing, Hypocotyl Length, and Flowering Time; *Plant Physiology* 139:1557-1569 (2005)

▶ **Chemiluminescent immunoblot: Stritzker et al. (2005):**

Enhanced Synthesis of Internalin A in *aro* Mutants of *Listeria monocytogenes* Indicates Posttranscriptional Control of the *inlAB* mRNA; *Journal of Bacteriology*, April 2005, p. 2836-2845, Vol. 187, No. 8

▶ **BLI & BFI (GFP) tumour monitoring in vivo: Li et al. (2005):**

Gene Therapy for Prostate Cancer by Controlling Adenovirus E1a and E4 Gene Expression with PSES Enhancer; *Cancer Research* 65, 1941-1951, March 1, 2005

▶ **Luciferase detection in cells: Pillon et al. (2005):**

Binding of Estrogenic Compounds to Recombinant Estrogen Receptor- α : *Environmental Health Perspectives* Volume 113, Number 3, March 2005

▶ **Bioluminescent AHL detection in bacteria: Heurlier et al. (2004):**

Positive Control of Swarming, Rhamnolipid Synthesis, and Lipase Production by the Posttranscriptional RsmA/RsmZ System in *Pseudomonas aeruginosa* PAO1; *Journal of Bacteriology*, May 2004, p. 2936-2945, Vol. 186, No. 10

▶ **Circadian rhythms: Somers et al. (2004):**

The F-Box Protein ZEITLUPE Confers Dosage-Dependent Control on the Circadian Clock, Photomorphogenesis, and Flowering Time; *The Plant Cell* 16:769-782 (2004)

▶ **BLI tumour monitoring in vivo: Le Pivert et al. (2004):**

Ultrasound guided combined cryoablation and microencapsulated 5-Fluorouracil inhibits growth of human prostate tumors in xenogenic mouse model assessed by luminescence imaging; *Technol Cancer Res Treat.* 2004 Apr;3(2):135-42

▶ **Reporter Mice - Review: Maggi et al.(2004):**

Techniques: reporter mice - a new way to look at drug action; *Trends Pharmacol Sci.* 2004 Jun;25(6):337-42.

Exhibit 12

97

▶ **GFP and luciferase detection in cells: Blum et al. (2004):**

Development and characterization of enhanced green fluorescent protein and luciferase expressing cell line for non-destructive evaluation of tissue engineering constructs; *Biomaterials* Volume 25, Issue 27 December 2004, Pages 5809-5819

▶ **Bioluminescent detection of Salmonella: Warriner et al. (2003):**

Internalization of bioluminescent *Escherichia coli* and *Salmonella* Montevideo in growing bean sprouts; *Journal of Applied Microbiology*, Volume 95 Issue 4 Page 719-727, October 2003

▶ **BLI of Plant Seedlings: Perl-Treves et al.(2004):**

Early induction of the *Arabidopsis* *GSTF8* promoter by specific strains of the fungal pathogen *Rhizoctonia solani*; *Molecular Plant-Microbe Interactions*, 2004 (Vol. 17) (No. 1) 70-80

▶ **Chemiluminescent Immunoblots: Hwang et al. (2003):**

Regulatory modes of rod outer segment membrane guanylate cyclase differ in catalytic efficiency and Ca^{2+} -sensitivity; *FEBS Journal* Volume 270, Number 18, September 2003, pp. 3814-3821(8)

▶ **Luciferase detection in bacteria: Hardie et al. (2003):**

Autoinducer 2 activity in *Escherichia coli* culture supernatants can be actively reduced despite maintenance of an active synthase, LuxS; *Microbiology* 149 (2003), 715-728;

▶ **Luciferase detection in cells: Dvorák et al. (2003):**

Colchicine Down-Regulates Cytochrome P450 2B6, 2C8, 2C9, and 3A4 in Human Hepatocytes by Affecting Their Glucocorticoid Receptor-Mediated Regulation; *Mol Pharmacol* 64:160-169, 2003

▶ **Chemotherapeutic activity in vivo by luminescent imaging of tumors: Caceres et al. (2003):**

Determination of chemotherapeutic activity in vivo by luminescent imaging of luciferase-transfected human tumors; *Anti-Cancer Drugs.* 14 (7):569-574, August 2003

▶ **Reactive oxygen species: Sakurai et al. (2003):**

Protective effect of zinc in ultra violet light-induced skin damage : Studies on im of ROS by chemiluminescence method; *BIOMEDICAL RESEARCH ON TRACE ELEMENTS*, 14(1) : 17-21, 2003.

▶ **Luminescence Immunoassay: Roda et al (2003):**

A rapid and sensitive 384-well microtitre format chemiluminescent enzyme immunoassay for 19-nortestosterone; *Luminescence*, Volume 18, Issue 2, Pages 72 - 78

▶ **Reactive oxygen species: Yasui & Sakurai (2003):**

Age-dependent generation of reactive oxygen species in the skin of live hairless rats exposed to UVA light; *Experimental Dermatology*; Volume 12 Issue 5 Page 655-661, October 2003

▶ **Chemiluminescence imaging of oxyradical generation in pig stomach: Ojetti et al. (2003):**

Real time endoscopic imaging of oxyradical generation in-pig stomach during ischemia-reperfusion; *Dig Liver Dis.* 2003 May;35(5):309-13

▶ **BLI & BFI (GFP) tumour monitoring in vivo: Caceres et al. (2003):**

Imaging of luciferase and GFP-transfected human tumours in nude mice; *Luminescence* 2003 Jul-Aug;18(4):218-23

▶ **Circadian rhythms: Devlin (2002):**

Signs of the time: environmental input to the circadian clock; *Journal of Experimental Biology* Vol. 53 No. 374 pp.1535-1550

▶ **GFP and luciferase detection in Staphylococcus: Qazi et al. (2002):**

agr Expression Precedes Escape of Internalized Staphylococcus aureus from the Host Endosome; *Infection and Immunity*, November 2001, p. 7074-7082, Vol. 69, No. 11

▶ **Luminescence Immunoassay: Roda et al. (2002):**

Microtiter Format for Simultaneous Multianalyte Detection and Development of a PCR-Chemiluminescent Enzyme Immunoassay for Typing Human Papillomavirus DNAs; *Clinical Chemistry*. 2002;48:1654-1660

▶ **BLI in vivo and in vitro: Yu and Szalay (2002):**

A Renilla luciferase-Aequorea GFP fusion gene construct (ruc-gfp) permits real-time detection of promoter activation by exogenously administered mifepristone in vivo; *Mol Genet Genomics* (2002) 268: 169-178

▶ **Chemiluminescence imaging of microparticles: Roda et al. (2002):**

Chemiluminescence, real time imaging of microparticles separation by field-flow fractionation of a GFFF microparticles separation: a useful tool for probing retention mechanisms at and ultra-low sensitive detection limits; *Luminescence* 2002

▶ **Northern Blot: Francois et al. (2002):**

Transgenic Expression in Arabidopsis of a Polyprotein Construct Leading to Production of Two Different Antimicrobial Proteins; *Plant Physiol*, April 2002, Vol. 128, pp. 1346-1358

▶ **Luciferase monitoring in plants: Iliev et al. (2002):**

Transcriptional and Posttranscriptional Regulation of Arabidopsis TCH4 Expression by Diverse Stimuli. Roles of cis Regions and Brassinosteroids; *Plant Physiol*. 2002 October; 130(2): 770-783

▶ **BLI in vivo of Salmonella in mice: Brovko et al. (2002):**

In vivo assessment of the effect of diet on time-course of infection in mice using bioluminescent bacterial pathogens; *Luminescence* 2002

▶ **AHL bioluminescence in bacteria: Burgess et al. (2002):**

LuxS-dependent quorum sensing in Porphyromonas gingivalis modulates protease and haemagglutinin activities but is not essential for virulence; *Microbiology* (2002), 148, 763-772

▶ **Fluorescence and chemiluminescence imaging of NO in aortas: Ozaki et al. (2002):**

Overexpression of endothelial nitric oxide synthase accelerates atherosclerotic lesion formation in apoE-deficient mice; *The Journal of Clinical Investigation*, August 2002, Volume 110, Number 3

▶ **Analysis of cells with microscope coupled to NightOWL camera: Martens et al.**

Mutant Luteinizing Hormone Receptors in a Compound Heterozygous Patient with Complete Leydig Cell Hypoplasia: Abnormal Processing Causes Signaling Deficiency; *The Journal of Clinical Endocrinology & Metabolism* Vol. 87, No. 6 2506-2513

▶ **Luminescence monitoring of tumor cell lines: Andreotti et al. (2002):**

Application of luciferase transfected human tumor cell lines for chemotherapeutic drug development; *Luminescence* 2002

▶ **Luciferase detection in cell lines: Paris et al.(2002):**

A New Recombinant Cell Bioassay for Ultrasensitive Determination of Serum Estrogenic Bioactivity in Children; *The Journal of Clinical Endocrinology & Metabolism* Vol. 87, No. 2 791-797

▶ **AHL bioluminescence in P. aeruginosa: Yates et al. (2002):**

N-Acylhomoserine Lactones Undergo Lactonolysis in a pH-, Temperature-, and Acyl Chain Length-Dependent Manner during Growth of Yersinia pseudotuberculosis and Pseudomonas aeruginosa; *Infection and Immunity*, October 2002, p. 5635-5646, Vol. 70, No. 10

▶ **AHL bioluminescence in P. aeruginosa: Diggle et al. (2002):**

Advancing the Quorum in Pseudomonas aeruginosa: MvaT and the Regulation of N-Acylhomoserine Lactone Production and Virulence Gene Expression; *J Bacteriol*. 2002 May; 184(10): 2576-2586

▶ **Bioluminescence imaging in mice: Coll et al. (2002):**

Exhibit 12

98

Non invasive optical imaging of firefly luciferase gene expression in mice using the Berthold Technologies Nightowl LB 981; *Luminescence* 2002

▶ **Luciferase imaging in cells: Michael et al. (2001):**

SdiA of *Salmonella enterica* Is a LuxR Homolog That Detects Mixed Microbial Communities; *Journal of Bacteriology*, October 2001, p. 5733-5742, Vol. 183, No. 19

▶ **Biochip: Stelzle et al. (2001):**

On-chip electrophoretic accumulation of DNA oligomers and streptavidin; *Fresenius' Journal of Analytical Volume* 371, Number 2 September 2001

▶ **GFP expression in bacteria: Qazi et al. (2001):**

agr Expression Precedes Escape of Internalized *Staphylococcus aureus* from the Host Endosome; *Infection and Immunity*, November 2001, p. 7074-7082, Vol. 69, No. 11

▶ **Imaging of Luciferase expression - review: Greer III & Szalay (2001):**

Imaging of light emission from the expression of luciferases in living cells and organisms: a review; *Luminescence* 2002 Jan-Feb;17(1):43-74

▶ **Circadian rhythms: Schultz et al.(2001):**

A Role for LKP2 in the Circadian Clock of Arabidopsis; *The Plant Cell*, Vol. 13, 2659-2670, December 2001

▶ **Reactive Oxygen Species: Addolorato et al. (2001):**

Oxygen Free Radical Production in Rat Liver; *Digestive Diseases and Sciences*, Volume 46, Number 5, May 2001, pp. 1057-1066(10)

▶ **Circadian Rhythms: Covington et al. (2001):**

ELF3 Modulates Resetting of the Circadian Clock in Arabidopsis; *Plant Cell*. 2001 June; 13(6): 1305-1316

▶ **BLI of Salmonella: Modi et al. (2001):**

Effect of phage on survival of *Salmonella enteritidis* during manufacture and storage of cheddar cheese made from raw and pasteurized milk; *J Food Prot* 2001 Jul;64(7):927-33

▶ **Microplates & Blots: Roda et al. (2000):**

Chemiluminescence imaging systems for the analysis of macrosamples: microtiter format, blot membrane, and whole organs; *Methods Enzymol* 2000;305:120-32

▶ **Reactive oxygen species: Yasui & Sakurai (2000):**

Chemiluminescent Detection and Imaging of Reactive Oxygen Species in Live Mouse Skin Exposed to UVA; *Biochemical and Biophysical Research Communications* Volume 269, Issue 1, 5 March 2000, Pages 131-136

▶ **BLI of bacteria: Griffiths et al. (2000):**

Rapid Methods for Testing the Efficacy of Sterilization-Grade Filter Membranes; *Applied and Environmental Microbiology*, August 2000, p. 3432-3437, Vol. 66, No. 8

▶ **Chemiluminescent detection: Roda et al. (2000):**

In situ hybridization and immunohistochemistry with enzyme-triggered chemiluminescent probes; *Methods Enzymol*. 2000;305:577-90

▶ **Luciferase imaging: Grant et al. (2000):**

Oxidative burst and cognate redox signalling reported by luciferase imaging: identification of a signal network that functions independently of ethylene, SA and Me-JA but is dependent on MAPKK activity; *Plant J*. 2000 Dec; 24(5):569-82

▶ **BLI & BFI (GFP) of bacteria: Brovko & Griffiths (2000):**

Sensitivity of Detection of Bacteria with Fluorescent and Luminescent; *Proceedings of SPIE - Volume 3921 Optical Diagnostics of Living Cells III*, April 2000, pp. 147-156

▶ **Imaging of Spotted Chemiluminescent Proteins: Roda et al. (2000):**

Protein microdeposition using a conventional ink-jet printer; *Biotechniques* 2000 Mar; 28(3):492-6

▶ **Imaging of Listeria: Wu et al. (2000):**

A comparison of the Bioscreen method and microscopy for the determination of lag times of individual cells of *Listeria monocytogenes*; *Letters in Applied Microbiology* 30 (6), 468-472

▶ **Luciferase detection in brain tissues: Beimesche et al.(1999):**

Tissue-Specific Transcriptional Activity of a Pancreatic Islet Cell-Specific Enhancer Sequence/Pax6- Binding Site Determined in Normal in Vivo; *Molecular Endocrinology* 13 (5): 718-728

▶ **BLI of plants: Baruah-Wolff et al. (1999):**

Luciferase as a reporter gene for transformation studies in rice (*Oryza sativa* L.); *Plant Cell Report* Volume 18, Number 9, Mai 1999

▶ **Western Blot: Manaresi et al. (1999):**

Chemiluminescence Western blot assay for the detection of immunity against parvovirus B19 VP1 and VP2 linear epitopes using a videocamera based luminograph; *J Virol Methods*. 1999 Aug;81(1-2):91-9

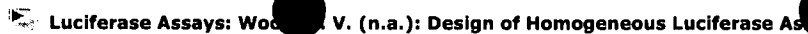
▶ **BLI of bacteria: Pfeifer et al. (1999):**

Salmonella typhimurium Virulence Genes Are Induced upon Bacterial Invasion into Phagocytic and Nonphagocytic Cells; *Infection and Immunity*,

November 1999, p. 5690, Vol. 67, No. 11

- Chemiluminescent in-situ hybridization: Musiani et al. (1999):**
 Prenatal diagnosis of parvovirus B19-induced hydrops fetalis by chemiluminescence in situ hybridization; *J Clin Microbiol.* 1999 Jul;37(7):2326-9
- Procedure for Luciferase Reporter Gene with NightOWL (1998): Hengerer & Herick**
 In vivo Procedure for the measurement Luciferase Reporter Gene Activity with a Low Light Imaging System; *Biospektrum* 4, 1998
- Chemiluminescent imaging of enzyme-labeled probes: Roda et al. (1998):**
 Chemiluminescent imaging of enzyme-labeled probes using an optical microscope-videocamera luminograph; *Analytical Anal Biochem.* 1998 Mar 1;257(1):53-62
- Chemiluminescent imaging of oxygen free radicals: Gasbarrini et al. (1997):**
 Chemiluminescent real time imaging of post-ischemic oxygen free radicals formation in livers isolated from young and old rats; *Free Radic Biol Med.* 1998 Jan 15;24(2):211-6
- Chemiluminescent in-situ hybridization: Musiani et al. (1997):**
 Sensitive chemiluminescence in situ hybridization for the detection of human papillomavirus genomes in biopsy specimens; *J Histochem Cytochem.* 1997 May;45(5):729-35
- Chemiluminescent in-situ hybridization: Gentilomi et al. (1997):**
 Co-localization of two different viral genomes in the same sample by double-chemiluminescence in situ hybridization; *Biotechniques* 1997 Dec;23(6):1076-80, 1082-3
- Calcium monitoring by Aequorine luminescence: Rosay et al. (1997):**
 Cell-type specific calcium signalling in a Drosophila epithelium; *Journal of Cell Science*, Vol 110, Issue 15 1683-1692
- Chemiluminescent in-situ hybridization: Musiani et al. (1996):**
 Detection of parvovirus B19 DNA in bone marrow cells by chemiluminescence in situ hybridization; *J Clin Microbiol.* 1996 May; 34(5): 1313-1316
- Chemiluminescent in-situ hybridization: Musiani et al. (1996):**
 Chemiluminescent in situ hybridization for the detection of cytomegalovirus DNA; *Am J Pathol.* 1996 Apr;148(4):1105-12
- Chemiluminescent imaging: Roda et al. (1996):**
 Chemiluminescent Low-Light Imaging of Biospecific Reactions on Macro- and Microsamples Using a Videocamera-Based Luminograph; *Anal. Chem.*, 68 (7), 1073 -1080, 1996
- Dot blot hybridization detection: Girotti et al. (1996):**
 Chemiluminescent immunoperoxidase assay for the dot blot hybridization detection of Parvovirus B19 DNA using a low light imaging device; *Anal Biochem.* 1996 May 1;236(2):290-5
- Chemiluminescent in-situ hybridization: Pasini et al.(1996):**
 Chemiluminescence in situ hybridization for the detection of viral genomes; *Chemiluminescence & Bioluminescence* 1996, 509-512
- Microscopic bioluminescent imaging: Pasini et al.(1996):**
 Oxygen free radical detection in isolated and perfused rat liver by chemiluminescent imaging; *Chemiluminescence & Bioluminescence* 1996, 505-508
- Dot blot hybridization detection: Girotti et al. (1995):**
 Application of a low-light imaging device and chemiluminescent substrates for quantitative detection of viral DNA in hybridization reactions; *Clin Chem.* 1995 Dec;41(12 Pt 1):1693-7
- Cameras for low light imaging: Ochs & Kuhles (1995):**
 Camera types for Low Level Light Imaging
- Imaging of chemiluminescence reactions: Kricka et al. (1994):**
 Imaging of chemiluminescent reactions in mesoscale silicon-glass microstructures; *J Biolumin Chemilumin.* 1994 May-Jun;9(3):135-8
- Low-light Imaging: Nicolas (1994):**
 Applications of low-light imaging to life sciences; *Journal of Bioluminescence and Chemiluminescence* Volume 9, Issue 3 , Pages 139 - 144
- BLI of bacteria: Hill et al.(1994):**
 Imaging bioluminescence in single bacteria; *Chemiluminescence & Bioluminescence* 1994, 629-632
- BLI: Hill et al.(1994):**
 Use of Lux Genes in Applied Biochemistry; *Chemiluminescence & Bioluminescence* 1994, 211-215
- Imaging system for luminescence and fluorescence: Berthold et al.(1994):**
 An Imaging System for Bio- and Chemiluminescence, Fluorescence and Radioactivity; *Chemiluminescence & Bioluminescence* 1994, 617-620
- Low light imaging system: Bräuer et al. (1993):**
 Measuring luminescence with a low light level imaging system using electronic light standards; *Chemiluminescence & Bioluminescence* 1993, 13-17

Exhibit 12
100

Luciferase Assays: Wood V. (n.a.): Design of Homogeneous Luciferase Assays

Design of Homogeneous Luciferase Assays; *Promega Notes 74*

© 2008 BERTHOLD TECHNOLOGIES GmbH & Co. KG

 Legal Notices

 Print Version

Exhibit 12
101

EXHIBIT 13

EXHIBIT 13

Exhibit 13
102

Non-viral delivery of the connexin 43 gene with histone deacetylase inhibitor to human nasopharyngeal tumor cells enhances gene expression and inhibits *in vivo* tumor growth

YOSHIYUKI HATTORI, MASAYOSHI FUKUSHIMA and YOSHIE MAITANI

Institute of Medicinal Chemistry, Hoshi University, Shinagawa-ku, Tokyo 142-8501, Japan

Received February 1, 2007; Accepted March 19, 2007

Abstract. Dysregulation of connexin expression is believed to have a role in carcinogenesis, because levels of connexin are reduced in various tumors. We examined the role of connexin 43 (Cx43) alone and combined with a histone deacetylase (HDAC) inhibitor in tumor growth inhibition. The transfection of Cx43 plasmid DNA (pCMV-Cx43) into human nasopharyngeal cancer KB cells using folate-linked nanoparticles induced inhibition of cell growth. Cx43 induced a tumor suppressive effect via a gap junctional intercellular communication-independent mechanism. The transfection of pCMV-Cx43 along with an HDAC inhibitor, 4-phenylbutyrate (4-PB), enhanced Cx43 expression greatly *in vitro*, and inhibited significantly the tumor growth of KB cells and xenografts compared with that of pCMV-Cx43 alone. 4-PB induced increased expression of genes of DNA damage checkpoints and of apoptosis via the down-regulation of anti-apoptotic bcl-2 mRNA expression and up-regulation of the activity of the apoptosis-associated enzyme caspase-3/7. Thus, the amplified Cx43 expression by an antitumor agent, an HDAC inhibitor, may have great potential as a growth inhibitor for nasopharyngeal tumors.

Introduction

Deregulation of connexin (Cx) expression is believed to play a part in carcinogenesis (1). Cx proteins have an essential role in gap junction intercellular communication (GJIC), which is often impaired among tumor cells and between tumor cells and surrounding normal cells. Connexin 43 (Cx43) is a tumor-suppressor (2), and its expression is reduced in various tumors (3-10). Forced expression of the Cx43 gene in several Cx43-deficient tumor cell lines attenuated their malignant

phenotype (8,11). However, a truncated Cx43 not forming gap junctions, also inhibited tumor growth (12). Thus, the mechanisms by which the Cx43 gene inhibits tumor growth remain unclear. Regarding tumor gene therapy using the Cx gene, there are many reports about co-administration of the herpes simplex thymidine kinase (HSV-tk) gene (13) or a chemotherapeutic agent (14,15). Enforced expression of Cx resulted in a dramatic suppression of tumor growth when Cx gene-transfected tumor cells were implanted into mice (1). However, the application of Cx gene delivery *in vivo* by direct injection into tumor-bearing mice with a vector has not been reported except for injection of the Cx26 gene with an adenoviral vector (16). One major obstacle to applications *in vivo* is poor transgene expression, therefore, a transfer system including an efficient vector for the Cx gene is required to strongly induce gene expression *in vivo*.

Histone deacetylase (HDAC) inhibitors such as sodium butyrate (SB), 4-phenylbutyrate (4-PB) and trichostatin A (TSA) cause cell-cycle arrest in the G₁ and/or G₂ phase and induce differentiation and/or apoptosis in a variety of cell types (17). Inhibition of HDAC activity induces the transcriptional activation of certain genes, such as that for the cyclin-dependent kinase inhibitor p21, which are thought to suppress tumor growth and prevent cell cycle progression (18,19). Several HDAC inhibitors inhibit tumor growth in animal models with little toxicity in non-tumor cells (20). Therefore, HDAC inhibitors are a new class of antitumor agent being evaluated in clinical trials. HDAC inhibitors also possess the capacity to enhance the expression of a wide variety of transiently transfected transgenes in tumors both *in vitro* and *in vivo* through their effect on the acetylation of histones (19,21). Combining of p53 gene therapy with an HDAC inhibitor, FR901228 or SB, enhanced therapeutic efficacy *in vitro* (22) and *in vivo* (23). The introduction of both the HSV-tk gene and FR901228 into melanoma xenografts enhanced the antitumor effect (24). However, the effect of transfection of the Cx gene combined with an HDAC inhibitor has not been reported.

The development of non-viral and tumor-selective delivery vectors for gene transfer *in vivo* is necessary for the clinical application of therapeutic genes. Folate receptor (FR) has been found to be overexpressed in a wide range of tumors (25). We previously reported that folate-linked nanoparticles (NP-F) could efficiently deliver DNA into human nasopharyngeal cancer KB cells, which overexpressed FR (26,27).

Correspondence to: Dr Yoshiyuki Hattori, Institute of Medicinal Chemistry, Hoshi University, Shinagawa-ku, Tokyo 142-8501, Japan
E-mail: yhattori@hoshi.ac.jp

Key words: connexin 43, histone deacetylase inhibitor, nasopharyngeal cancer, 4-phenylbutyrate, gene therapy, folate-linked nanoparticle, transfection, gap junction, apoptosis

Therefore, we used NP-F as a DNA transfection vector for cancer gene therapy.

In the present study, we investigated whether the transfection of plasmid DNA (pCMV-Cx43) coding for the Cx43 gene by NP-F combined with an HDAC inhibitor induced inhibition of KB cell growth. A novel combination of pCMV-Cx43 and an HDAC inhibitor, 4-PB enhanced the expression of Cx43 protein and induced significantly greater growth inhibition in KB cells and the tumor xenografts compared with pCMV-Cx43 alone. This combination increased apoptosis via down-regulation of bcl-2 mRNA expression and up-regulation of caspase-3/7 activity.

Materials and methods

Materials. SB and 4-PB were purchased from Wako Pure Chemicals (Osaka, Japan). TSA was supplied by Sigma Chemical Co. (St. Louis, MO, USA). 1,1'-Dioctadecyl-3, 3', 3'-tetramethylindocarbocyanine perchlorate (DiI) was obtained from Lambda Probes & Diagnostics (Graz, Austria). Calcein-AM was purchased from Dojindo (Kumamoto, Japan). The Pica gene luciferase assay kit was obtained from Toyo Ink Mfg. Co. Ltd. (Tokyo, Japan). Bicinchonnic acid (BCA) protein assay reagent was purchased from Pierce (Rockford, IL, USA). All reagents were of analytical grade. All other chemicals used were of reagent grade. Folate-deficient RPMI-1640 medium and fetal bovine serum were purchased from Life Technologies, Inc. (Grand Island, NY, USA).

Preparation of plasmid DNA. In the construction of the plasmid pCMV-Cx43 encoding the Cx43 gene under the control of the CMV promoter, the Cx43 and CMV promoter DNAs were amplified as described previously (28). After the Cx43 DNA amplification, this DNA was subcloned into an *Nco*I/*Xba*I-digested pGL3-control (Promega, Madison, WI, USA). Subsequently, the amplified CMV promoter DNA was subcloned into the *Hind*III and *Kpn*I restriction sites of the above plasmid.

In the construction of the plasmid pCMV-Cx43-EGFP, EGFP was fused in frame to the carboxyl terminus of Cx43. The DNA coding for EGFP was amplified by PCR using pEGFP-C1 (Clontech, CA, USA) as a template and the following EGFP-specific primers: EGFP forward primer (5'-TTGCGCCCGTGGGCAAGGGCGAGGAGCTG-3'), EGFP reverse primer (5'-TTTCTAGATTAGGACTTGTACAGCTCCTCC-3'). The forward primer contained a *Nar*I restriction site (underlined). The reverse primer contained an *Xba*I restriction site (underlined). The cDNA encoding bp 1-1146 of human Cx43 was amplified by PCR using the following Cx43-specific primers: Cx43 forward primer (5'-GCAAGCTTaccATGGGTGACTGGAGCGCCT-3'), Cx43 reverse primer (5'-ATGGCGCCGATCTCCAGGTCATCAGGCC-3'). The forward primer contained a 3-bp optimal Kozak sequence (in lower case letters) together with a *Hind*III restriction site (underlined). The reverse primer coded for bp 1129-1146 of Cx43 with a *Nar*I restriction site (underlined). After the DNA amplification of EGFP, this DNA was digested with *Nar*I and *Xba*I and was ligated into a *Nar*I and *Xba*I-digested pGL3-enhancer (Promega). Subsequently, the amplified PCR fragment of Cx43 was cloned into the *Hind*III and *Nar*I-

restriction sites of the above plasmid, and then the CMV promoter DNA was subcloned into the *Hind*III and *Kpn*I-restriction sites as described above.

In the construction of the plasmid pCMV-luc encoding the luciferase gene under the control of the CMV promoter, the CMV promoter DNA was subcloned into the *Hind*III and *Kpn*I restriction sites of pGL3-enhancer. pGL3-basic encoding the luciferase gene without promoter was obtained from Promega and used as a control plasmid. A protein-free preparation of these plasmids was purified following alkaline lysis using maxiprep columns (Qiagen, Hilden, Germany).

Preparation of folate-linked nanoparticles. Cholesteryl-3β-carboxyamidoethylene-N-hydroxyethylamine (OH-Chol) was synthesized as previously reported (27). NP-F as a gene transfection reagent was prepared with lipids [OH-Chol: Tween-80 (NOF Co. Ltd., Tokyo, Japan): folate-polyethylene glycol-distearoylphosphatidylethanolamine (mean molecular weight of PEG: 2,000 kDa) = 94:5:1, molar ratio = 10:1.3:0.65 weight] in 10 ml of water using a modified ethanol injection method as described previously (27).

Cell culture. KB cells were from the Cell Resource Center for Biomedical Research, Tohoku University (Miyagi, Japan). Prostate cancer LNCaP cells were supplied by the Department of Urology, Keio University Hospital (Tokyo, Japan). All the cell lines used in this study were grown in a folate-deficient RPMI-1640 medium supplemented with 10% heat-inactivated fetal bovine serum and kanamycin (100 μg/ml) at 37°C in a 5% CO₂ humidified atmosphere.

In vitro transfection. Cell cultures were prepared by plating cells in a 35-mm culture dish 24 h prior to each experiment. Based on preliminary experiments *in vitro*, the optimized charge ratio (+/-) of cationic lipid to DNA was determined as 3:1 (27). The NP-F and plasmid DNA complex (NP-F nanoplex) at a charge ratio (+/-) of cationic lipid to DNA of 3/1 was formed by addition of NP to 2 μg of plasmid DNA in 50 mM NaCl with gentle shaking and left at room temperature for 10 min. The NP-F nanoplex was diluted in 1 ml of medium supplemented with 10% serum and then incubated with cells for 24 h. For the co-introduction of the HDAC inhibitor, the NP-F nanoplex was diluted in the medium containing the HDAC inhibitor to the concentration indicated in the figure legends.

In vitro cell growth. KB cells were seeded separately at a density of 1 × 10⁴ cells per well in 96-well plates and maintained for 24 h before transfection in RPMI medium supplemented with 10% serum. The cells at 30% confluence in the well were transfected with the NP-F nanoplexes using 0.2 μg of pCMV-Cx43 or pGL3-basic in the presence or absence of the HDAC inhibitor and incubated for 48 h. The cell number was determined with a WST-8 assay (Dojindo Laboratories).

Immunoblotting. KB cells were seeded in a 35-mm culture dish and incubated overnight. The cells at 30% confluency were transfected with pCMV-Cx43 or pGL3-basic in the presence or absence of the HDAC inhibitor and then incubated for 24 h. The cells were suspended in lysis buffer [1%

Triton X-100 in phosphate-buffered saline pH 7.4 (PBS)], and then centrifuged at 15,000 rpm for 10 min. The supernatants (10 μ g protein) were resolved on a 12% sodium dodecyl sulphate-polyacrylamide gel by electrophoresis (SDS-PAGE) and transferred to a polyvinylidene difluoride (PVDF) membrane (FluoroTrans[®] W, PALL Gelman Laboratory, Ann Arbor, MI, USA). Expression of the Cx43 protein was identified using a specific rabbit antiserum (Sigma) and acetylated histone H3 was detected by rabbit anti-human acetyl histone H3 antibody (Sigma). The goat anti-rabbit IgG peroxidase conjugate (Santa Cruz Biotechnology, Inc., Santa Cruz, CA, USA) was used as secondary antibody. These proteins were detected with peroxidase-induced chemiluminescence (Super Signal West Pico Chemiluminescent Substrate, Pierce).

RNA isolation and RT-PCR. KB cells were seeded in a 35-mm culture dish and incubated overnight. The cells at 30% confluency were transfected with pCMV-Cx43 or pGL3-basic in the presence or absence of 1 μ M TSA, 1 mM SB or 1 mM 4-PB, and then incubated for 24 h. Total RNA was isolated from the cells using NucleoSpin RNA II (Macherey-Nagel, Germany). First-strand cDNA was synthesized from 5 μ g of total RNA as previously described (28). For RT-PCR, the 25- μ l reaction volume contained the following: 1 μ l of synthesized cDNA, 10 pmol of each specific primer pair, and 0.25 units of Ex Taq DNA polymerase (Takara Shuzo Co., Ltd) with a PCR buffer containing 1.5 mM MgCl₂ and 0.2 mM of each dNTP. The profile of PCR amplification consisted of denaturation at 94°C for 0.5 min, primer annealing at 58°C for 0.5 min, and elongation at 72°C for 1 min for 25 cycles. For the amplification of human Cx43, the primers Cx43-FW, 5'-CTC ATGTGTTCTATGTGATG-3', and Cx43-RW, 5'-ATTGCG GCAAGAAGAATTGT-3', were used. For the amplification of human bcl-2, the primers bcl-2-FW, 5'-TGGAGAGCGTC AACCGGGAG-3', and bcl-2-RW, 5'-CCGTACAGTTCCAC AAAGGC-3', were used. For the amplification of the housekeeping gene β -actin, the primers β -actin-FW, 5'-ACCCACA CTGTGCCCCATCTA-3', and β -actin-RW, 5'-CTGCTTGCT GATCCACATCT-3', were used. PCRs of Cx43, bcl-2 and β -actin were performed at the same cycle run for all samples. The PCR products for Cx43, bcl-2 and β -actin were analyzed by 1.5% agarose gel electrophoresis in a Tris-borate-EDTA (TBE) buffer. The products were visualized by ethidium bromide staining.

Real-time PCR was performed on the corresponding cDNA synthesized from each sample described above. The optimized settings were transferred to the real-time PCR protocol with the iCycler MyiQ detection system (Bio-Rad Laboratories, Hercules, CA, USA) and SYBR-Green I assay (iQ[™] SYBR-Green Supermix, Bio-Rad Laboratories) was used for quantification. Samples were run in triplicate and the expression levels of Cx43 and bcl-2 mRNA were normalized to the amount of β -actin in the same sample.

cDNA array. KB cells were seeded in a 35-mm culture dish and incubated overnight. The cells at 30% confluency were transfected with pGL3-basic or pCMV-Cx43 in the presence or absence of 1 μ M TSA or 1 mM 4-PB. After 24 h of incubation, total RNA was isolated from the cells as described

above. A non-radioactive human cell cycle gene array (GEArray Q series human cell cycle gene assay, Super Array Inc., MD, USA) was used to analyze the gene expression profile of the cell cycle, DNA damage checkpoint and ATM pathway. Briefly, 5 μ g of total RNA was used as a template to produce biotinylated cDNA probes. RNA was reverse-transcribed using gene-specific primers with biotin-16-dUTP. Biotinylated cDNA probes were denatured and hybridized to cell cycle gene-specific cDNA fragments spotted on membranes. The GEArray membranes were then washed and blocked with GEA blocking solution, and incubated with alkaline phosphatase-conjugated streptavidin. The hybridized biotinylated probes on the membrane were detected by a chemiluminescent method using the alkaline phosphatase substrate, CDP-Star. The membranes were exposed to chemiluminescence film (Hyperfilm[™] ECL[™], Amersham Bioscience Corp., Piscataway, NJ, USA) for 10 sec. The results were analyzed using free ScanAlyze software (developed by Dr Michael Eisen), which converts a grayscale TIFF image of spots into numerical data (median pixel intensity), and then the gene expression profiles were compared using GEArray analyzer software (Super Array, Inc.). Each array comprised 96 marker genes in quadruplicate, 4 positive controls including β -actin, glyceraldehyde-3-phosphate dehydrogenase (GAPDH), cyclophilin A (PPIA) and ribosomal protein L13a, and a negative control, the bacterial plasmid pUC18. Intensity was calculated from each array by subtracting the negative control from each spot and normalized against the housekeeping gene PPIA. Gene expression ratios from each experiment were calculated by using the average normalized intensities from each array.

Cell cycle analysis. KB cells were seeded in a 35-mm culture dish and incubated overnight. The cells at 30% confluency were transfected with pCMV-Cx43 or pGL3-basic in the presence or absence of 1 μ M TSA, 1 mM SB or 1 mM 4-PB in medium. After 24 h of incubation, the cells were harvested with EDTA after a wash with ice-cold PBS. Detached cells were washed once with ice-cold PBS and gently suspended in PBS-EtOH (70%) and fixed overnight at 4°C. For staining, the fixed cells were washed once in PBS and then resuspended in PBS with 50 μ g/ml propidium iodide (PI) and 0.5% RNase A. After 30 min at 37°C, the cells were processed for FACS analysis of the PI-fluorescence by a FACScalibur flow cytometer (Becton-Dickinson, San Jose, CA) equipped with a 488-nm argon ion laser. Data for 10,000 fluorescent events were obtained by recording forward scatter (FSC), side scatter (SSC), and PI-fluorescence (585/42 nm).

Assessment of gap junctional intercellular communication. The FACS analysis of the GJIC reported by Robe *et al* (29) was modified. Briefly, cells grown in 35-mm dishes were labeled for 1-h incubation with either 5 μ M calcein-AM or 5 μ M DiI in the medium. The two labeled cells were mixed in equal proportions in 35-mm dishes and incubated for 24 h. Subsequently, pCMV-Cx43 or pGL3-basic was transfected with NP-F into the mixed cells in the presence or absence of 1 mM SB, 1 mM 4-PB or 1 μ M TSA. After 24 h of incubation, the cells were trypsinized, washed in PBS and processed for a FACS analysis of the calcein-AM- and

DiI-fluorescences with a FACSCalibur flow cytometer as described above. Data for 10,000 fluorescent events were obtained by recording calcein-AM-fluorescence (530/30 nm) and DiI-fluorescence (585/42 nm).

Confocal microscopy. KB and LNCaP cells, respectively, were plated into 35-mm culture dishes. The cells at 30% confluency were transfected with pCMV-Cx43-EGFP in the presence or absence of 1 μ M TSA or 1 mM 4-PB by incubation for 24 h. Examinations were performed with a Radiance 2100 confocal laser scanning microscope (Bio-Rad Laboratories) as previously described (28). Cx43-EGFP was imaged using the 488-nm excitation line of an argon laser, and fluorescence emission was observed with a filter, HQ515/30.

Luciferase and caspase-3/7 activities. KB cells were seeded in a 35-mm culture dish and incubated overnight. The cells at 30% confluency were transfected with pGL3-basic or pCMV-Cx43 in the presence or absence of 1 μ M TSA, 1 mM SB or 1 mM 4-PB by incubation for 24 h. For measuring caspase-3/7 activity, a homogenous assay (Caspase-Glo™ 3/7 assay, Promega, Madison, WI, USA) was performed as described in the assay instructions. Luciferase activity was measured using the luciferase assay system (Pica Gene, Toyo Ink Mfg. Co. Ltd., Tokyo, Japan) as previously reported (30).

Gene expression in vivo. To generate KB tumor xenografts, 1×10^7 cells suspended in 50 μ l of RPMI medium were inoculated subcutaneously into the flanks of male BALB/c nu/nu mice (7 weeks of age, Clea Japan, Inc., Tokyo, Japan). The tumor volume was calculated using the formula: tumor volume = $0.5 \times a \times b^2$, where a and b are the larger and smaller diameters, respectively. Based on a preliminary experiment of gene expression induced by intratumoral injection, the optimized ratio of cationic lipid to DNA was determined as 1.5:1. For detection of luciferase gene expression in tumor, the nanoplex was formed by addition of NP-F (23.8 μ l) to 10 μ g of pCMV-luc with gentle shaking and standing at room temperature for 10 min. When the average volume of KB xenograft tumors reached approximately 600 mm³, the NP-F nanoplexes of 10 μ g of plasmid per tumor were directly injected into xenografts. Twenty-four hours after injections, the mice were injected with D-luciferin (potassium salt, Wako Pure Chemicals, Osaka, Japan) dissolved in PBS (125 mg/kg of body weight) into the peritoneal cavity and subsequently anesthetized by i.m. injection of 50 mg/kg body weight of pentobarbital (Nembutal, Dainippon Pharmaceutical Co., Ltd., Osaka, Japan). *In vivo* bioluminescence imaging was performed by using a NightOWL LB981 NC100 system (Berthold Technologies, Bad Wildbad, Germany). A gray scale body-surface reference image was collected using the NightOWL LB981 CCD camera. Photons emitted from luciferase within the mice were collected and integrated for a 2-min period. A pseudocolor luminescent image from blue (least intense) to red (most intense), representing the spatial distribution of the detected photons emitted within the mice, was generated using WinLight software (Berthold Technologies). The overlay of the real image and the luminescence representation allowed the localization and measurement of luminescence emitted from the tumor xenografts.

For detection of EGFP expression in tumor, the NP-F nanoplexes of 10 μ g of pEGFP-C1 plasmid per tumor were directly injected into KB xenografts. Twenty-four hours after injections, tumors were removed for preparation of cryosections. The excised tumors were immediately frozen, sectioned at 20 μ m thick and mounted. The expression of EGFP protein was observed using fluorescence microscopy.

Assessment of KB tumor growth. When the average volume of KB xenograft tumors reached 150 mm³ (day 0), these mice were divided into four groups: group I, pGL3-basic (10 μ g) as a control; group II, pCMV-Cx43 (10 μ g); group III, pGL3-basic (10 μ g) plus 1 mg 4-PB; and group IV, pCMV-Cx43 (10 μ g) plus 1 mg 4-PB. Each experimental group consisted of 4 tumors. The NP-F nanoplexes at a charge ratio (+/-) of 1.5/1 of cationic lipid to DNA were formed as described in the above section. The nanoplexes of 10 μ g of plasmid per tumor were directly injected into xenografts on days 0, 2 and 4. At 10 min after each DNA transfection, 20 μ l of 50 mg/ml 4-PB dissolved in DMSO was directly injected into the xenografts. The tumor volume was measured at days 0, 2, 4, 6, 8, 11 and 13. At day 13, all mice were sacrificed, and the tumor weights were measured. Tumor volume and weight are shown as the mean \pm SE and \pm SD, respectively. The excised tumors were immediately frozen, sectioned 20- μ m thick and mounted. The sections were stained with hematoxylin and pure eosin (Muto Pure Chemicals Co., Ltd., Tokyo, Japan) for histopathological examination.

Statistical analysis. The statistical significance of differences between mean values was determined using Welch's t-test. Multiple comparisons were performed with an analysis of variance followed by the Bonferroni/Dunn test. P-values <0.05 were considered significant.

Exhibit 13 106

Results

Amplification of Cx43 gene expression by HDAC inhibitors. In this study, we used NP-F for *in vitro* and *in vivo* DNA transfection into KB tumor. The *in vitro* transfection efficiency of pEGFP-C1 into KB cells by NP-F was ~20-30% at 30% confluency by flow cytometric analysis (data not shown). Commercially available transfection reagent Lipofectamine 2000 (Invitrogen Corp., Carlsbad, CA, USA) exhibited 40-50% transfection efficiency of the cells at 30% confluency, however, Lipofectamine 2000 is known to be cytotoxic and to induce expression of many apoptotic genes. In fact, the Lipofectamine 2000 significantly decreased cell viability after transfection into KB cells. Therefore, we decided to use NP-F for DNA transfection into KB cells.

To investigate whether the transfection of pCMV-Cx43 induced growth inhibition in the cells, we initially examined cell growth after transfection using a colorimetric viability assay. In this study, we used pGL3-basic as a control plasmid. Forty-eight hours after transfection, pCMV-Cx43 had a significant suppressive effect in KB cells (Fig. 1A).

Next, to induce the complete growth suppression of KB cells, we investigated whether the transfection of pCMV-Cx43 with an HDAC inhibitor, TSA, SB or 4-PB, enhanced the expression of Cx43. In a preliminary study, we observed

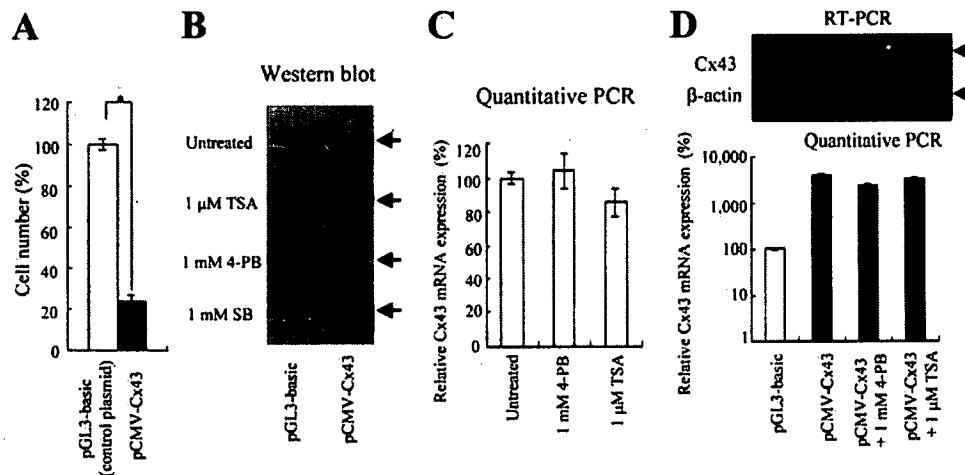


Figure 1. Effect on cell growth of expression of Cx43 (A). pGL3-basic was used as a control plasmid. The cells at 30% confluency were transfected with pCMV-Cx43 or pGL3-basic. Cell number was measured 48 h after transfection. Statistical significance of the data was evaluated with the Welch's t-test. * $P < 0.05$, compared with pGL3-basic. Effect of HDAC inhibitors on the expression of Cx43 protein (B) and mRNA (C and D) in KB cells. The cells transfected with pCMV-Cx43 or pGL3-basic were exposed to 1 μ M TSA, 1 mM 4-PB or 1 mM SB for 24 h (B and D). The cells were exposed to 1 μ M TSA or 1 mM 4-PB for 24 h (C). Western blot (B) and quantitative PCR (C and D) and RT-PCR (D) analyses were performed 24 h after transfection. (B and C) The β -actin housekeeping gene was used as the control. The relative amount of Cx43 mRNA in the cells was compared with a SYBR-Green I-based quantitative PCR analysis. The y-axis indicates Cx43 mRNA expression (%) of untreated (C) or pGL3-basic-transfected cells (D). The expression level of Cx43 mRNA was normalized to the amount of β -actin in the same sample. Each result represents the mean \pm SD ($n=3$).

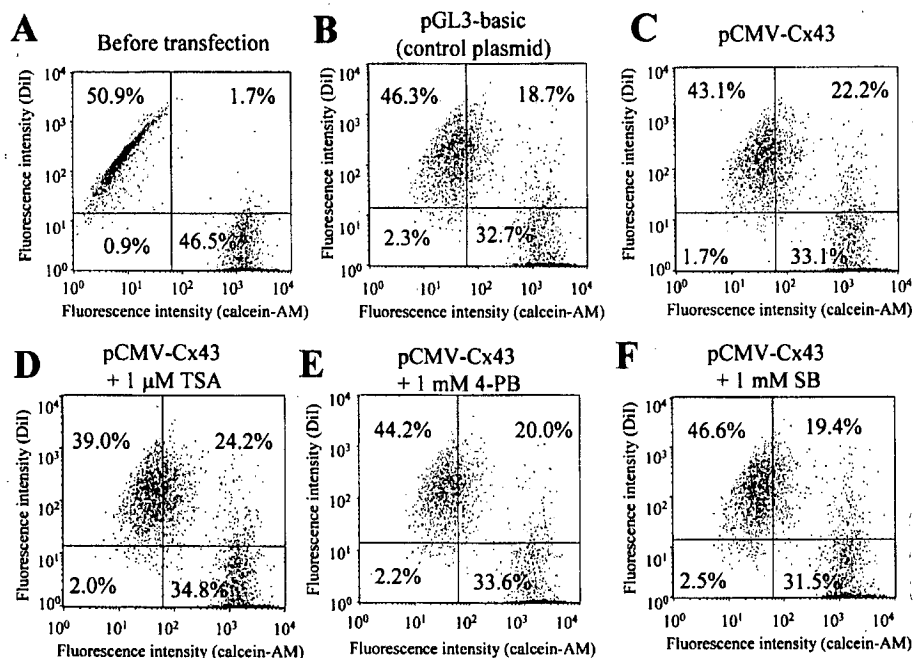


Figure 2. Gap junction-mediated transfer of fluorescent dyes in the presence and absence of HDAC inhibitors by FACS analysis. KB cells were pre-loaded with Dil and calcein-AM fluorescent probes. While Dil was retained in the preloaded cells, calcein-AM spread to Dil-positive cells, indicating gap junction-mediated transfer. The cells preloaded with Dil and calcein-AM were mixed in equal proportions, plated, and incubated for 24 h. The cells were transfected with pCMV-Cx43 or pGL3-basic in the presence or absence of 1 μ M TSA, 1 mM SB or 1 mM 4-PB and incubated for another 24 h. Upper left quadrant, calcein-AM-loaded cells; lower right quadrant, Dil-tagged cells; upper right quadrant, Dil-tagged cells that have incorporated calcein-AM. Histogram of Dil-tagged and calcein-AM-loaded cells before co-incubation (A); pGL3-basic-transfected cells (B); pCMV-Cx43-transfected cells (C); pCMV-Cx43 plus TSA-transfected cells (D); pCMV-Cx43 plus 4-PB-transfected cells (E); pCMV-Cx43 plus SB-transfected cells (F).

the highest levels of Cx43 protein when the cells were co-introduced with 1 μ M TSA, 1 mM SB and 1 mM 4-PB, respectively (data not shown). Therefore, in the subsequent

experiment, we used these concentrations as optimal. The expression of endogenous Cx43 protein was detected moderately in KB cells (Fig. 1B, untreated cells transfected with

Exhibit 13
107

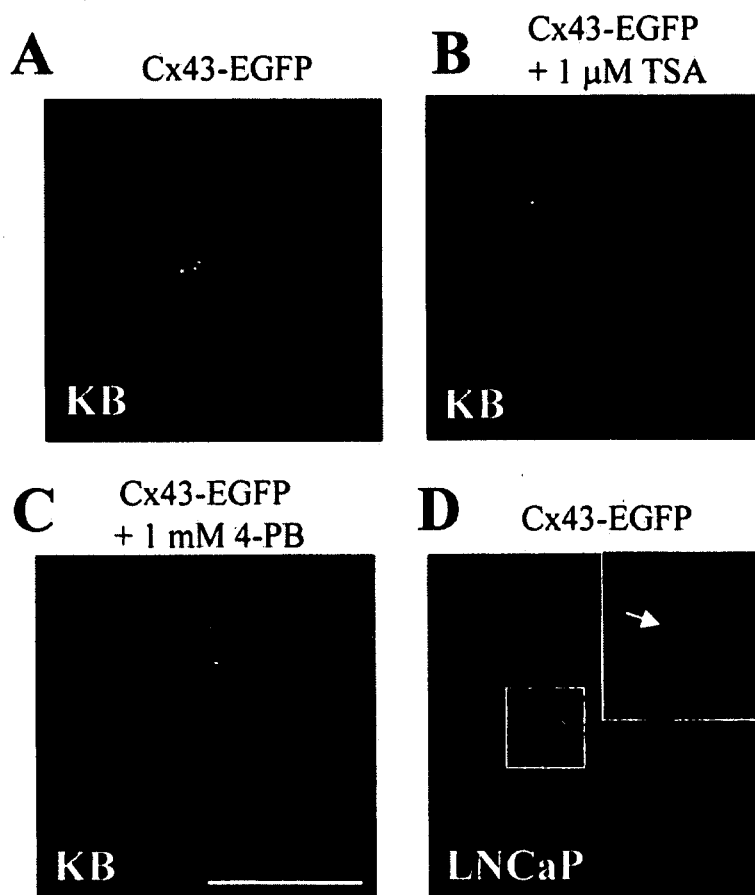


Figure 3. Localization of Cx43-EGFP in KB (A-C) and LNCaP cells (D). KB cells were transfected with pCMV-Cx43-EGFP in the absence (A) or presence of 1 μ M TSA (B) or 1 mM 4-PB (C) for 24 h. LNCaP cells were transfected with pCMV-Cx43-EGFP for 24 h (D). The Cx43-EGFP was visualized by confocal microscopy (magnification $\times 1,200$). The red signals show the location of the nucleus, and the green signals, that of the Cx43-EGFP. Scale bar, 50 μ m. Confocal images revealed that Cx43-EGFP was transported inefficiently to the cell surface and assembled into gap junctions in KB cells (A-C) while Cx43 was assembled more efficiently into gap junctions in LNCaP cells (D). Arrowheads indicate the junctional plaque.

Exhibit 13
108

pGL3-basic), and was weakly increased when the cells were treated with 4-PB or SB, but not TSA (Fig. 1B, pGL3-basic). When the cells were co-transfected with pCMV-Cx43 plus an HDAC inhibitor, the exogenous expression of Cx43 protein was strongly increased in the cells treated with each inhibitor, compared with those not treated with an inhibitor (Fig. 1B, pCMV-Cx43). Furthermore, we confirmed the increased expression of exogenous protein by HDAC inhibitors using pCMV-luc in the cells; the luciferase activity increased ~2- and 6-fold on treatment with TSA, and 4-PB and SB, respectively (data not shown). To confirm the effect on acetylation in histone by HDAC inhibitors, we analyzed the intracellular level of histone H3 acetylation using a specific antibody against acetylated histone H3. When KB cells were co-transfected with pCMV-Cx43 and TSA, SB or 4-PB, the increased Cx43 expression correlated with the increased acetylation of histone H3 (data not shown). The acetylation levels of histone H3 by HDAC inhibitors corresponded with a previous report (31).

To analyze the effect of HDAC inhibitors on the transcription of Cx43 mRNA, RT-PCR and quantitative PCR analyses were carried out in the cells transfected with pCMV-Cx43 in the presence or absence of HDAC inhibitors. As

shown in Fig. 1C, endogenous Cx43 mRNA did not increase on treatment with 4-PB or TSA. In the cells transfected with pCMV-Cx43, the expression of Cx43 mRNA was ~40-fold higher than that with pGL3-basic (Fig. 1D). However, in the cells co-transfected with TSA or 4-PB, no amplification of Cx43 mRNA was observed compared to the cells without an HDAC inhibitor (Fig. 1D). Thus the amplified expression of Cx43 protein might result from an increase in Cx43 gene translation and/or from an indirect effect on stabilization of Cx43 protein by HDAC inhibitors.

Defective GJIC in KB tumor cells. To investigate whether the amplified expression of Cx43 protein by pCMV-Cx43 plus the HDAC inhibitor caused gap junctions to form, we assessed the transfer of calcein-AM, a cytoplasmic dye that crosses gap junctions, in a co-culture of calcein-AM-loaded cells and cells marked with DiI, a non-diffusible membrane fluorescent dye, by FACS analysis. pGL3-basic-transfected cells showed slight GJIC-mediated transfer of calcein-AM (18.7%) after 48-h culture (Fig. 2B), indicating that other kinds of Cx endogenously expressed in KB cells induced GJIC. The pCMV-Cx43-transfected cells did not exhibit a great increase

Table I. Differential expression of genes related to the cell cycle in KB cells on transfection of pCMV-Cx43 and/or treatment with HDAC inhibitors.

Gene name	pGL3-basic-transfected cells	pCMV-Cx43-transfected cells	pCMV-Cx43-transfected cells + 1 mM 4-PB	pCMV-Cx43-transfected cells + 1 μ M TSA
G₁				
CDC7	17.1	58.2 (3.4)	77.0 (4.5)	81.2 (4.7)
cdk2	N.D	18.3	13.5	9.1
p16	12.3	79.1 (6.5)	70.6 (5.8)	41.7 (3.4)
Cks1p9	42.6	84.1 (2.0)	74.6 (1.8)	26.3 (0.6)
Cullin2	N.D	60.9	66.2	48.8
Cullin3	N.D	22.2	10.2	30.1
Cullin4B	N.D	19.7	26.3	10.5
E2F-4	45.0	89.2 (2.0)	86.8 (1.9)	78.0 (1.7)
Nedd8	13.8	42.3 (3.1)	39.1 (2.8)	17.8 (1.3)
skp1	N.D	31.5	16.0	35.2
skp2	10.0	21.1 (2.1)	40.4 (4.1)	17.9 (1.8)
S				
Cyclin C	31.8	32.2 (1.0)	23.3 (0.7)	17.7 (0.6)
Cyclin G	42.2	67.8 (1.6)	79.5 (1.9)	72.7 (1.7)
Cyclin G2	16.6	15.2 (0.9)	27.6 (1.7)	17.5 (1.1)
CDC6	36.0	73.9 (2.1)	75.8 (2.1)	49.2 (1.4)
CDK7	17.1	58.2 (3.4)	77.0 (4.5)	81.2 (4.7)
MCM6	53.0	69.0 (1.3)	69.9 (1.3)	62.7 (1.2)
G₂				
Cyclin B	31.5	46.5 (1.5)	49.7 (1.6)	40.2 (1.3)
Cyclin B2	130.6	114.4 (0.9)	111.2 (0.9)	110.1 (0.8)
M				
cdk1	74.8	86.5 (1.2)	91.3 (1.2)	79.1 (1.1)
Cdc27	123.7	102.0 (0.8)	96.8 (0.8)	90.9 (0.7)
MAD2L1	N.D	14.4	11.1	3.9
PRC1	101.1	99.9 (1.0)	100.8 (1.0)	100.9 (1.0)
Rbx-1	12.6	36.0 (2.9)	15.8 (1.3)	5.7 (0.5)
DNA damage checkpoint and ATM pathway				
Apaf-1	97.9	102.6 (1.1)	105.1 (1.1)	99.3 (1.0)
ATM	73.1	84.5 (1.2)	87.3 (1.2)	79.9 (1.1)
chk1	18.9	58.8 (3.1)	61.4 (3.3)	40.3 (2.1)
MRE11A	N.D	27.8	28.5	13.3
MRE11B	N.D	19.3	48.2	26.7
nibrin	30.0	54.5 (1.8)	71.4 (2.4)	27.2 (0.9)
chk2	108.7	98.8 (0.9)	101.4 (0.9)	92.7 (0.9)
UBE1	23.1	70.6 (3.1)	73.4 (3.2)	56.4 (2.5)
E6-AP	N.D	23.2	14.8	11.7
SUMO-1	N.D	8.8	18.6	6.2
Control				
GAPDH	70.5	87.5 (1.2)	96.8 (1.4)	86.0 (1.2)
PPIA	100.0	100.0 (1.0)	100.0 (1.0)	100.0 (1.0)

This table shows the optical density of the spots in cDNA array. Median pixel intensity of each spot in cDNA array was calculated using ScanAnalyze software, which is a program for DNA microarray imaging and extracts median pixel intensity from the image data of spots. The gene expression levels are shown as a percentage of the intensity compared with the corresponding internal control, PPIA. The ratio of gene expression between control cells and HDAC inhibitor-treated and/or pCMV-Cx43-transfected cells was assessed by the fold difference.

Exhibit 13
109

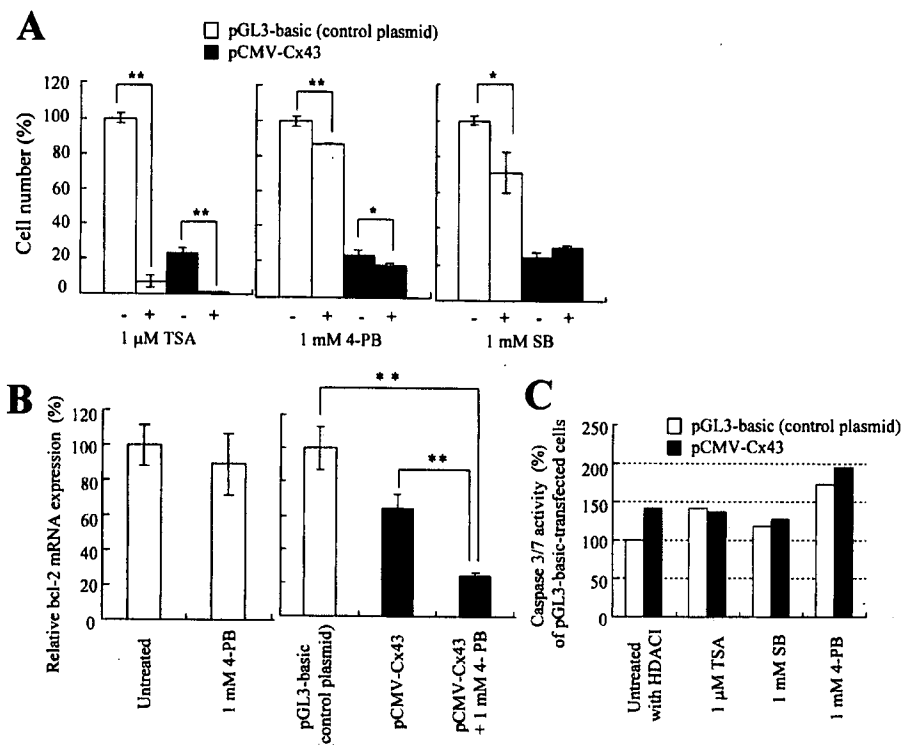


Figure 4. Effect of HDAC inhibitors on cytotoxicity in Cx43-transfected cells (A). KB cells were transfected with pCMV-Cx43 or pGL3-basic in the presence of 1 μ M TSA, 1 mM SB or 1 mM 4-PB and incubated for 48 h. (B) Quantitative PCR analysis of bcl-2 mRNA expression in KB cells transfected with pCMV-Cx43 and/or 1 mM 4-PB. The y-axis indicates bcl-2 mRNA expression (%) of untreated or pGL3-basic-transfected cells. The expression level of bcl-2 mRNA was normalized to the amount of β -actin in the same sample. Each result represents the mean \pm SD (n=3). Statistical significance of the data was evaluated with Welch's t-test. **P<0.01, compared with pCMV-Cx43 plus 4-PB. (C) Effects of caspase-3/7 activities on Cx43-overexpressing KB cells by HDAC inhibitors. KB cells were transfected with pCMV-Cx43 or pGL3-basic in the presence of 1 μ M TSA, 1 mM SB or 1 mM 4-PB and incubated for 24 h. The results show caspase-3/7 activity as a percentage of the control (pGL3-basic-transfected cells). Each result represents the mean (n=2).

Exhibit 13

110

in GJIC (22.2%) (Fig. 2C), compared with the pGL3-basic-transfected cells. Moreover, in the pCMV-Cx43-transfected cells, TSA, 4-PB and SB did not increase the GJIC (24.2%, 20.0% and 19.4%, respectively) even though they induced the overexpression of Cx43 (Fig. 2D-F). These findings indicated that the transfection of Cx43 with an HDAC inhibitor could not increase the GJIC compared with Cx43 alone.

Next, to examine whether the Cx43 was transported properly to the plasma membrane and formed fluorescent puncta at cell-cell interfaces, we constructed a plasmid encoding a Cx43-EGFP chimera and investigated the localization of Cx43-EGFP protein in the cells. Confocal micrographs revealed that the Cx43-EGFP was localized to the intracellular compartment (Fig. 3A), suggesting that the defect of GJIC in the cells was due to an inability to assemble functional gap junctions. Furthermore, the transport of Cx43-EGFP was not affected by the co-introduction of TSA or 4-PB (Fig. 3B and C). In LNCaP cells, known to form assemblies of functional gap junctions at the membrane on transfection of the Cx43 gene (32), Cx43-EGFP showed the expected localization at sites of contact between the cells (Fig. 3D, arrow), suggesting that the subcellular targeting of Cx43-EGFP was not affected by the tagging with EGFP. From these results, KB cells could not correctly transport Cx43 protein into the membrane, therefore, the GJIC-mediated transfer shown in Fig. 2B might be regulated by another endogenous Cx species. Although

functional gap junctions did not form in KB cells transfected with pCMV-Cx43, the expression of Cx43 could induce cell cycle arrest. There is evidence of gap junction-independent roles of Cx in the control of cell growth and the suppression of tumorigenicity (33). This finding suggests that the Cx43 expression in KB cells induced the cell growth inhibition via a GJIC-independent mechanism.

DNA array. To investigate the mechanism of growth inhibition by Cx43, we generated cDNA probes from KB cells transfected with pCMV-Cx43 or pGL3-basic in the presence or absence of TSA or 4-PB for 24 h, and evaluated the effect on the expression of cell cycle-related genes which were among the key genes that affect progression through the cell cycle (Table I). PPIA and GAPDH were used as internal standards. In Cx43-transfected cells, compared with pGL3-basic-transfected cells, the expression of genes involved in the G₁ phase, DNA damage checkpoint, and ATM pathway, was up-regulated. An up-regulated mRNA expression was found in 11 genes in G₁ phase (CDC7, cdk2, p16, Cks1p9, Cullin 2, Cullin 3, Cullin 4B, E2F-4, Nedd8, skp1 and skp2), 2 genes in S phase (CDC6 and CDK7), 2 genes in M phase (MAD2L1 and Rbx-1) and 6 genes involved in the DNA damage checkpoint and ATM pathway (chk1, MRE11A, MRE11B, UBE1, SUMO-1 and E6-AP) (Table I), with a difference of ≥ 2 -fold from pGL3-basic-transfected cells. The introduction of pCMV-

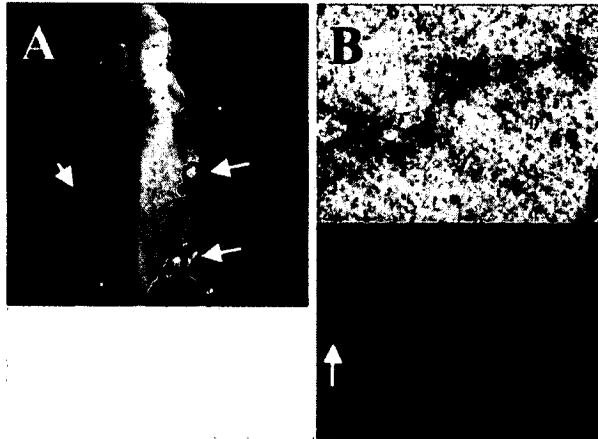


Figure 5. Tumor transfection *in vivo*. Xenografts of KB tumor cells were intratumorally injected with NP-F nanoplex of pCMV-luc (A) or pEGFP-C1 (B). (A) Twenty-four hours after intratumoral injections, mice were imaged and pseudocolor images representing light emitted from tumors superimposed over grayscale reference image of representative mice. (B) Photomicrographs of tumor after cryosection were taken with a x40 objective. Arrow, injection sites.

Cx43 plus 4-PB up-regulated mRNA expression in 2 genes in G₁ phase (CDC7 and *skp2*), 2 genes in S phase (cyclin G2 and CDK7) and 3 genes involved in the DNA damage checkpoint (MRE11B, *nibirin* and SUMO-1) compared with that of pCMV-Cx43 alone. The introduction of pCMV-Cx43 plus TSA up-regulated mRNA expression in 1 gene in G₁ phase (CDC7) and 1 gene in S phase (CDK7), compared with that of pCMV-Cx43 alone.

We also assessed the effect of pCMV-Cx43 on the cell cycle 24 h after transfection into KB cells (data not shown). Flow cytometric analysis revealed that transfection of pCMV-Cx43 caused an increase in the percentage of cells in G₁ phase (76%) compared with transfection of pGL3-basic (70%). Co-transfection with 4-PB or SB did not result in a substantial accumulation in G₁ phase induced by Cx43 expression (77%), but that with TSA caused a decrease in the percentage of cells in G₁ phase (58%).

Combined delivery of pCMV-Cx43 with HDAC inhibitors *in vitro*. HDAC inhibitors including TSA, 4-PB and SB have been used as antineoplastic agents (20). We investigated the cell viability 48 h after treatment with the HDAC inhibitor alone at optimal concentration for increased expression of Cx43 protein. As the result, 1 mM TSA showed high cytotoxicity for the cells (7.3% in cell viability), but 1 mM 4-PB and 1 mM SB did not (71% and 87% in cell viability, respectively) (Fig. 4A). Next, we explored whether the co-introduction of pCMV-Cx43 plus a HDAC inhibitor increased cytotoxicity. The co-introductions of pCMV-Cx43 plus TSA and 4-PB into the cells suppressed significantly tumor growth compared to that of pCMV-Cx43 alone, but pCMV-Cx43 plus SB did not (Fig. 4A). These results suggested that 1 mM 4-PB and 1 μ M TSA could induce a high level of Cx43 protein, and could increase suppression of cell growth by the co-introduction of pCMV-Cx43. However, to confirm suppression of tumor

growth by overexpressed Cx43, co-introduction of pCMV-Cx43 plus 4-PB was adequate, because 1 μ M TSA exhibited strong cytotoxicity without Cx43 expression. Thereafter, we investigated the mechanism of inhibition of cell growth by the co-introduction of pCMV-Cx43 plus 4-PB and applied this combination to xenografts.

Effect of Cx43 with HDAC inhibitors on apoptosis *in vitro*. Tanaka and Grossman reported that overexpression of Cx26 in human bladder and prostate cancer enhanced the cytotoxicity of chemotherapy by down-regulating the expression of anti-apoptotic *bcl-2* (15,16). Therefore, we examined the effect on the expression of *bcl-2* mRNA 24 h after the transfection of Cx43 into KB cells by quantitative PCR analysis. pCMV-Cx43 transfection resulted in a down-regulation of *bcl-2* mRNA expression compared with pGL3-basic transfection (~64%) (Fig. 4B). Furthermore, the transfection of pCMV-Cx43 plus 4-PB induced a significantly greater down-regulation (~24% of pGL3-basic, respectively) of *bcl-2* mRNA expression, whereas 4-PB alone did not.

Next, to examine the effect of Cx43 on the expression of apoptosis-associated enzymes, we measured caspase-3/7 activity 24 h after pCMV-Cx43-transfection with or without HDAC inhibitors (Fig. 4C). Caspase-3/7 activity in pCMV-Cx43-transfected cells was approximately 1.4-fold higher than that in pGL3-basic-transfected cells. The treatments with SB and TSA in pGL3-basic-transfected cells induced a 1.4- and 1.2-fold increase in activity, respectively, compared with pGL3-basic alone, and the co-introduction of pCMV-Cx43 and SB or TSA did not increase the activity (1.4- and 1.3-fold that of levels in pGL3-basic-transfected cells, respectively). In contrast, the treatment with 4-PB in pGL3-basic-transfected cells induced the most potent caspase-3/7 activity (1.7-fold that of activity of pGL3-basic-transfected cells), and the co-introduction of pCMV-Cx43 and 4-PB enhanced the activity (1.9-fold that in pGL3-basic-transfected cells). These findings suggest that combining pCMV-Cx43 with 4-PB might result in an induction of caspase-3/7 activity in the cells.

***In vivo* transfection.** To test the utility of NP-F for gene delivery *in vivo*, we evaluated transfection efficiency by intratumoral injection of NP-F nanoplex of pCMV-luc or pEGFP-C1 into KB tumor xenografts. NP-F induced luciferase expression at a high level around KB tumors (Fig. 5A), however, the distribution of EGFP-expressed cells was restricted to the center of the tumor mass in the vicinity of the injection site (Fig. 5B).

Combination gene therapy in KB tumor xenografts. To evaluate the potential for *in vivo* therapy in KB tumor xenografts, we evaluated the anti-tumor effect by directly injecting the NP-F nanoplex of pCMV-Cx43 or pGL3-basic following a direct injection of 4-PB once a day three times into the xenografts. Yamano *et al* reported that an intratumoral injection of HDAC inhibitor, FR901228, enhanced luciferase expression in solid tumors which were intratumorally injected with luciferase plasmid, whereas the intraperitoneal injection did not (21). Transfection with pCMV-Cx43 alone did not inhibit tumor growth compared with that by pGL3-basic (Fig. 6A). pGL3-basic plus 4-PB treatment moderately suppressed

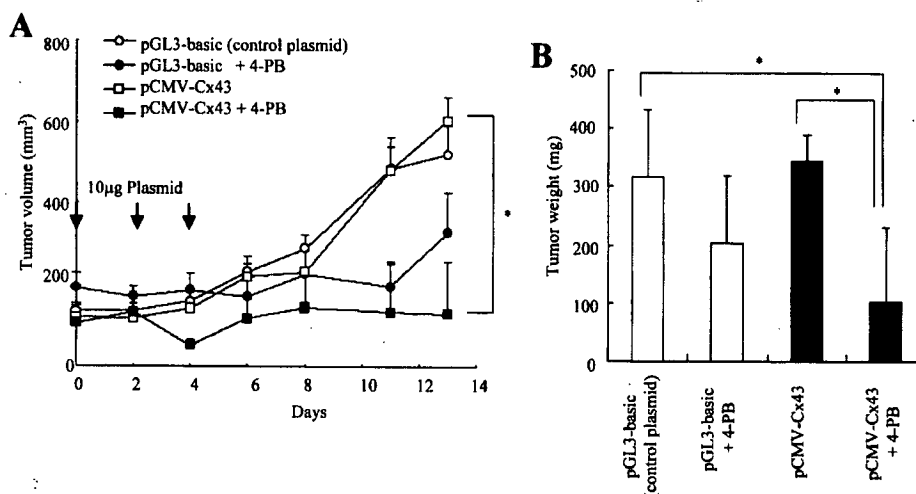


Figure 6. Tumor growth after intratumoral injection of pCMV-Cx43 plus 4-PB. An NP-F nanoplex of 10 μ g of pCMV-Cx43 or 10 μ g of pGL3-basic was injected on day 0, 2 and 4 with or without 1 mg of 4-PB as described in Materials and methods. Tumor volume was measured and the growth ratio was calculated as an increase in tumor volume (A). Tumor weight when all mice were sacrificed at day 13 (B). The results indicate the mean volume and weight \pm SE or SD, respectively (n=4). Statistical significance of the data was evaluated with Fisher's exact test. * $P < 0.05$, compared with the pCMV-Cx43 plus 4-PB.

tumor growth, but the effect was not statistically significant ($P > 0.05$). The introduction of pCMV-Cx43 plus 4-PB significantly suppressed tumor growth, and complete regression was observed in 2 of 4 tumors on day 13 after treatment. A comparison of tumor weight after excision also demonstrated that the tumor growth was significantly attenuated in the mice treated with pCMV-Cx43 plus 4-PB compared with just pGL3-basic (Fig. 6B). Neither the transfection of pCMV-Cx43 alone, the injection of 4-PB alone, nor the introduction of pCMV-Cx43 plus 4-PB altered the change in body weight during 2 weeks of treatment (data not shown).

To determine the fate of tumor cells after gene therapy with pCMV-Cx43, KB tumor xenografts were analyzed by histological examination. The tumors treated with 4-PB showed no evidence of tumor cell death (Fig. 7B) even though the treatment suppressed tumor growth (Fig. 6A and B). Tumors transfected with pCMV-Cx43 exhibited many aggregated cells in the eosinophilic mass although transfection did not suppress tumor growth (Fig. 7C and E). The tumors transfected with pCMV-Cx43 plus 4-PB showed cell death in the eosinophilic mass (Fig. 7D and F). These findings suggested that the introduction of pCMV-Cx43 plus 4-PB had a strong anti-tumor effect on KB tumor xenografts.

Discussion

Restoring Cx expression and/or GJIC in Cx-deficient tumor cells by gene delivery may decrease tumor cell growth (8,11). In the present study, we found that Cx43 expression induced significantly tumor growth inhibition in nasopharyngeal cancer KB cells via a GJIC-independent mechanism. Furthermore, enforced expression of Cx43 by 4-PB enhanced the cell death through activation of the apoptosis pathway, and the combined delivery of Cx43 with 4-PB suppressed the growth of tumor xenografts *in vivo*. This is the first report that enforced expression of Cx43 by 4-PB has potential as a tumor growth inhibitor.

The transfection of pCMV-Cx43 into KB cells inhibited the cell growth (Fig. 1A), but Cx43 was localized to the intracellular compartment (Fig. 3A). Regarding the function of Cx43 in growth inhibition, a truncated Cx43 having the intracellular C-terminal domain of Cx43 could not form gap junctions but inhibited the tumor growth (12), indicating that Cx43 suppresses tumor growth via a GJIC-independent mechanism (33). The mechanistic aspects of the GJIC-independent functions of Cxs remain largely unknown. Several possible mechanisms have been hypothesized (34). In Cx43-transfected cells, we found up-regulated mRNA expression in the G_1 phase and DNA damage checkpoint and ATM pathway genes by cDNA array analysis (Table I). Cx43 transfection induced p16 expression, and the DNA-damage-response by regulating the expression of Mre11A, Mre11B and nibrin, known to be important for mediating ATM-dependent checkpoint pathways (35). p16 is an important regulator of the cell cycle at the G_1 phase (36). The expression of the nibrin and Mre11 genes was induced in an irradiation-evoked DNA damage checkpoint response (37,38), suggesting that the transfection of pCMV-Cx43 had a similar or even identical underlying sensitivity to irradiation, and function in a similar signal pathway, in response to DNA damage. These findings corresponded with the result that Cx43-transfected cells had increased caspase-3/7 activity (Fig. 4C). Seul *et al* reported that the adenoviral delivery of Cx37 induced endothelial cell death through apoptosis (39). Overexpression of Cx43 in KB cells appears to regulate the expression of many genes involved in the G_1 phase of the cell cycle and apoptosis. This is the first report that Cx43 gene delivery induced effective growth inhibition via a GJIC-independent mechanism in KB cells.

Co-introduction of pCMV-Cx43 and TSA, SB or 4-PB into the cells up-regulated the expression of Cx43 protein (Fig. 1B). The amplification of Cx43 expression resulted from an increase in translation from Cx43 mRNA rather than in transcription from pCMV-Cx43. As another possibility,

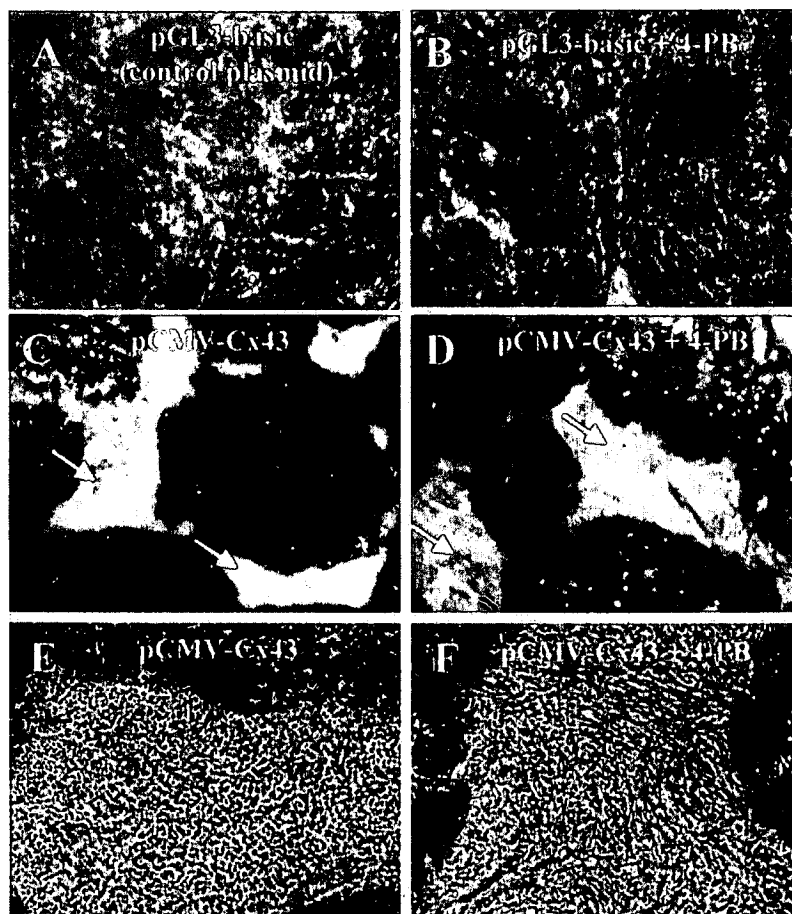


Figure 7. Histological analysis of tumors after Cx43 transfection and/or 4-PB treatment. Tumors were obtained when all mice were sacrificed at day 13. Photomicrographs of hematoxylin and eosin-stained sections of tumors were taken with x40 (A and D) and x100 (E and F) objectives. Tumor injected with 10 μ g of pGL3-basic (A), tumor injected with 10 μ g of pGL3-basic plus 1 mg 4-PB (B), tumor injected with 10 μ g of pCMV-Cx43 (C and E), and tumor injected with 10 μ g of pCMV-Cx43 plus 1 mg 4-PB (D and F). Arrowheads: tumor death areas. (E and F) Magnifications of the area of tumor death observed as an eosinophilic mass in C and D, respectively.

the amplified expression might result from an indirect effect on stabilization of Cx43 protein by HDAC inhibitors. Expression of endogenous Cx43 protein in KB cells was also weakly increased when the cells were treated with 4-PB or SB (Fig. 1B). Among the HDAC inhibitors, 4-PB up-regulated the expression of endogenous Cx43 in human gliomas (40,41). Thus, pCMV-Cx43 plus either 4-PB or SB will be greater inducers for endogenous and exogenous Cx43 expression in nasopharyngeal tumors.

Combining pCMV-Cx43 with 4-PB or TSA in the cells enhanced the cytotoxicity, but that with SB did not (Fig. 4A). Several groups have reported that combining Cx gene therapy with a chemotherapeutic agent resulted in greater suppression of tumor growth (14,15). Cx43 expression could enhance the sensitivity of human glioblastoma cells to doxorubicin, paclitaxel and etoposide (14). Transfection with the Cx26 gene induced down-regulation of bcl-2 expression in prostate cancer cells (15). Transfection of pCMV-Cx43 induced down-regulation of bcl-2 expression in prostate cancer PC-3 cells, and increased sensitivity to docetaxel (42). In this study, the introduction of pCMV-Cx43 plus 4-PB in KB cells resulted

in greater reduction of bcl-2 mRNA expression and induced caspase-3/7 activity (Fig. 4B and C). From the result obtained with the cDNA array, the co-introduction of 4-PB up-regulated mRNA expression in DNA damage checkpoint-related genes such as MRE11B, nibirin and SUMO-1 (Table I), suggesting an enhancement of the signal pathway in response to DNA damage. Furthermore, on the overexpression of Cx43 by 4-PB, strong expression of p16 protein was observed (Table I). Transfection of the p16 gene into nasopharyngeal carcinoma increased sensitivity to chemotherapeutic drugs such as 5FU and cisplatin (43). Therefore, the possible mechanism of enhanced efficacy with pCMV-Cx43 plus 4-PB might result from the effect of Cx43 overexpressed by 4-PB to induce growth inhibition and the effect on increased cytotoxicity of 4-PB by down-regulating bcl-2 expression. This may provide valuable molecular therapeutic information to improve the clinical applications of both HDAC inhibitors and Cx43 gene therapy.

The introduction of pCMV-Cx43 plus TSA also resulted in significant reduction of tumor growth (Fig. 4A). However, from DNA array analysis, the introduction of pCMV-Cx43 plus

TSA slightly affected mRNA expression of genes involved in DNA damage checkpoint and ATM pathway, compared with that of pCMV-Cx43 alone (Table I). These findings suggested that the mechanism of induction of apoptosis might be different between TSA and 4-PB. However, it was not clear why different responses to 4-PB and TSA in the induction of genes involved in the cell cycle, DNA damage checkpoint, and ATM pathway were observed.

In *in vivo* Cx43 gene therapy, pCMV-Cx43 could not suppress the growth of KB tumor xenografts (Fig. 6A), but the tumors exhibited cell death (Fig. 7C and E). The observed restricted cell death in tumors may be due to the effect of Cx43 since the distribution of Cx expression by NP-F transfection into tumors was restricted to the center of the tumor mass in the vicinity of the injection site (Fig. 5B). Therefore, to induce inhibition of tumor growth by Cx43 expression alone, it is necessary to develop a gene carrier with the ability to introduce DNA widely into the tumor. 4-PB with pGL3-basic suppressed tumor growth, but the tumors exhibited no evidence of cell death (Fig. 7B). HDAC inhibitors including 4-PB have been reported to inhibit the process of new capillary blood vessel formation or tumor angiogenesis, in addition to the inhibitory effect on cancer cell proliferation (44-46). The reduction in tumor size may be due to the antitumor effects of 4-PB. The combination of pCMV-Cx43 and 4-PB suppressed significantly tumor growth and weight *in vivo* compared with the control (Fig. 6), and resulted in massive tumor cell death (Fig. 7D and F), suggesting that the combined delivery showed a synergistic or additive effect in terms of growth inhibition and tumor toxicity. One explanation for enhanced growth inhibition by combination therapy might be that Cx43 increased sensitivity for 4-PB via the down-regulation of bcl-2. As another possibility, the reduction in tumor size by 4-PB may increase the transfection efficiency of pCMV-Cx43, because significant tumor growth inhibition by intratumoral injection was obtained in tumor gene therapy when the tumor volume was <50 mm³ (47). The combination of pCMV-Cx43 and an HDAC inhibitor transfected with NP-F has great potential as a tumor-targeted carrier for *in vivo* cancer gene therapy.

In conclusion, we demonstrated that Cx43 transfected by nanoparticle had a tumor suppressive effect via a mechanism that was independent of GJIC in KB cells, and combining pCMV-Cx43 with 4-PB resulted in significantly greater growth suppression of the cells and xenografts. Thus, the combination of Cx43 expression and an HDAC inhibitor may serve as a novel tool for gene therapy.

Acknowledgements

This project was supported in part by a grant from the Promotion and Mutual Aid Corporation for Private Schools of Japan, and by a Grant-in-Aid for Scientific Research from the Ministry of Education, Culture, Sports, Science, and Technology of Japan.

References

- Vine AL and Bertram JS: Cancer chemoprevention by connexins. *Cancer Metastasis Rev* 21: 199-216, 2002.
- Yamasaki H and Naus CC: Role of connexin genes in growth control. *Carcinogenesis* 17: 1199-1213, 1996.
- Lee SW, Tomasetto C, Paul D, Keyomarsi K and Sager R: Transcriptional downregulation of gap-junction proteins blocks junctional communication in human mammary tumor cell lines. *J Cell Biol* 118: 1213-1221, 1992.
- Tomasetto C, Neveu MJ, Daley J, Horan PK and Sager R: Specificity of gap junction communication among human mammary cells and connexin transfectants in culture. *J Cell Biol* 122: 157-167, 1993.
- Habermann H, Ray V, Habermann W and Prins GS: Alterations in gap junction protein expression in human benign prostatic hyperplasia and prostate cancer. *J Urol* 167: 655-660, 2002.
- Huang RP, Hossain MZ, Sehgal A and Boynton AL: Reduced connexin43 expression in high-grade human brain glioma cells. *J Surg Oncol* 70: 21-24, 1999.
- Sawey MJ, Goldschmidt MH, Risek B, Gilula NB and Lo CW: Perturbation in connexin 43 and connexin 26 gap-junction expression in mouse skin hyperplasia and neoplasia. *Mol Carcinog* 17: 49-61, 1996.
- Zhang ZQ, Zhang W, Wang NQ, Bani-Yaghoob M, Lin ZX and Naus CC: Suppression of tumorigenicity of human lung carcinoma cells after transfection with connexin43. *Carcinogenesis* 19: 1889-1894, 1998.
- Oyamada Y, Oyamada M, Fusco A and Yamasaki H: Aberrant expression, function and localization of connexins in human esophageal carcinoma cell lines with different degrees of tumorigenicity. *J Cancer Res Clin Oncol* 120: 445-453, 1994.
- Pelin K, Hirvonen A and Linnainmaa K: Expression of cell adhesion molecules and connexins in gap junctional intercellular communication deficient human mesothelioma tumour cell lines and communication competent primary mesothelial cells. *Carcinogenesis* 15: 2673-2675, 1994.
- Mehta PP, Perez-Stable C, Nadji M, Mian M, Asotra K and Roos BA: Suppression of human prostate cancer cell growth by forced expression of connexin genes. *Dev Genet* 24: 91-110, 1999.
- Zhang YW, Kaneda M and Morita I: The gap junction-independent tumor-suppressing effect of connexin 43. *J Biol Chem* 278: 44852-44856, 2003.
- Nicholas TW, Read SB, Burrows FJ and Kruse CA: Suicide gene therapy with Herpes simplex virus thymidine kinase and ganciclovir is enhanced with connexins to improve gap junctions and bystander effects. *Histol Histopathol* 18: 495-507, 2003.
- Huang RP, Hossain MZ, Huang R, Gano J, Fan Y and Boynton AL: Connexin 43 (cx43) enhances chemotherapy-induced apoptosis in human glioblastoma cells. *Int J Cancer* 92: 130-138, 2001.
- Tanaka M and Grossman HB: Connexin 26 induces growth suppression, apoptosis and increased efficacy of doxorubicin in prostate cancer cells. *Oncol Rep* 11: 537-541, 2004.
- Tanaka M and Grossman HB: Connexin 26 gene therapy of human bladder cancer: induction of growth suppression, apoptosis, and synergy with Cisplatin. *Hum Gene Ther* 12: 2225-2236, 2001.
- Peart MJ, Tainton KM, Ruefli AA, *et al*: Novel mechanisms of apoptosis induced by histone deacetylase inhibitors. *Cancer Res* 63: 4460-4471, 2003.
- Blagosklonny MV, Robey R, Sackett DL, *et al*: Histone deacetylase inhibitors all induce p21 but differentially cause tubulin acetylation, mitotic arrest, and cytotoxicity. *Mol Cancer Ther* 1: 937-941, 2002.
- Ishiguro K and Sartorelli AC: Activation of transiently transfected reporter genes in 3T3 Swiss cells by the inducers of differentiation/apoptosis-dimethylsulfoxide, hexamethylene bisacetamide and trichostatin A. *Eur J Biochem* 271: 2379-2390, 2004.
- Piekarz R and Bates S: A review of depeptide and other histone deacetylase inhibitors in clinical trials. *Curr Pharm Des* 10: 2289-2298, 2004.
- Yamano T, Ura K, Morishita R, Nakajima H, Monden M and Kaneda Y: Amplification of transgene expression *in vitro* and *in vivo* using a novel inhibitor of histone deacetylase. *Mol Ther* 1: 574-580, 2000.
- Imanishi R, Ohtsuru A, Iwamatsu M, *et al*: A histone deacetylase inhibitor enhances killing of undifferentiated thyroid carcinoma cells by p53 gene therapy. *J Clin Endocrinol Metab* 87: 4821-4824, 2002.
- Takimoto R, Kato J, Terui T, *et al*: Augmentation of antitumor effects of p53 gene therapy by combination with HDAC inhibitor. *Cancer Biol Ther* 4: 421-428, 2005.
- Yamamoto S, Yamano T, Tanaka M, *et al*: A novel combination of suicide gene therapy and histone deacetylase inhibitor for treatment of malignant melanoma. *Cancer Gene Ther* 10: 179-186, 2003.

25. Parker N, Turk MJ, Westrick E, Lewis JD, Low PS and Leamon CP: Folate receptor expression in carcinomas and normal tissues determined by a quantitative radioligand binding assay. *Anal Biochem* 338: 284-293, 2005.
26. Hattori Y and Maitani Y: Folate-linked lipid-based nanoparticle for targeted gene delivery. *Curr Drug Delivery* 2: 243-252, 2005.
27. Hattori Y, Kubo H, Higashiyama K and Maitani Y: Folate-linked nanoparticles formed with DNA complexes in sodium chloride solution enhance transfection efficiency. *J Biomed Nanotech* 1: 176-184, 2005.
28. Hattori Y and Maitani Y: Folate-linked nanoparticle-mediated suicide gene therapy in human prostate cancer and nasopharyngeal cancer with herpes simplex virus thymidine kinase. *Cancer Gene Ther* 12: 796-809, 2005.
29. Robe PA, Jolais O, N'Guyen M, *et al*: Modulation of the HSV-TK/ganciclovir bystander effect by n-butyrate in glioblastoma: correlation with gap-junction intercellular communication. *Int J Oncol* 25: 187-192, 2004.
30. Hattori Y and Maitani Y: Enhanced *in vitro* DNA transfection efficiency by novel folate-linked nanoparticles in human prostate cancer and oral cancer. *J Control Release* 97: 173-183, 2004.
31. Bartova E, Pachernik J, Harnicarova A, *et al*: Nuclear levels and patterns of histone H3 modification and HP1 proteins after inhibition of histone deacetylases. *J Cell Sci* 118: 5035-5046, 2005.
32. Govindarajan R, Zhao S, Song XH, *et al*: Impaired trafficking of connexins in androgen-independent human prostate cancer cell lines and its mitigation by alpha-catenin. *J Biol Chem* 277: 50087-50097, 2002.
33. Jiang JX and Gu S: Gap junction- and hemichannel-independent actions of connexins. *Biochim Biophys Acta* 1711: 208-214, 2005.
34. Zhang YW, Nakayama K, Nakayama K and Morita I: A novel route for connexin 43 to inhibit cell proliferation: negative regulation of S-phase kinase-associated protein (Skp 2). *Cancer Res* 63: 1623-1630, 2003.
35. Lee JH and Paull TT: ATM activation by DNA double-strand breaks through the Mre11-Rad50-Nbs1 complex. *Science* 308: 551-554, 2005.
36. Shapiro GI, Edwards CD and Rollins BJ: The physiology of p16(INK4A)-mediated G1 proliferative arrest. *Cell Biochem Biophys* 33: 189-197, 2000.
37. Desai-Mehta A, Cersaletti KM and Concannon P: Distinct functional domains of nibrin mediate Mre11 binding, focus formation, and nuclear localization. *Mol Cell Biol* 21: 2184-2191, 2001.
38. Gatei M, Young D, Cersaletti KM, *et al*: ATM-dependent phosphorylation of nibrin in response to radiation exposure. *Nat Genet* 25: 115-119, 2000.
39. Seul KH, Kang KY, Lee KS, Kim SH and Beyer EC: Adenoviral delivery of human connexin37 induces endothelial cell death through apoptosis. *Biochem Biophys Res Commun* 319: 1144-1151, 2004.
40. Asklund T, Appelskog IB, Ammerpohl O, Ekstrom TJ and Almquist PM: Histone deacetylase inhibitor 4-phenylbutyrate modulates glial fibrillary acidic protein and connexin 43 expression, and enhances gap-junction communication, in human glioblastoma cells. *Eur J Cancer* 40: 1073-1081, 2004.
41. Ammerpohl O, Thormeyer D, Khan Z, *et al*: HDACi phenylbutyrate increases bystander killing of HSV-tk transfected glioma cells. *Biochem Biophys Res Commun* 324: 8-14, 2004.
42. Fukushima M, Hattori Y, Yoshizawa T and Maitani Y: Combination of non-viral connexin 43 gene therapy and docetaxel inhibits the growth of human prostate cancer in mice. *Int J Oncol* 30: 225-231, 2007.
43. Chow LS, Wang X, Kwong DL, Sham JS, Tsao SW and Nicholls JM: Effect of p16INK4a on chemosensitivity in nasopharyngeal carcinoma cells. *Int J Oncol* 17: 135-140, 2000.
44. Pili R, Kruszewski MP, Hager BW, Lantz J and Carducci MA: Combination of phenylbutyrate and 13-cis retinoic acid inhibits prostate tumor growth and angiogenesis. *Cancer Res* 61: 1477-1485, 2001.
45. Williams RJ: Trichostatin A, an inhibitor of histone deacetylase, inhibits hypoxia-induced angiogenesis. *Expert Opin Investig Drugs* 10: 1571-1573, 2001.
46. Kim MS, Kwon HJ, Lee YM, *et al*: Histone deacetylases induce angiogenesis by negative regulation of tumor suppressor genes. *Nat Med* 7: 437-443, 2001.
47. Galaup A, Opolon P, Bouquet C, *et al*: Combined effects of docetaxel and angiostatin gene therapy in prostate tumor model. *Mol Ther* 7: 731-740, 2003.

Exhibit 13**115**

